



UNIVERSIDAD NACIONAL AUTÓNOMA DE MÉXICO

Maestría y Doctorado en Ciencias Bioquímicas

Supresión por dosis génica de la sensibilidad a tunicamicina revela nuevas funciones de
la MAPK Hog1 en *Saccharomyces cerevisiae*

TESIS

QUE PARA OPTAR POR EL GRADO DE:

Doctora en Ciencias

PRESENTA:

Mariana Hernández Elvira

TUTOR PRINCIPAL:

Dr. Roberto Coria Ortega

[Instituto de Fisiología Celular](#)

MIEMBROS DEL COMITÉ TUTOR:

Dra. Soledad Funes Argüello

[Instituto de Fisiología Celular](#)

Dra. Romina Rodríguez Sanoja

[Instituto de Investigaciones Biomédicas](#)

Ciudad Universitaria, Cd de México. Octubre, 2019



UNAM – Dirección General de Bibliotecas

Tesis Digitales
Restricciones de uso

DERECHOS RESERVADOS ©
PROHIBIDA SU REPRODUCCIÓN TOTAL O PARCIAL

Todo el material contenido en esta tesis está protegido por la Ley Federal del Derecho de Autor (LFDA) de los Estados Unidos Mexicanos (Méjico).

El uso de imágenes, fragmentos de videos, y demás material que sea objeto de protección de los derechos de autor, será exclusivamente para fines educativos e informativos y deberá citar la fuente donde la obtuvo mencionando el autor o autores. Cualquier uso distinto como el lucro, reproducción, edición o modificación, será perseguido y sancionado por el respectivo titular de los Derechos de Autor.

CONTENIDO

CONTENIDO	2
LISTA DE FIGURAS Y TABLAS	4
LISTA DE ABREVIATURAS	5
AGRADECIMIENTOS	6
AGRADECIMIENTOS PERSONALES	8
RESUMEN	9
ABSTRACT	10
INTRODUCCIÓN.....	11
La síntesis de proteínas en el retículo endoplásmico	11
El estrés del retículo endoplásmico y la respuesta a las proteínas mal plegadas.....	15
Las vías alternativas de la respuesta al estrés de RE.....	17
JUSTIFICACIÓN	20
HIPÓTESIS.....	21
OBJETIVOS.....	22
Objetivo general.....	22
Objetivos específicos	22
METODOLOGÍA	23
Condiciones de cultivo y cepas	23
Ensayos de la sensibilidad a estrés	23
Ensayo de la búsqueda de los genes supresores de la sensibilidad a la Tn.....	23
Transformación de las células.....	24
Extracción del plásmido de las levaduras	25
Sobreexpresión de los genes	25
Generación de las mutantes nulas.....	26
Ensayo de las interacciones físicas	26
Construcción de la red de interacción.....	26
Cuantificación del dolicol	27
RESULTADOS.....	28
La rama SLN1 participa en la resistencia a la Tn y no a otros inductores del estrés del RE.....	28
Identificación de los genes supresores de la sensibilidad a la Tn en la mutante <i>hog1Δ</i>	29

Los genes supresores se clasifican como generales o específicos de la vía de HOG....	32
La inactivación de algunos genes supresores afecta la resistencia a la Tn	34
Los genes supresores no son interactores físicos de Hog1.....	35
Los supresores forman una red de interacción con Hog1	36
La síntesis de dolicol es un proceso importante para responder a la Tn	39
DISCUSIÓN	43
CONCLUSIONES	49
REFERENCIAS	50
ANEXOS	56
1. Lista de cepas	56
2. Lista de oligonucleótidos.....	57
3. Publicaciones	58

LISTA DE FIGURAS Y TABLAS

Figura 1: La síntesis y el procesamiento de las proteínas en el retículo endoplásmico.	12
Figura 2: La síntesis del dolicol y la <i>N</i> -glicosilación.....	14
Figura 3: La respuesta a las proteínas mal plegadas (UPR).....	17
Figura 4: La respuesta al estrés hiperosmótico (HOG).....	18
Figura 5: Búsqueda de los genes supresores de la sensibilidad a la Tn.....	24
Figura 6: El efecto de la ausencia de los componentes de la rama SLN1 en la resistencia al estrés del RE.....	28
Figura 7: La supresión de la sensibilidad a la Tn de la mutante <i>hog1Δ</i> por los plásmidos de la biblioteca genómica.	30
Figura 8: La supresión de la sensibilidad a la Tn de la mutante <i>hog1Δ</i> por la sobreexpresión de los genes aislados.	31
Figura 9: El efecto de la sobreexpresión de los genes supresores en las mutantes de distintas vías de señalización.	33
Tabla 1: Las características funcionales y localización de los genes supresores de la sensibilidad a la Tn.....	34
Figura 10: El efecto de la inactivación de los genes supresores en la sensibilidad a la Tn.	35
Tabla 2: La evaluación de las interacciones físicas entre Hog1 y los supresores específicos.	36
Figura 11: La red de interacción entre Hog1 y los genes supresores.....	39
Figura 12: El efecto de la modificación de la síntesis de dolicol en la resistencia a la Tn.	42
Figura 13: Las funciones celulares de Hog1 en respuesta al estrés.	43
Figura 14: Los supresores de la sensibilidad a la Tn participan en limitados procesos celulares.	44

LISTA DE ABREVIATURAS

2-DOG	2-deoxiglucosa
ABC	<i>ATP-binding cassette</i>
BiFC	<i>Bimolecular fluorescence complementation</i>
cis-PT	<i>Cis</i> -preniltransferasa
CWI	<i>Cell wall integrity</i>
Dol-Glc	Dolicol-Glucosa
Dol-Man	Dolicol-Manosa
ERAD	<i>Endoplasmic reticulum-associated degradation</i>
FPP	Farnesil difosfato
Glc	Glucosa
GlcNAc	<i>N</i> -acetil glucosamina
HOG	<i>High Osmolarity Glycerol</i>
IPP	Isopentenil difosfato
Man	Manosa
MAPK	<i>Mitogen-activated protein kinase</i>
OST	Oligosacariltransferasa
PDI	<i>Protein disulfide isomerase</i>
RE	Retículo endoplásmico
S1P	Ser-proteasa sitio 1
S2P	Metaloproteasa sitio 2
SRP	<i>Signal recognition particle</i>
Tn	Tunicamicina
UGT1	UDP-glucosa glucosiltransferasa
UPR	<i>Unfolded protein response</i>
VC	Extremo carboxilo de Venus
VN	Extremo amino de Venus

AGRADECIMIENTOS

Agradezco al Consejo Nacional de Ciencia y Tecnología (CONACyT) por la beca de Doctorado 366635. Así como al Programa de Apoyo a Proyectos de Investigación e Innovación Tecnológica (PAPIIT) por el apoyo económico para concluir el proyecto.

Al Programa de Maestría y Doctorado en Ciencias Bioquímicas y al Programa de Apoyo a Estudios de Posgrado (PAEP) por el apoyo para la participación en eventos académicos.

Este trabajo se desarrolló en el Instituto de Fisiología Celular (IFC) en la Universidad Nacional Autónoma de México (UNAM), bajo la dirección del Dr. Roberto Coria Ortega a quien agradezco la oportunidad, orientación y ayuda.

Este trabajo se realizó a través del apoyo para los proyectos CONACyT: CB-254978; PAPIIT, DGAPA, UNAM: IN210616 y IN210519.

Agradezco a la Dra. Laura Kawasaki Watanabe por los consejos, asesoría técnica y administración del laboratorio.

Agradezco a la Dra. Soledad Funes Argüello y a la Dra. Romina Rodríguez Sanoja, miembros de mi comité tutor, por las aportaciones que enriquecieron el proyecto y mi formación.

Agradezco a los Dres. María Alicia González Manjarrez, Jesús Aguirre Linares, Manuel Gutiérrez Aguilar, Bertha María Josefina González Pedrajo y Patricia Coello Coutiño por los comentarios para el mejoramiento de este escrito.

Agradezco al Dr. Francisco Torres Quiroz por todas las sugerencias y discusiones científicas que me ayudaron a resolver problemas a lo largo del proyecto.

Agradezco al Dr. Gabriel del Río Guerra y a la Dra. Teresa Lara Ortíz por la facilitación de cepas y plásmidos.

Agradezco al Dr. Antonio Peña Díaz, a la Dra. Martha Calahorra y a la M. en C. Norma Sánchez por la asesoría técnica y apoyo en el préstamo de equipo y material esencial para la conclusión del proyecto.

A la Dra. Laura Ongay Larios, a la Lic. Guadalupe Códiz y a la M. en C. Minerva Trejo, miembros de la Unidad de Biología Molecular por la asesoría técnica y ayuda prestada a lo largo de mis estudios de Doctorado.

A los miembros de la Unidad de Cómputo y del Taller de Mantenimiento por la asesoría técnica y ayuda prestada a lo largo de mis estudios de Doctorado.

AGRADECIMIENTOS PERSONALES

*"Nada en la vida debe ser temido, solo entendido.
Ahora es el momento de entender más para temer menos".
Marie Curie*

A mis padres, por ser siempre la dirección hacia donde quiero moverme. Su ejemplo de amor, felicidad y compañerismo me ha formado y enseñado a disfrutar el camino. Gracias por creer en mí y darme la motivación para seguir adelante. Cada logro parte de ustedes y de la gran familia que formaron.

A mi hermana, por ser un punto de apoyo fundamental en mi vida. y ayudarme en cada etapa. Tu ejemplo de dedicación y humanidad me ha ayudado a crecer en todos los aspectos. A mi hermano, recién agregado, por formar parte de esta nueva etapa familiar y por todos los momentos felices que hemos compartido.

Akram, gracias por compartir conmigo la vida y los sueños. Por ser mi mejor amigo y equipo siempre. Por hacer mejor cada día y ayudarme a ser mejor persona. Gracias por la vida que hemos construido y por ser mi lugar favorito. "...*Que no importa si hay destino, siempre y cuando en el camino vayas tú*".

A los amigos, que también son familia, por crecer juntos y volver divertido el proceso. Espero que la vida siempre nos acerque y nos permita seguir disfrutando nuestra compañía. Gracias por todos los momentos que hemos compartido, definitivamente son parte importante de quién soy.

A todos los miembros del laboratorio 124 Norte (y amigos anexos), por ser parte de esta familia extendida en la que viví y crecí durante estos años. Por hacer más disfrutable el trabajo y la ciencia. Gracias por todas las enseñanzas que contribuyeron a mi crecimiento personal y profesional.

A todos los que trabajan por hacer ciencia abierta, compartida y equitativa. Espero que no tardemos mucho en alcanzar la equidad de género en ámbitos científicos (y humanos).

RESUMEN

Todos los organismos cuentan con mecanismos celulares de adaptación que les permiten crecer y desarrollarse en condiciones adversas. En la levadura *Saccharomyces cerevisiae* la vía de respuesta a condiciones de hiperosmolaridad (HOG) también es esencial para la resistencia a otros tipos de estrés, incluyendo el estrés de retículo endoplásmico (RE). Esta condición se genera por la acumulación de proteínas mal plegadas en el lumen del organelo y puede ser inducida experimentalmente por un tratamiento con el antibiótico tunicamicina (Tn), inhibidor de la *N*-glicosilación de proteínas. Sin embargo, el mecanismo celular empleado en esta respuesta es distinto al conocido para el estrés hiperosmótico, por lo que este trabajo se enfocó en identificar proteínas involucradas en la respuesta al estrés de RE reguladas por Hog1, la cinasa MAPK de la vía de HOG. Para esto, se desarrolló una búsqueda de supresores que por dosis génica revirtieran la sensibilidad de la mutante *hog1Δ* a la Tn. Los supresores aislados participan en un limitado número de procesos celulares, incluyendo de manera general, el transporte y la glicosilación de proteínas, la desintoxicación celular y la biogénesis de la pared celular. Notablemente, los supresores Rer2 y Srt1 participan en la vía de síntesis de dolícol, lípido esencial en la *N*-glicosilación, y concluimos que, en respuesta a la Tn, la mutante *hog1Δ* muestra un metabolismo deficiente de poliprenoles. Este trabajo revela nuevos interactores genéticos y funcionales de Hog1 y contribuye a un mejor entendimiento de la participación de esta MAPK en la respuesta al estrés de RE.

ABSTRACT

All organisms have adaptive cellular mechanisms that allow them to grow and to develop in adverse conditions. In the yeast *Saccharomyces cerevisiae*, the High Osmolarity Glycerol (HOG) pathway is essential for resistance to a variety of stresses, including endoplasmic reticulum stress (ER stress). This condition caused by the accumulation of unfolded proteins in the lumen of this organelle can be achieved by treatment with tunicamycin (Tn), a *N*-glycosylation inhibitor. However, the molecular mechanism that participates in the ER stress response is different from the one involved in hyperosmotic stress. This work focused on identifying proteins involved in the ER stress response regulated by Hog1, the MAPK of the HOG pathway. A gene dosage suppression screening allowed us to identify genes that suppress Tn sensitivity of a *hog1Δ* strain. The suppressors participate in a limited number of cellular processes, including protein transport and glycosylation, cellular detoxification and cell wall biogenesis. Notably, the finding of the suppressors Rer2 and Srt1, involved in the dolichol biosynthesis pathway, essential lipid in the *N*-glycosylation process, revealed that the *hog1Δ* strain has a defective polyprenol metabolism in response to Tn. This work uncovers new genetic and functional interactors of Hog1 and contributes to a better understanding of the participation of this MAPK in the ER stress response.

INTRODUCCIÓN

La síntesis de proteínas en el retículo endoplásmico

Las proteínas son moléculas esenciales que realizan funciones básicas para el desarrollo de la vida de todos los organismos; regulan y efectúan procesos metabólicos y fisiológicos, así como también participan en mecanismos de transporte, estructura y almacenamiento, entre otras cosas. El funcionamiento adecuado de las proteínas es dependiente de la fidelidad de su síntesis. Todas las proteínas se producen en ribosomas a partir de una secuencia lineal de ARN y alcanzan un estado funcional tridimensional mediante mecanismos de plegamiento, modificación y degradación estrictamente regulados dentro de la célula (Figura 1). Cerca de un tercio del proteoma de la célula, principalmente proteínas transmembranales y de secreción, es sintetizado en ribosomas adheridos a la membrana del retículo endoplásmico (RE) y co-traduccionalmente son transportadas al lumen de este organelo, donde son blanco de modificaciones co- y post-traduccionales con las que alcanzan un estado funcional. Finalmente, de acuerdo al estado de conformación que presenten, son transportadas hacia su destino final a través del sistema de transporte vesicular o son eliminadas mediante mecanismos de degradación (McCaffrey & Braakman, 2016).

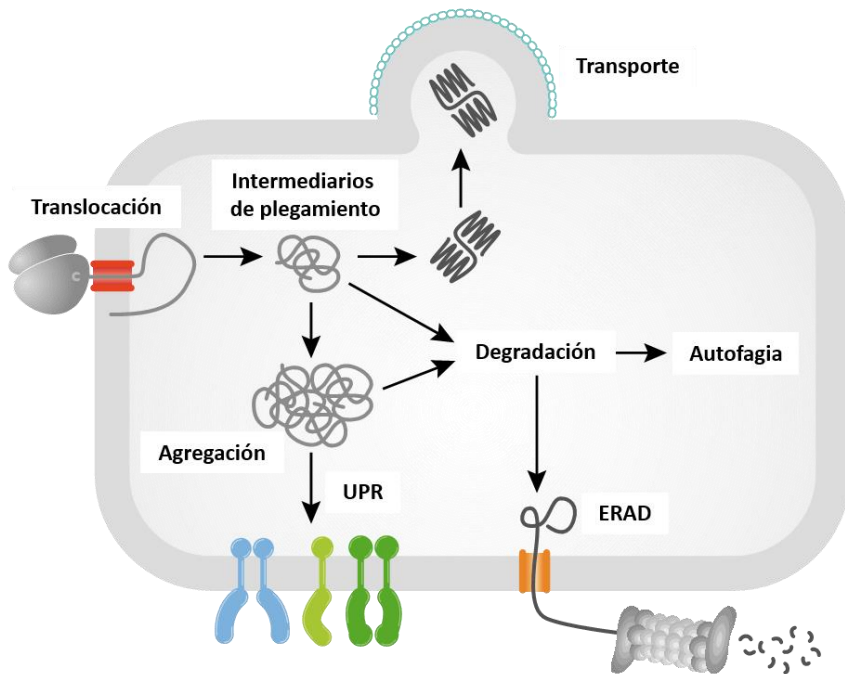


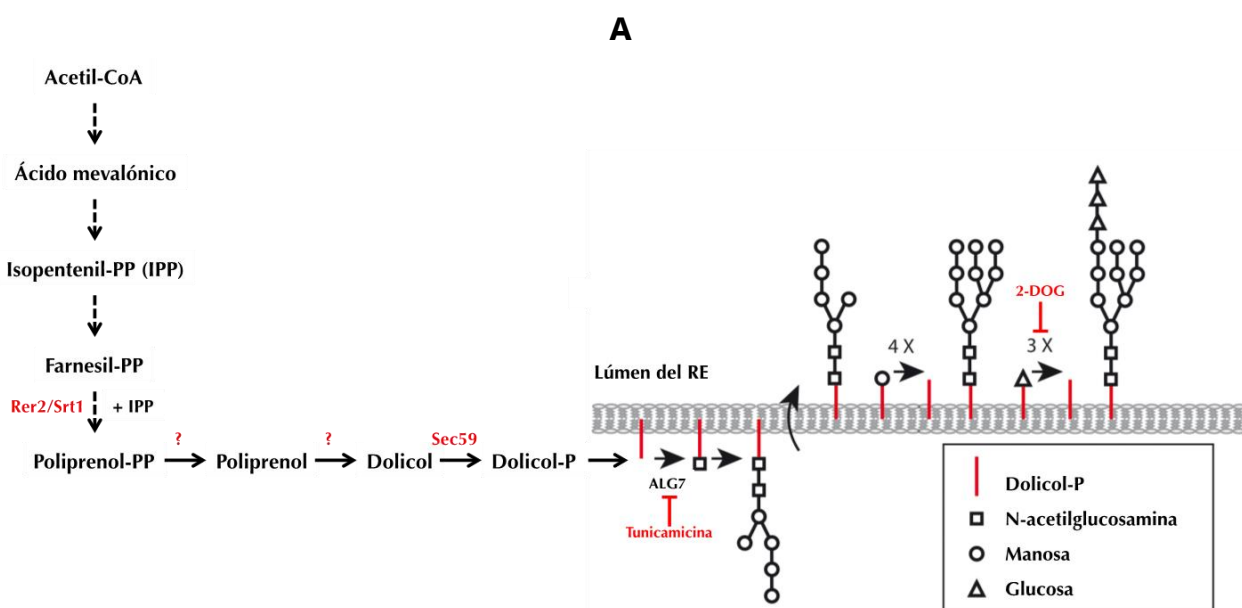
Figura 1: La síntesis y el procesamiento de las proteínas en el retículo endoplásmico.

Las proteínas transmembranales y de secreción son traducidas en ribosomas unidos a la membrana del RE. Las proteínas son transportadas co-traduccionalmente hacia el lumen del RE donde son modificadas por enzimas residentes para alcanzar un estado funcional y ser transportadas hacia su destino final. Ciertas proteínas pueden permanecer en un estado intermedio de plegamiento, favoreciendo la agregación de proteínas desplegadas. Esta condición desencadena la activación de la vía de respuesta a proteínas desplegadas (UPR) o mecanismos de degradación como autofagia y ERAD (Cyr & Hebert, 2009).

Todas las proteínas comienzan su traducción en ribosomas citosólicos, sin embargo, aquellas destinadas al RE presentan en el amino terminal de su secuencia un péptido señal (región de 6 a 12 residuos hidrofóbicos) que es reconocido por la proteína SRP (del inglés, *signal recognition particle*), la cual induce un retraso en la traducción y en el reclutamiento del ribosoma hacia la membrana del RE, donde la proteína naciente se inserta en el lumen a través del complejo Sec61. En el interior del RE, el péptido señal es eliminado por una peptidasa, liberando el extremo amino de la proteína (Lodish, 2000). Estas proteínas son plegadas co-traduccionalmente por chaperonas de la familia Hsp70 y Hsp90. La proteína BiP, perteneciente a la familia Hsp70, es una de las chaperonas más abundantes en el RE y es esencial para el plegamiento y degradación de las proteínas. BiP se une a regiones hidrofóbicas de las proteínas recién sintetizadas, evitando su agregación y asistiendo en el plegamiento a través de ciclos de hidrólisis del ATP. BiP es auxiliada por co-chaperonas de la familia Hsp40 (Araki & Nagata, 2011). Asimismo, la adición de puentes disulfuro es esencial para el plegamiento al estabilizar la estructura de las proteínas. Esta modificación es catalizada por las enzimas oxidorreductasas de la familia PDI (del inglés, *protein disulfide isomerase*), encargadas de oxidar dos residuos cisteína cercanos (Cys-X-X-Cys) para formar un enlace disulfuro (Braakman & Hebert, 2013).

En el RE también ocurre la *N*-glicosilación, una modificación co-traduccional esencial para el plegamiento adecuado de las proteínas. En este proceso se adicionan 14 residuos de carbohidratos (2 *N*-acetil glucosaminas, 9 manosas y 3 glucosas: GlcNAc₂-Man₉-Glc₃) a un residuo Asn en la secuencia consenso Asn-X-Ser/Thr (Breitling & Aebi, 2013). Este polisacárido, denominado *N*-glucano, es preensamblado sobre una molécula de dolicol fosfato (Figura 2A). El dolicol es un lípido isoprenoide localizado en la membrana del RE, esencial para la *N*- y *O*-glicosilación pues funciona como base para la formación del *N*-glucano y como donador de azúcares en estos procesos (Cantagrel & Lefèbvre, 2011). La síntesis de dolicol (Figura 2A) ocurre por la vía del mevalonato a partir de Acetil-CoA, resultando en la formación del farnesil difosfato (FPP), molécula compartida como sustrato para la síntesis de dolicoles, esteroles y ubiquinonas, así como para la

prenilación de proteínas (Grabiska & Palamarczyk, 2002). La enzima *cis*-preniltransferasa (*cis*-PT) es la primera enzima específica para la síntesis de dolicol; es la encargada de la condensación del FPP con unidades de isopentenil difosfato (IPP) para la formación del poliprenol difosfato. En *Saccharomyces cerevisiae* existen dos *cis*-PTs, Rer2 que cataliza la formación de dolicoles con 11 a 15 unidades de isopreno (Sato et al., 1999) y Srt1 que sintetiza dolicoles más largos con 18 a 23 unidades de isopreno (Schenk, Rush, Waechter, & Aebi, 2001), estas enzimas funcionan como heterodímeros con la proteína Nus1 (Harrison et al., 2011). El poliprenol difosfato es convertido a dolicol y posteriormente es fosforilado para su utilización en la *N*-glicosilación (Grabiska & Palamarczyk, 2002). Este proceso comienza en el lado citosólico, donde la enzima Alg7 adiciona una molécula de GlcNAc al dolicol fosfato, para después extender el polisacárido hasta GlcNAc₂-Man₅. La orientación del dolicol se invierte por una flipasa y en el lumen del RE se completa el proceso hasta formar el *N*-glucano con GlcNAc₂-Man₉-Glc₃. Finalmente, el polisacárido es transferido en bloque a las proteínas nacientes por el complejo enzimático oligosacariltransferasa (OST) (Breitling & Aebi, 2013). La presencia de carbohidratos incrementa la solubilidad y estabilidad de las proteínas contribuyendo al plegamiento y al control de calidad en el RE. Asimismo, un desequilibrio o inhibición de este proceso incrementa la presencia de proteínas mal plegadas. Como se ilustra en la Figura 2B, el antibiótico tunicamicina (Tn) inhibe específicamente a la enzima Alg7 pues compite por el sitio activo debido a su similitud estructural con el sustrato GlcNAc; también la *N*-glicosilación puede ser bloqueada por el análogo de la glucosa, 2-deoxiglucosa (2-DOG) al integrarse al *N*-glucano y evitar su elongación.



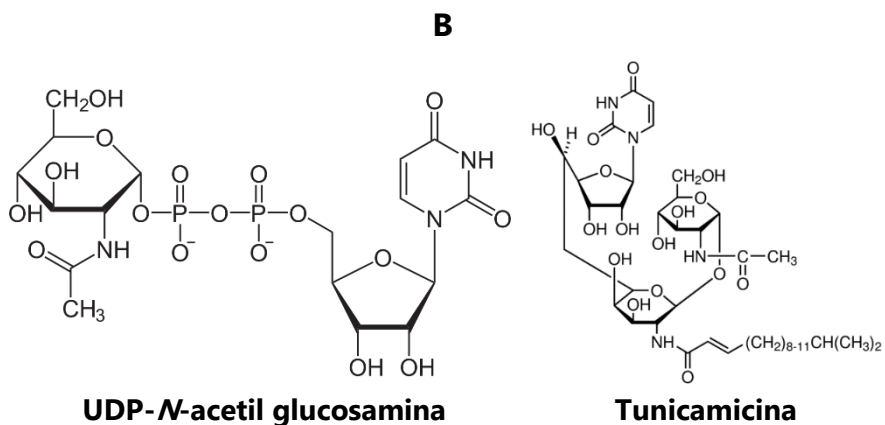


Figura 2: La síntesis del dolicol y la *N*-glicosilación.

A: El dolicol se sintetiza a partir de Acetil-CoA por la vía del mevalonato que produce farnesil difosfato (PP), sustrato de las *cis*-preniltransferasas Rer2/Srt1 que adicionan secuencialmente moléculas de isopentenil difosfato (IPP) para la producción de poliprenol-PP y posteriormente dolicol. El dolicol es fosforilado por la cinasa Sec59 y funciona como base para la formación del polisacárido empleado en la *N*-glicosilación. En el citosol se añaden dos moléculas de *N*-acetil glucosamina y 5 moléculas de manosa, posteriormente la orientación del dolicol es invertida y en el lumen del RE se termina su elongación al agregar 4 moléculas de manosa y 3 de glucosa, donadas por dolicol-manosa (Dol-Man) y dolicol-glucosa (Dol-Glc), respectivamente. Este *N*-glucano es transferido a las proteínas nacientes. La *N*-glicosilación puede ser bloqueada en distintos pasos, la tunicamicina inhibe a la enzima Alg7, primer paso de este proceso, mientras que la 2-deoxiglucosa (2-DOG) se integra al polisacárido y evita su elongación (Modificado de Rauthan & Pilon, 2011).

B: Estructuras de la molécula UDP-*N*-acetilglucosamina, sustrato de la enzima Alg7, y del antibiótico tunicamicina, inhibidor competitivo de la misma enzima.

Cuando el plegamiento de las proteínas es incompleto, estas se retienen en el RE a través de interacciones con chaperonas que las mantienen solubles en el lumen y evitan su agregación. La presencia del *N*-glucano, es importante en este control de calidad. A este polisacárido se le eliminan 2 glucosas terminales, permitiendo así su detección por las chaperonas calnexina y, su ortólogo soluble, calreticulina que promueven el plegamiento de las proteínas. La eliminación de la glucosa restante, cuando la proteína alcanza su plegamiento funcional, evita la interacción con estas chaperonas, liberando a la proteína. El sensor UGT1 (UDP-glucosa glucosiltransferasa) detecta el estado de plegamiento de estas proteínas y adiciona una molécula de glucosa cuando este es incompleto, induciendo el reclutamiento por calnexina/calreticulina. Aquellas proteínas con plegamiento funcional son empacadas en vesículas y liberadas hacia su destino final a través de la vía de secreción (Braakman & Hebert, 2013). Sin embargo, aquellas proteínas mal plegadas o desplegadas son marcadas para su degradación a través del mecanismo de degradación asociada al retículo endoplasmático (ERAD, del inglés *endoplasmic reticulum-associated degradation*) que consiste en retro-translocar y degradar a las

proteínas por el sistema ubiquitina-proteasoma. Por otra parte, cuando los agregados de las proteínas mal plegadas son muy grandes, la degradación se realiza a través de mecanismos de autofagia, es decir, por el encapsulamiento de estos agregados en vesículas de doble membrana que se fusionan al lisosoma donde liberan su contenido para ser degradado (Thibault & Ng, 2012).

El estrés del retículo endoplásmico y la respuesta a las proteínas mal plegadas

El control de la síntesis y degradación de las proteínas es un mecanismo altamente regulado, sin embargo, ciertas condiciones (estrés ambiental, patógenos, incremento en la demanda de proteínas, etc.) pueden generar un incremento en la cantidad de proteínas mal plegadas, induciendo su agregación y acumulación en el lumen del RE, condición conocida como estrés de RE (Shamu, Cox, & Walter, 1994). El estrés de RE se ha asociado con el desarrollo de diversas enfermedades como diabetes, cáncer, enfermedades neurodegenerativas, infecciones virales y bacterianas, entre otras (Kaufman, 2002).

La vía de respuesta a proteínas desplegadas (UPR, del inglés *unfolded protein response*) es una cascada de señalización conservada en todos los eucariontes que está encargada de responder a condiciones de estrés de RE con la finalidad de incrementar la capacidad de procesamiento y degradación del organelo (Figura 3). Se han identificado 3 sensores: IRE1, PERK y ATF6, localizados en la membrana del RE, que responden de manera paralela y con mecanismos específicos ante la presencia de proteínas mal plegadas (Chakrabarti, Chen, & Varner, 2011).

Ire1 es el sensor más conservado y el único presente en levaduras. Es una proteína transmembranal con un dominio luminal de detección de proteínas mal plegadas y un dominio citosólico con actividades catalíticas de cinasa y endorribonucleasa (RNAsa) (Cox, Shamu, & Walter, 1993). En condiciones basales, el dominio de detección se encuentra inhibido por la interacción con la chaperona BiP. En cambio, en presencia de las proteínas mal plegadas la chaperona se disocia de Ire1, induciendo una oligomerización y trans-autofosforilación (Shamu & Walter, 1996; Welihinda & Kaufman, 1996). Esta activación permite el procesamiento (eliminación de un intrón) del ARNm *XBP1/HAC1*. El ARNm procesado es eficientemente traducido en un factor de transcripción llamado Xbp1 en mamíferos o Hac1 en levaduras y es translocado al núcleo donde se une a promotores de genes que codifican para enzimas de plegamiento, modificación y degradación de las proteínas, entre otros (Cox & Walter, 1996; Mori, Ogawa, Kawahara, Yanagi, & Yura, 1998;

Sidrauski, 1998). En *S. cerevisiae* el procesamiento de *HAC1* es el único mecanismo de respuesta a estrés de RE, mediado por la UPR. En mamíferos, en cambio, existen otras respuestas adaptativas mediadas por este sensor; Ire1 degrada selectivamente ARN mensajeros dirigidos al RE para disminuir la carga del organelo, lo que ayuda a que el procesamiento de las proteínas ya acumuladas sea más eficiente. Asimismo, Ire1 activa mecanismos apoptóticos a través de la vía de señalización JNK (Chakrabarti et al., 2011).

Por otra parte, PERK es una proteína transmembranal del RE cuyo principal mecanismo es la modulación de la traducción. Presenta un dominio luminal de detección de proteínas mal plegadas que se activa por la disociación de la chaperona BiP. La activación de PERK, dada por autofosforilación, permite la fosforilación de la proteína eIF2 α , la cual es un regulador del inicio de la traducción. La fosforilación de eIF2 α atenúa la traducción general con lo que se reduce la carga de proteínas que llegan al RE. El mismo factor fosforilado estimula la traducción del ARNm de ATF4 el cual es un activador transcripcional de genes involucrados en la secreción de las proteínas y la síntesis y el transporte de aminoácidos, entre otros (Chakrabarti et al., 2011).

Finalmente, el sensor ATF6 es una proteína transmembranal con un dominio luminal de interacción con la chaperona BiP. Cuando se disocian, ATF6 es transportada a Golgi donde es blanco de proteólisis por las enzimas S1P (Ser-proteasa sitio 1) y S2P (metaloproteasa sitio 2). El procesamiento de ATF6 permite que el dominio amino con actividad transcripcional se transloque al núcleo donde regula la expresión de diversos genes que auxilian en la respuesta a proteínas mal plegadas (Chakrabarti et al., 2011).

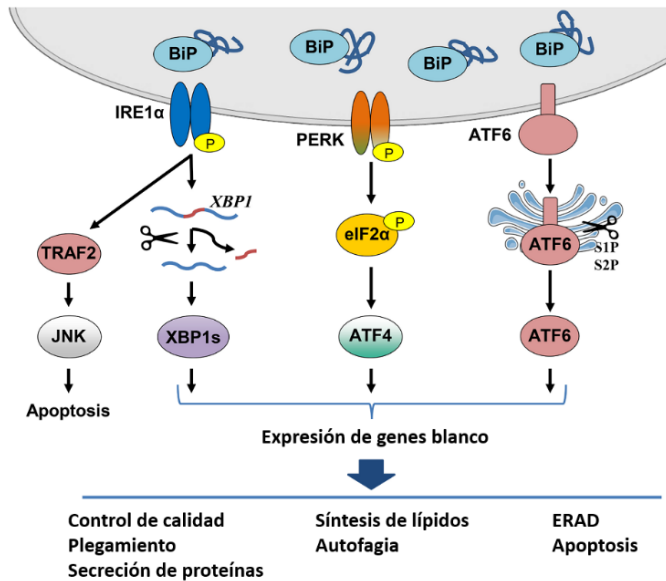


Figura 3: La respuesta a las proteínas mal plegadas (UPR).

En mamíferos existen tres sensores de la vía UPR (IRE1, PERK y ATF6) que se activan por la presencia de proteínas mal plegadas y por la disociación de la chaperona BiP. IRE1 se trans-autofosforila y su dominio RNAsa procesa al mensajero XBP1, el cual se traduce en el factor de transcripción Xbp1; adicionalmente, Ire1 activa mecanismos de apoptosis cuando el estrés no es controlado. PERK se activa también por trans-autofosforilación, induciendo la fosforilación del factor de inicio de la traducción eIF2 α lo que produce la atenuación de la traducción y activación del factor de transcripción ATF4. ATF6 se activa y se transporta a Golgi donde es procesado por las proteasas S1P y S2P, liberando su dominio transcripcional. Los factores de transcripción son translocados al núcleo donde incrementan la expresión de genes involucrados en el plegamiento, modificación y degradación de proteínas, así como en mecanismos de autofagia y apoptosis (Storm, Sheng, Arnoldussen, & Saatcioglu, 2016).

Las vías alternativas de la respuesta al estrés de RE

En *S. cerevisiae* se ha reportado la participación de otras vías de señalización en la respuesta a estrés de RE (Chen, 2005). Particularmente, la vía de respuesta a estrés hiperosmótico es esencial para responder a la acumulación de proteínas mal plegadas (Bicknell, Tourtellotte, & Niwa, 2010; Torres-Quiroz, García-Marqués, Coria, Randez-Gil, & Prieto, 2010). Esta vía, denominada HOG (del inglés, *high osmolarity glycerol*), se activa a través de dos ramas mecanísticamente distintas acopladas a un módulo de MAPK (del inglés, *mitogen-activated protein kinase*) (Figura 4). La rama SLN1, denominada por el osmosensor Sln1, es un sistema de fosforrelevo que en condiciones basales se trans-autofosforila y transfiere ese grupo fosfato a la proteína Ypd1 y posteriormente a Ssk1; en ambientes con hiperosmolaridad se inhibe la transferencia del fosfato, lo que permite que Ssk1 desfosforilado interaccione con la MAPKKK Ssk2, o su parálogo Ssk22, con lo que se induce su autofosforilación. Por otro lado, la rama SHO1 recluta proteínas de señalización

en la membrana plasmática que generan la activación de la cinasa Ste20 y posteriormente de la MAPKKK Ste11. Ambas ramas convergen en la unión y activación de la MAPKK Pbs2 que a su vez interacciona y fosforila a la MAPK Hog1. Hog1 es translocado al núcleo donde activa un programa transcripcional para regular el metabolismo y transporte de osmolitos, principalmente glicerol. Asimismo, Hog1 regula el arresto del ciclo celular e inhibe la traducción para contender contra el incremento de la osmolaridad (Saito & Posas, 2012).

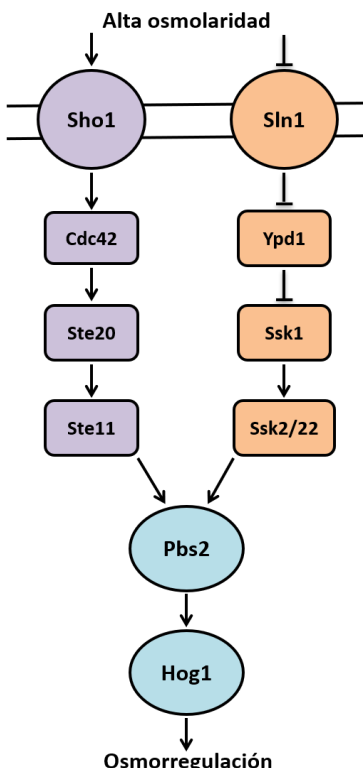


Figura 4: La respuesta al estrés hiperosmótico (HOG).

En condiciones de alta osmolaridad se activan dos ramas acopladas a un módulo de MAPK. La rama SHO1 (marcada en morado) tiene como sensor a Sho1, una proteína de andamiaje que recluta proteínas para la activación de la cinasa Ste20 que a su vez fosforila a la MAPKKK Ste11. La rama SLN1 (marcada en naranja) es activada por el sensor Sln1, parte de un sistema de fosforrelevo que se inhibe en condiciones de hiperosmolaridad y activa a la MAPKKK Ssk2/22. Ambas ramas convergen (marcado en azul) en la activación de la MAPKK Pbs2 que interacciona y fosforila a la MAPK Hog1, la cual regula la síntesis de osmolitos y arresto del ciclo celular, entre otras cosas.

Experimentalmente, la acumulación de proteínas desplegadas y por lo tanto el estrés de RE se puede inducir, entre otras cosas, con el antibiótico Tn, inhibidor de la N -glicosilación. En estas condiciones, los genes *PBS2* y *HOG1* son esenciales, adicionalmente la rama SLN1 es importante pues una mutante *sho1Δ* es resistente a este antibiótico mientras que la cepa *ssk1Δ* es sensible (Bicknell et al., 2010; Torres-Quiroz et al., 2010).

Además, Hog1 requiere su actividad cinasa para contender contra el estrés de RE, pues una mutante de Hog1 catalíticamente inactiva es incapaz de crecer en presencia de Tn, mientras que la activación de Hog1, a través de la fosforilación por la MAPKK Pbs2, no es requerida en condiciones de estrés inducido por Tn. Estos datos en conjunto con la ausencia de localización nuclear de Hog1 sugieren que Hog1 participa en la regulación de blancos extra nucleares en respuesta a la Tn (Torres-Quiroz et al., 2010). En resumen, la actividad de Hog1 es importante para contender contra el estrés de RE, sin embargo, el mecanismo involucrado es, en ciertos pasos, distinto del conocido para estrés hiperosmótico, por lo que resulta importante explorar con mayor profundidad la participación de Hog1 en la respuesta al estrés de RE y de esta manera incrementar nuestro conocimiento sobre alternativas de respuesta a condiciones ambientales dañinas.

JUSTIFICACIÓN

El estrés de RE es una condición asociada al desarrollo de numerosas patologías por lo que los mecanismos celulares de respuesta representan un importante blanco terapéutico; asimismo, la generación de estrés de RE es un paso limitante en procesos industriales como en la producción de proteínas recombinantes. La UPR es la vía canónica de respuesta a estrés de RE. Sin embargo, se ha reportado la participación de otras vías de señalización entre las que se encuentra la vía de respuesta al estrés hiperosmótico o vía de HOG. Es importante identificar y profundizar en el estudio de otros procesos celulares involucrados en esta respuesta y de esta manera conocer nuevos mecanismos alternativos de resistencia al estrés de RE. Una de las estrategias experimentales empleadas para esto es el estudio de interacciones genéticas; este análisis es útil en la determinación de relaciones funcionales entre genes y su posible participación en procesos celulares relacionados. Particularmente, mediante el análisis de supresión por dosis génica se pueden encontrar interactores funcionales como blancos enzimáticos, interactores físicos, modificadores transcripcionales, traduccionales o postraduccionales, entre otras cosas. Por lo anterior, en este trabajo se propuso analizar genes cuya sobreexpresión revierta la sensibilidad de una mutante *hog1Δ* a la Tn y de esta manera encontrar proteínas involucradas en la respuesta al estrés de RE relacionadas con la vía de HOG o independientes de esta.

HIPÓTESIS

Para responder a estrés de RE, Hog1 regula la actividad de proteínas extra nucleares. La búsqueda de supresores que por dosis génica reviertan la sensibilidad de la mutante *hog1Δ* a la Tn permitirá la identificación de nuevas proteínas involucradas en este proceso.

OBJETIVOS

Objetivo general

Identificar genes supresores que por dosis génica reviertan la sensibilidad a la Tn de la mutante *hog1Δ* y analizar su relación con la vía de HOG.

Objetivos específicos

- Identificar genes cuya sobreexpresión revierta la sensibilidad a la Tn de la mutante *hog1Δ*.
- Analizar la supresión en mutantes de otros componentes de la vía HOG y UPR.
- Analizar la participación de estos genes en la respuesta a estrés de RE.
- Estudiar la interacción genética entre *HOG1* y los genes supresores en la resistencia a la Tn.
- Determinar si las proteínas codificadas por los supresores interactúan físicamente con Hog1.
- Analizar la relación entre las interacciones físicas de las proteínas supresoras y Hog1.

METODOLOGÍA

Condiciones de cultivo y cepas

En este trabajo se emplearon levaduras de la especie *Saccharomyces cerevisiae*, isogénicas de la cepa BY4742 o BY4741 (Anexo 1). Las levaduras se crecieron a 30 °C en medio completo YPD (1% extracto de levadura, 2% peptona y 2% glucosa) o medio mínimo sintético SD (0.69% base nitrogenada, 2% glucosa y 20 µg/mL de cada aminoácido necesario para el crecimiento y selección de los plásmidos). En algunos casos la glucosa se intercambió por galactosa o rafinosa, según los requerimientos de cada experimento. Para la selección de las mutantes dobles, el medio de cultivo YPD se adicionó con 100µg/mL del antibiótico nourseotricina.

Las bacterias *Escherichia coli* de la cepa DH5 α se utilizaron para replicar los plásmidos. Las bacterias se crecieron a 37 °C en medio de cultivo LB (1% triptona, 0.5% extracto de levadura y 0.5% NaCl) adicionado con 100µg/mL de ampicilina o 50µg/mL de kanamicina para la selección de los plásmidos, según el caso.

Ensayos de la sensibilidad a estrés

Cultivos líquidos de cada cepa se crecieron en medio selectivo hasta saturación y se ajustaron a una DO₆₀₀=0.5. Alícuotas de 5 diluciones seriales (1:10) de este cultivo se depositaron en medio sólido SD o SGAL suplementado con inductores de estrés. Las cajas se incubaron a 30 °C durante 72 horas y se escanearon.

Para la determinación de las curvas de crecimiento, los mismos cultivos líquidos se ajustaron por triplicado a una DO₆₀₀=0.05 y se crecieron a 30 °C con agitación en cajas de 100 pozos. La DO₆₀₀ se registró cada hora durante 48 horas en un espectrofotómetro de placas (Bioscreen C). El promedio de la DO₆₀₀ de las 3 réplicas se graficó y la tasa de crecimiento se calculó como el valor de la pendiente de una regresión lineal de la fase exponencial.

Ensayo de la búsqueda de los genes supresores de la sensibilidad a la Tn

El ensayo se realizó siguiendo el protocolo ilustrado en la Figura 5. La cepa *hog1 Δ* se transformó con una biblioteca genómica (Jones et al., 2008), compuesta por más de 1000 fragmentos únicos y sobrelapantes del genoma de la cepa FY4 de *S. cerevisiae*.

clonados en el plásmido pGP564 (2μ , LEU2). Las transformantes se plaquearon en medio SD-leu suplementado con 1 μ g/mL de Tn. Posteriormente, se evaluó el crecimiento de cada una de las transformantes en presencia de 0.5 μ g/mL Tn o 1M KCl, seleccionando aquellas resistentes a la Tn y sensibles a KCl. El plásmido de la biblioteca genómica se extrajo de cada una de las transformantes. Bacterias *E. coli* se electroporaron con la extracción para replicar los plásmidos. Este plásmido se empleó para transformar la cepa *hog1Δ* y las nuevas transformantes se evaluaron en presencia de Tn o KCl, seleccionando aquellas resistentes a la Tn. Los extremos de estos plásmidos se secuenciaron con los oligonucleótidos M13 y T3 (Anexo 2) para conocer la región cromosomal clonada en cada uno. Los procedimientos particulares para cada paso se describirán a continuación.

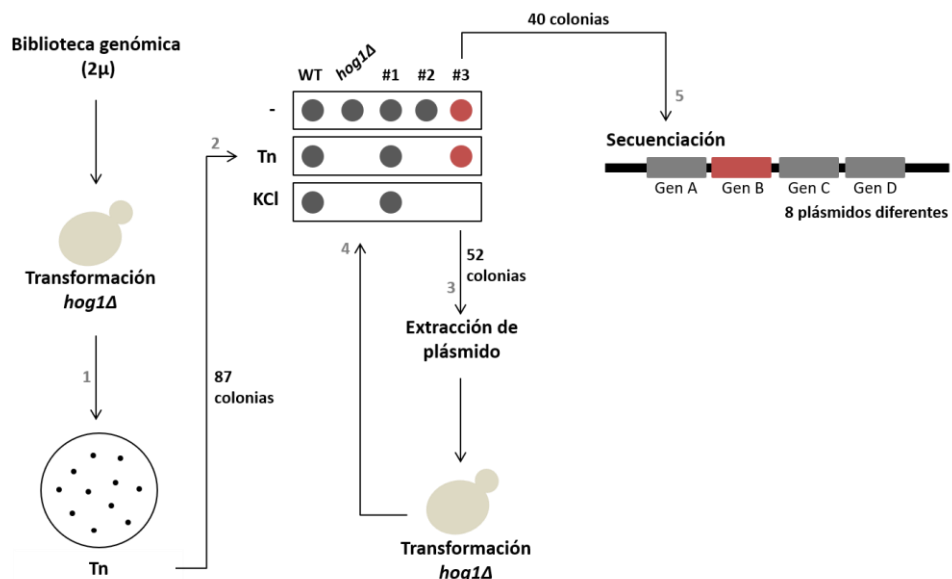


Figura 5: Búsqueda de los genes supresores de la sensibilidad a la Tn.

(1) La cepa *hog1Δ* se transformó con una biblioteca genómica y plaqueó en SD-leu con 1 μ g/mL Tm. (2) Las transformantes se crecieron en 0.5 μ g/mL Tn o 1M KCl y se seleccionaron las resistentes a la Tn y sensibles a KCl (marcadas en rojo). (3) Se extrajo el plásmido de las transformantes seleccionadas. (4) La mutante *hog1Δ* se transformó con los plásmidos extraídos y se repitió el paso de selección. (5) Se secuenció el plásmido de las colonias seleccionadas para conocer la región cromosomal clonada en cada uno.

Transformación de las células

Las levaduras se crecieron en YPD hasta la fase exponencial ($DO_{600}=0.5$), posteriormente se centrifugaron y lavaron con agua y buffer (0.1M TE pH 7.5, 0.1M LiOAc pH 7.5). Las células se resuspendieron en el mismo buffer y una alícuota de estas se mezcló con 10ng de plásmido y 50 μ g de ADN de esperma de salmón. A esta mezcla se agregó buffer (40%PEG, 0.1M TE pH 7.5, 0.1 M LiOAc pH 7.5) e incubó durante 30 minutos a 30

°C. Posteriormente, se agregó DMSO e incubó a 42 °C por 15 minutos. Finalmente, las transformantes se plaquearon en medio selectivo, de acuerdo al plásmido utilizado en cada transformación.

Las bacterias quimiocompetentes se incubaron con 10ng de plásmido durante 30 minutos en hielo. Después se sometieron a un choque térmico a 42°C durante 45 segundos y se agregó LB para recuperar durante 1 hora a 37 °C en agitación. Las transformantes se plaquearon en LB suplementado con 100µg/mL de ampicilina.

Para electroporar, las bacterias se crecieron en LB hasta una DO₆₀₀=0.6, se lavaron tres veces con agua fría y una vez con 10% glicerol frío. Las células se resuspendieron en 10% glicerol y una alícuota de las células se colocó en la celda de electroporación. En el electroporador Micropulser (Biorad) se aplicó un pulso de 2.5kV durante 5 segundos. Posterior al pulso, las bacterias se resuspendieron en LB y se recuperaron por 2 horas a 37 °C. Finalmente, se plaquearon en LB suplementado con 50µg/mL de kanamicina.

Extracción del plásmido de las levaduras

Las transformantes seleccionadas se crecieron hasta saturación en SD-leu. Las células se centrifugaron y lavaron con agua. Posteriormente, se resuspendieron en buffer (2% Triton X-100, 1% SDS, 100 mM NaCl, 10mM Tris pH 8, 1mM EDTA pH 8) y adicionó una mezcla de fenol:cloroformo (1:1 v/v). Las células se rompieron durante 3 minutos con perlas de vidrio. Después, las células se centrifugaron y se recuperó la fase acuosa, que se precipitó con 3M acetato de sodio y 100% etanol frío. Esta mezcla se centrifugó y la pastilla se lavó con 70% etanol. Finalmente, después de centrifugar, la pastilla se resuspendió en agua. Esta extracción se empleó para electroporar bacterias, que se plaquearon en LB con 50µg/mL kanamicina.

Sobreexpresión de los genes

Los ORFs con regiones regulatorias se amplificaron usando los oligonucleótidos marcados en el Anexo 2. Los productos de las PCRs se purificaron con el kit Geneclean y clonaron en el vector pGEM-T Easy (Promega). Los fragmentos insertados se comprobaron por secuenciación con los oligonucleóticos T7 y SP6. Posteriormente, los insertos se subclonaron en el vector Yep352 (2µ, URA3) o pYES2 (P_{GAL}, 2µ, URA3). Los plásmidos se replicaron en bacterias. Bacterias se transformaron con estas clonaciones y se plaquearon en LB con 100µg/mL ampicilina.

Generación de las mutantes nulas

Las mutantes sencillas se obtuvieron de la colección de EUROSCARF. Las mutantes dobles se generaron por recombinación homóloga, interrumpiendo la secuencia codificante de *HOG1* al insertar el gen *NAT1*, de resistencia a nourseotricina. Para hacerlo, se amplificó el gen *NAT1*, a partir del plásmido pAG25, con oligonucleótidos con 40 nt de homología con el locus de *HOG1* (Anexo 2). Las mutantes sencillas se transformaron con el producto de esta PCR y las transformantes se plaquearon en YPD suplementado con 100µg/mL de nourseotricina. Para comprobar las dobles mutantes se extrajo el ADN genómico y se comprobó la integración del gen *NAT1* por PCR y secuenciación.

Ensayo de las interacciones físicas

Las interacciones físicas se determinaron usando el método de complementación bimolecular de la fluorescencia (BiFC). De la colección de Bioneer se obtuvieron los genes (Yor1, Kin1, Kin2, Rer1, Rer2, Nab6 y Ecm13) fusionados al extremo amino de la proteína fluorescente Venus (VN), integrados en la cepa BY4741. Para construir la fusión de Hog1 con el carboxilo de Venus (VC), se amplificó el fragmento del plásmido pFA6a+VC usando oligonucleótidos con extremos con homología para recombinar en el extremo 3' de la región codificante de *HOG1*. La cepa BY4742 WT se transformó con el producto de esta PCR y las transformantes se plaquearon en YPD con 200µg/mL G418. Para co-expresar los dos fragmentos, ambas cepas se aparearon y seleccionaron las células diploides por el crecimiento en SD-lys-met. Las células diploides se crecieron hasta fase exponencial en medio selectivo e incubaron durante 2 horas con 1µg/mL de Tn para inducir estrés de RE. Posteriormente, se fijaron con 3.7% formaldehído durante 15 minutos. La fluorescencia se detectó en el citómetro Attune Acoustic Focusing con el filtro BL2. La intensidad de la fluorescencia se determinó con el software Attune versión 2.1 y el promedio de la intensidad de fluorescencia se normalizó respecto a la detectada en la cepa diploide Hog1VC y WT (Hog1/-).

Construcción de la red de interacción

Los datos de las interacciones reportadas para cada uno de los genes supresores y de Hog1 se obtuvieron de la base de datos BioGRID versión 3.4.144, repositorio de interacciones genéticas y físicas obtenidos mediante diversos ensayos experimentales. Los datos se visualizaron en Cytoscape. Únicamente se analizaron las interacciones físicas. Las

proteínas que interaccionaban con un solo nodo de la red se eliminaron para mejorar la visualización. La red se agrupó empleando la configuración establecida en el elemento “*force-directed layout*”, dentro del software, y la visualización se mejoró manualmente. Los ejes se colorearon de acuerdo al ensayo experimental que apoya esa interacción.

Cuantificación del dolicol

La extracción del dolicol se hizo a partir de 4 gramos de células (peso húmedo). Las levaduras se crecieron en YPD hasta la fase exponencial y se trajeron con 1 μ g/mL Tn durante 2 horas. Los cultivos se centrifugaron y se lavaron con agua. Las células se resuspendieron en agua y se rompieron en vórtex con perlas de vidrio durante 15 ciclos (1min en vórtex y 1 min en hielo). Posteriormente, se agregó una mezcla de cloroformo: metanol (2:1) y se trajeron los lípidos durante 1 hora a temperatura ambiente en agitación. Las mezclas se centrifugaron. La fase orgánica se recuperó y se lavó con 1/5 volumen de 10mM EDTA en 0.9% NaCl y se evaporó en un rotovapor a 55 °C. Los lípidos se resuspendieron en 15% KOH en metanol: agua (10:1) e hirvieron durante 2 horas a 95 °C. Después, los lípidos se trajeron dos veces con una mezcla de éter dietílico y agua utilizando un embudo de separación. La fase orgánica se evaporó y se resuspendió en hexano. Los lípidos se pasaron por una columna de sílica equilibrada con hexano. La columna se lavó con 3% éter dietílico en hexano y la fracción de interés se eluyó con 17% éter dietílico en hexano. La fracción de poliprenoles se evaporó y se resuspendió en 500 μ l de hexano. El análisis de los poliprenoles se hizo por HPLC usando el equipo Waters Alliance e2695/2489/2414. Los extractos se corrieron a 25° con un flujo de 1.2 mL/min en una elución isocrática con 55% metanol, 23% isopropanol y 22% hexano. Los poliprenoles se detectaron con una lámpara UV a 210 nm. Como estándar interno se utilizó Dolicol-18 (18 unidades de isopreno) a una concentración de 1 μ g/ μ l. La concentración de poliprenoles se cuantificó midiendo el área bajo la curva de cada pico de las muestras respecto al área bajo la curva del estándar. La cuantificación se expresó por mg de proteína, cuantificada con el kit BCA Pierce (Thermo Fisher Scientific). Los valores de la cuantificación de cada cepa se graficaron.

RESULTADOS

La rama SLN1 participa en la resistencia a la Tn y no a otros inductores del estrés del RE.

Anteriormente se reportó la participación de la vía de HOG en respuesta a estrés de RE, específicamente, se determinó que la presencia de componentes de la rama SLN1 son esenciales para resistir al antibiótico Tn (Torres-Quiroz et al., 2010). En la Figura 6, se observa que las cepas *hog1Δ*, *pbs2Δ* y *ssk1Δ* tienen un defecto en el crecimiento en presencia de Tn, mientras que son capaces de resistir a una inducción de estrés de RE con 2-DOG (análogo de la glucosa) o DTT (agente reductor). Por el contrario, la ausencia del gen *HAC1*, de la vía UPR, induce una fuerte sensibilidad a cualquier inductor de estrés de RE. De la misma manera, la falta del gen *slt2Δ*, que codifica para la MAPK de la vía de integridad de la pared celular (CWI, del inglés *cell wall integrity*), genera una elevada sensibilidad a cualquier inductor de estrés de RE. Esto sugiere que la participación de la vía de HOG en la respuesta a estrés de RE es un mecanismo específicamente involucrado con el mecanismo de acción de la Tn. A partir de esto, se analizó el papel de Hog1 en respuesta a la Tn, empleando a la cepa *hac1Δ* como un control de sensibilidad a la Tn.

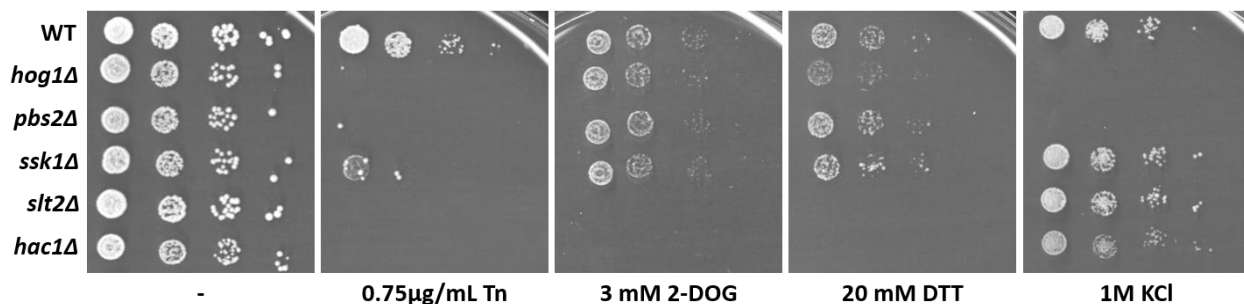


Figura 6: El efecto de la ausencia de los componentes de la rama SLN1 en la resistencia al estrés del RE.

Ensayo de crecimiento en medio sólido de mutantes nulas de componentes de la vía de HOG (*hog1Δ*, *pbs2Δ* y *ssk1Δ*), UPR (*hac1Δ*) y CWI (*slt2Δ*). Las levaduras se crecieron en YPD a una $DO_{600} = 0.05$ y diluciones seriadas (1:10) se depositaron en medio sólido SD con o sin los inductores de estrés marcados en la imagen. Las cajas se incubaron por 72 horas y se escanearon. El crecimiento en KCl (estrés hiperosmótico) se usó como control.

Identificación de los genes supresores de la sensibilidad a la Tn en la mutante *hog1 Δ*

Para profundizar en la participación de Hog1 en la resistencia a la Tn e identificar proteínas y procesos celulares involucrados en esta respuesta, se propuso aislar supresores de la sensibilidad a la Tn, es decir, genes cuya sobreexpresión revirtieran la sensibilidad a la Tn de una mutante *hog1 Δ* y no su sensibilidad a KCl. En este análisis se empleó una biblioteca genómica formada por una colección de más de 1500 plásmidos de sobreexpresión que representa el 95% del genoma de *S. cerevisiae* (Jones et al., 2008). En primer lugar, la cepa *hog1 Δ* se transformó con la biblioteca genómica y las transformantes se plaquearon en cajas con 1 μ g/mL de Tn para aislar aquellas resistentes. En este caso se seleccionaron 87 colonias. Las transformantes se crecieron en Tn y en KCl y se seleccionaron aquellas resistentes al primero y sensibles al segundo. 52 transformantes de las 87 cumplieron con esta condición. A las 52 clonas seleccionadas se les extrajo el plásmido y este se reintrodujo en la mutante *hog1 Δ* para comprobar el fenotipo de resistencia a la Tn y sensibilidad a KCl, recuperando en este caso 40 transformantes. Los plásmidos de estas 40 transformantes se secuenciaron para conocer la región del genoma contenida en cada uno. Con esto se encontró que solamente 8 plásmidos diferentes estaban representados en estas 40 clonas. El nivel de resistencia a la Tn que confieren los 8 plásmidos diferentes y el número de veces que se encontraron en las 40 clonas se muestra en la Figura 7B. Las regiones genómicas tienen un tamaño que va de 9 a 12 kb y están distribuidas en 6 diferentes cromosomas. Es importante notar la diversidad de repetición de cada plásmido; el Sup8 fue aislado 14 veces mientras que Sup70, Sup86 y Sup87 se aislaron una vez cada uno (Figura 7A). Asimismo, el nivel de supresión es heterogéneo en relación a la resistencia a la Tn de la mutante *hog1 Δ* transformada con el plásmido vacío. Los plásmidos Sup8, Sup39 y Sup70 son los que generan mayor supresión mientras que el Sup11 es el supresor más débil (Figura 7A,B).

A

Nombre	Coordenadas cromosomales	Tamaño (bp)	Región cromosomal	Repeticiones	Nivel de supresión
Sup8	II: 702,406-712,203	9,797	<i>YBR241C</i> <i>YBR242C</i> <i>ALG7</i> <i>GPX2</i> <i>ISW1</i> <i>RRT2</i>	14	+++++
Sup39	XI: 238,339-250,650	12,311	<i>AAT1</i> <i>SEG2</i> <i>GFA1</i> <i>APE1</i> <i>YKL102C</i> <i>HSL1</i>	13	+++++
Sup47	VII: 1,050,372-1,061,331	10,959	<i>PXR1</i> <i>YOR1</i> <i>BGL2</i> <i>YGR283C</i> <i>ERV29</i>	3	+++
Sup11	XIII: 28,455-38,857	10,402	<i>ND11</i> <i>YML119W</i> <i>NGL3</i> <i>NAB6</i> <i>YML116W-A</i> <i>ATR1</i>	5	++
Sup31	XII: 330,854-341,756	10,911	<i>IOC2</i> <i>KIN2</i> <i>HRT3</i> <i>CHA4</i> <i>ICT1</i> <i>MIM2</i>	2	+++
Sup70	II: 239,720-249,439	9,719	<i>NTH2</i> <i>RER2</i> <i>COO1</i> <i>GPI18</i> <i>RCR1</i> <i>UGA2</i> <i>DSF2</i>	1	+++++
Sup86	II: 133,290-141,740	8,450	<i>PSY4</i> <i>COR1</i> <i>YBL044W</i> <i>ECM13</i> <i>FU11</i> <i>PRE7</i>	1	++
Sup87	III: 111,555-122,059	10,504	<i>YCL002C</i> <i>RER1</i> <i>YCL001W-A</i> <i>YCL001W-B</i> <i>YCR001W</i> <i>CDC10</i> <i>MRPL32</i> <i>YCP4</i> <i>CIT2</i>	1	++

B

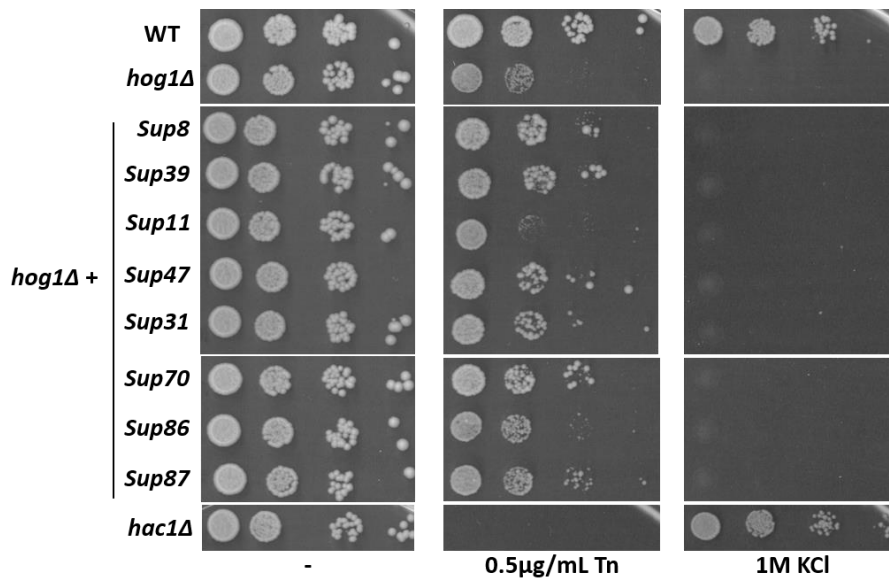


Figura 7: La supresión de la sensibilidad a la Tn de la mutante *hog1Δ* por los plásmidos de la biblioteca genómica.

A: Representación esquemática de los plásmidos supresores de la sensibilidad a la Tn de la cepa *hog1Δ*. Las coordenadas cromosomales y el tamaño se identificaron por secuenciación. Se muestra la orientación de cada gen y aquellos marcados en rojo son los causantes de la supresión a la Tn. Las repeticiones indican el número de veces que se aisló ese plásmido y el nivel de supresión es la resistencia a la Tn que generan respecto a la mutante *hog1Δ* con plásmido vacío, determinado por el crecimiento de cada transformante en presencia de Tn (inciso B).

B: Ensayo de crecimiento en medio sólido de la mutante *hog1Δ* transformada con plásmido vacío o con los 8 plásmidos aislados. Las levaduras se crecieron en YPD a una D_{600} = 0.05 y diluciones seriales (1:10) se depositaron en medio sólido SD con o sin los inductores de estrés marcados en la imagen. Las cajas se incubaron por 72 horas y se escanearon. Las cepas WT y *hac1Δ* se utilizaron como control de resistencia y sensibilidad a la Tn, respectivamente.

Cada fragmento genómico clonado en los plásmidos contiene en promedio 6 ORFs (Figura 7A). Para identificar al gen responsable de la supresión, se subclonó cada ORF, de cada plásmido, de manera independiente en el vector de sobreexpresión YEp352. De esta manera se identificaron 8 genes capaces de suprimir la sensibilidad a la Tn y no la sensibilidad a KCl de la mutante *hog1Δ* (Figura 8). El nivel de supresión es variable, determinado tanto por el crecimiento en medio sólido como por la tasa de crecimiento en cultivos líquidos. Todos los genes inducen resistencia a la Tn en la mutante *hog1Δ*, lo que implica que todos se comportan como supresores. El supresor más débil es el gen *ECM13* el cual genera un crecimiento 0.4 veces mayor y el supresor más fuerte es el gen *ALG7* que genera un crecimiento aproximadamente 5 veces mayor (Figura 8). El gen *KIN1* no se identificó como supresor en este ensayo, sin embargo, también se probó por ser parálogo del gen *KIN2*. Se encontró que *KIN1* causa el mismo efecto de supresión de la sensibilidad a la Tn que *KIN2*.

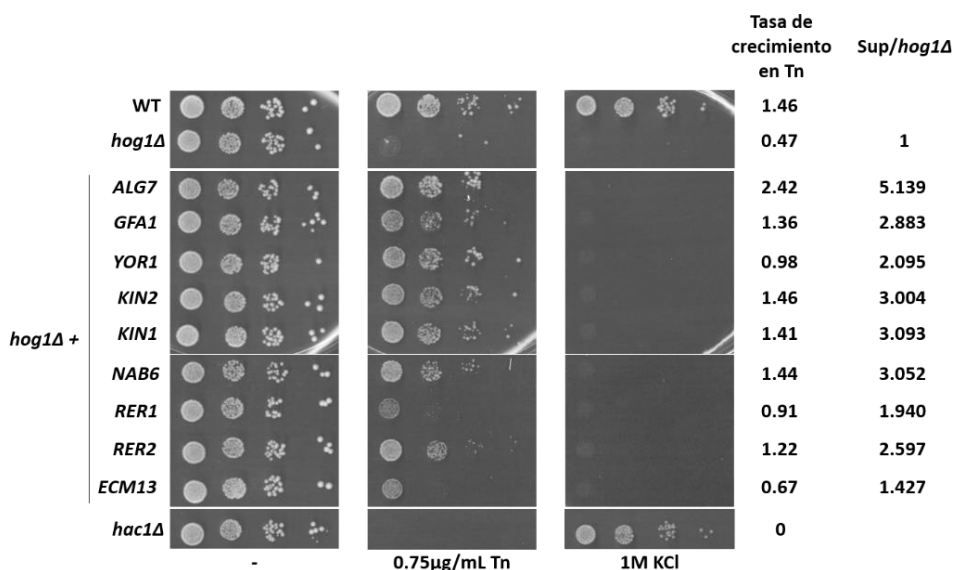


Figura 8: La supresión de la sensibilidad a la Tn de la mutante *hog1Δ* por la sobreexpresión de los genes aislados.

Los genes mostrados en la figura se sobreexpresaron en el plásmido YEp352 y su capacidad de supresión a la Tn se evaluó en la mutante *hog1Δ*. Se muestra un ensayo de crecimiento en medio sólido de la mutante *hog1Δ* transformada con plásmido vacío o con los genes identificados en el ensayo. Las levaduras se crecieron en YPD a una $DO_{600} = 0.05$ y diluciones seriadas (1:10) se depositaron en medio sólido SD con o sin los inductores de estrés marcados en la imagen. Las cajas se incubaron por 72 horas y se escanearon. Las cepas WT y *hac1Δ* se utilizaron como controles de resistencia y sensibilidad a la Tn, respectivamente. La tasa de crecimiento en Tn se calculó a partir de la pendiente de la fase exponencial determinada en cultivos líquidos medidos en espectrofotómetro. La relación Sup/*hog1Δ* se calculó de acuerdo a la tasa de crecimiento de las transformantes con los genes supresores respecto a la mutante *hog1Δ* con plásmido vacío.

Los genes supresores se clasifican como generales o específicos de la vía de HOG

Posteriormente, para determinar si el mecanismo de supresión es específico para la vía de HOG, se probó el efecto de la sobreexpresión de estos genes en la sensibilidad a la Tn de las mutantes *pbs2Δ*, *ssk1Δ*, *hac1Δ* y *slt2Δ*. Como se observa en la Figura 9, la sobreexpresión de cada uno de los 8 genes suprimió la sensibilidad a la Tn de las mutantes *pbs2Δ* y *ssk1Δ*. Mientras que únicamente tres supresores (*ALG7*, *GFA1* y *YOR1*) revirtieron la sensibilidad a la Tn de las mutantes *slt2Δ* y *hac1Δ*, indicando que estos tienen un mecanismo general de supresión. Por lo tanto, clasificamos a los genes *ALG7*, *GFA1* y *YOR1* como supresores generales y a los genes *NAB6*, *KIN1*, *KIN2*, *RER1*, *RER2* y *ECM13* como supresores específicos. Los supresores generales son los más representados en el ensayo, pues 75% (30 de 40) de los genes aislados son supresores generales, mientras que los supresores específicos representan el 15% restante (10 de 40) (Figura 9). Asimismo, la sobreexpresión de los genes supresores no afecta la sensibilidad a estrés hiperosmótico de la mutante *hog1Δ*.

Las características de cada supresor se resumen en la Tabla 1. Los supresores generales participan en mecanismos de resistencia a la Tn. De manera particular, el gen *ALG7* codifica para la enzima UDP-*N*-acetilglucosamina fosfotransferasa que cataliza el primer paso de la *N*-glicosilación, adición de una molécula de *N*-acetil glucosamina al dolícol fosfato (Barnes, Hansen, Holcomb, & Rine, 1984; Rine, Hansen, Hardeman, & Davis, 1983). Esta enzima es inhibida específicamente por la Tn. El gen *GFA1* codifica para la enzima glutamina-fructosa-6-fosfato amidotransferasa, que está involucrada tanto en la síntesis de *N*-acetilglucosamina como en la síntesis de quitina. Esta última es un componente esencial de la pared celular de la levadura (Bowman & Free, 2006; Watzele & Tanner, 1989). El gen *YOR1* codifica para un transportador ABC (del inglés, *ATP-binding cassette*) localizado en la membrana plasmática y que participa en la desintoxicación celular (Katzmann et al., 1995; Rogers et al., 2001).

Por su parte, los supresores específicos participan en una variedad de funciones relacionadas con el procesamiento de proteínas. El gen *NAB6* codifica para una proteína de probable unión a ARN mensajeros. Esta proteína está relacionada con el metabolismo de los ARN mensajeros que codifican para componentes de la pared celular (Abruzzi et al., 2007). Los genes *KIN2* y *KIN1* codifican para Ser/Thr cinasas involucradas en la exocitosis y en la polarización celular (Elbert, Rossi, & Brennwald, 2005; Yuan, Nie, He, Jia, & Gao, 2016). El gen *RER2* codifica para una *cis*-PT involucrada en la vía de síntesis de dolícol, el

cual es esencial en la *N*-glicosilación (Sato et al., 1999). El gen *RER1* codifica para una proteína involucrada en el transporte vesicular retrógrado y en la retención de proteínas en el lumen del RE (Nishikawa & Nakano, 1993; Sato, Sato, & Nakano, 1997). El producto del gen *ECM13* no se ha caracterizado, pero se ha reportado su probable participación en la respuesta a daño de ADN y a la biosíntesis de pared celular (García et al., 2004; Lussier et al., 1997).

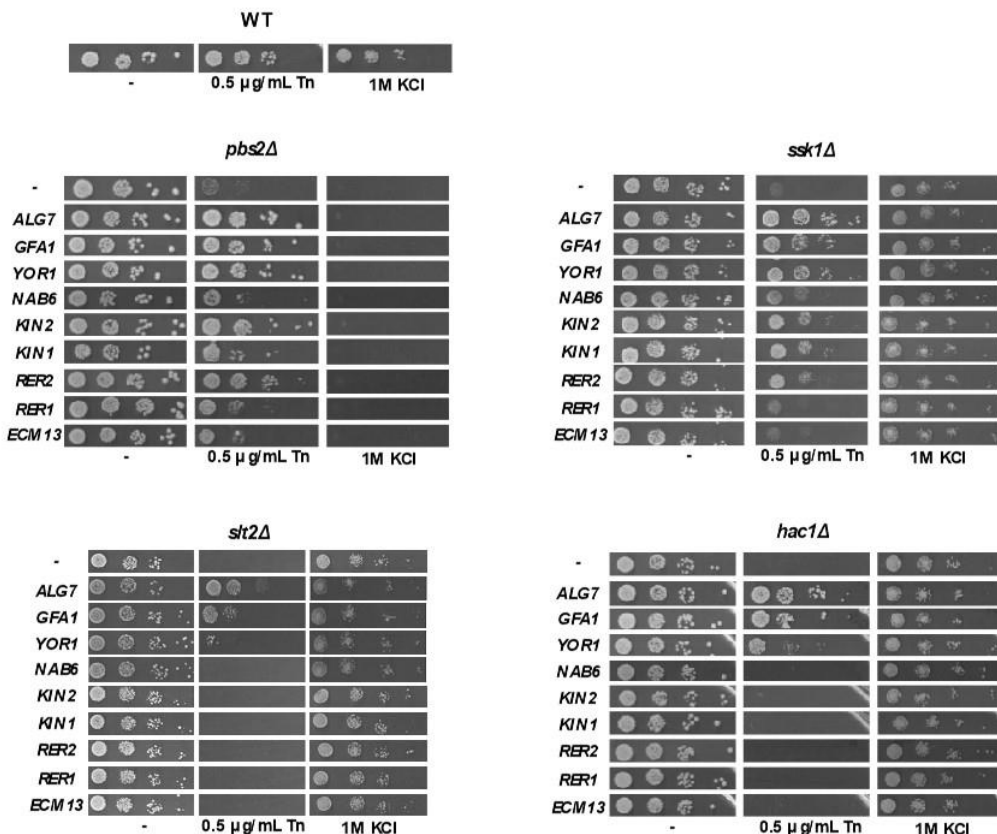


Figura 9: El efecto de la sobreexpresión de los genes supresores en las mutantes de distintas vías de señalización.

Los genes supresores se evaluaron en las mutantes *pbs2Δ*, *ssk1Δ*, *hac1Δ* y *slt2Δ*. Se muestran ensayos de crecimiento en medio sólido de las mutantes transformadas con plásmidos que contienen los genes supresores o con el vector vacío. Las levaduras se crecieron en YPD a una $OD_{600}=0.05$ y diluciones seriadas (1:10) se depositaron en medio sólido SD con o sin inductores de estrés marcados en la imagen. Las cajas se incubaron por 72 horas y se escanearon. La cepa WT se utilizó como control de resistencia a estrés.

Gen	Función molecular	Proceso biológico	Componente celular
<i>ALG7</i>	UDP-N-acetil glucosamina fosfotransferasa	N-glicosilación	Retículo endoplásmico
<i>GFA1</i>	Glutamina-fructosa-6-fosfato amidotransferasa	Biosíntesis de pared celular	Desconocido
<i>YOR1</i>	Transportador con actividad ATPasa (familia ABC)	Transporte de xenobióticos	Membrana plasmática
<i>NAB6</i>	Proteína putativa de unión a mRNA	Desconocido (Metabolismo de mRNAs de biosíntesis de pared celular)	Citoplasma
<i>KIN2</i>	Ser/Thr cinasa	Exocitosis Polarización celular Respuesta a estrés de RE	Membrana plasmática
<i>KIN1</i>	Ser/Thr cinasa	Exocitosis Polarización celular Respuesta a estrés de RE	Membrana plasmática
<i>RER2</i>	Cis-preniltransferasa	N-glicosilación	Retículo endoplásmico
<i>RER1</i>	Desconocida	Transporte vesicular ER-Golgi/Golgi-ER Retención de proteínas en lumen del RE	Vesículas COPI Vacuola
<i>ECM13</i>	Desconocida	Desconocido (Respuesta a daño de DNA; biosíntesis de pared celular)	Desconocida

Tabla 1: Las características funcionales y localización de los genes supresores de la sensibilidad a la Tn.

La información se obtuvo de las bases de datos *Saccharomyces* Genome Database y Gene Ontology database. Los colores indican la clasificación de los supresores, en rojo están marcados los supresores generales mientras que en azul se indican los supresores específicos.

La inactivación de algunos genes supresores afecta la resistencia a la Tn

Para saber si las proteínas codificadas por los genes supresores están involucradas con la respuesta a estrés de RE, se evaluó el crecimiento de las mutantes nulas de estos genes en presencia de Tn (Figura 10). Los genes *ALG7*, *GFA1* y *RER2* no se incluyeron dentro del análisis ya que son genes esenciales y la falta de ellos causa letalidad. Como se muestra en la Figura 10, la ausencia de los genes *YOR1*, *NAB6*, *KIN2* y *RER1* induce sensibilidad a altas concentraciones de Tn (a partir de 1µg/mL). Mientras que las mutantes *kin1Δ* y *ecm13Δ* tienen un fenotipo de resistencia a la Tn parecido a una cepa silvestre. Particularmente, la mutante *kin1Δ* es menos sensible a la Tn que la mutante *kin2Δ*, sugiriendo que estos genes parálogos pueden participar de manera distinta en esta respuesta. También se observó que ninguna de las mutante evaluadas es sensible a estrés hiperosmótico.

Asimismo, se evaluó la interacción epistática de cada supresor con *HOG1* por medio del crecimiento en Tn de dobles mutantes. Como puede observarse en la Figura 10, las mutantes dobles de *hog1Δ* con *yor1Δ*, *nab6Δ*, *kin2Δ* y *kin1Δ* son más sensibles a la Tn que la mutante nula sencilla *hog1Δ*, sugiriendo que estos genes participan de manera independiente a Hog1 para responder a la Tn. En cambio, las mutantes dobles *hog1Δrer1Δ* y *hog1Δecm13Δ* no presentan cambios en la sensibilidad a la Tn respecto a la mutante *hog1Δ*, indicando que podrían formar parte de la vía de HOG en la respuesta a la Tn.

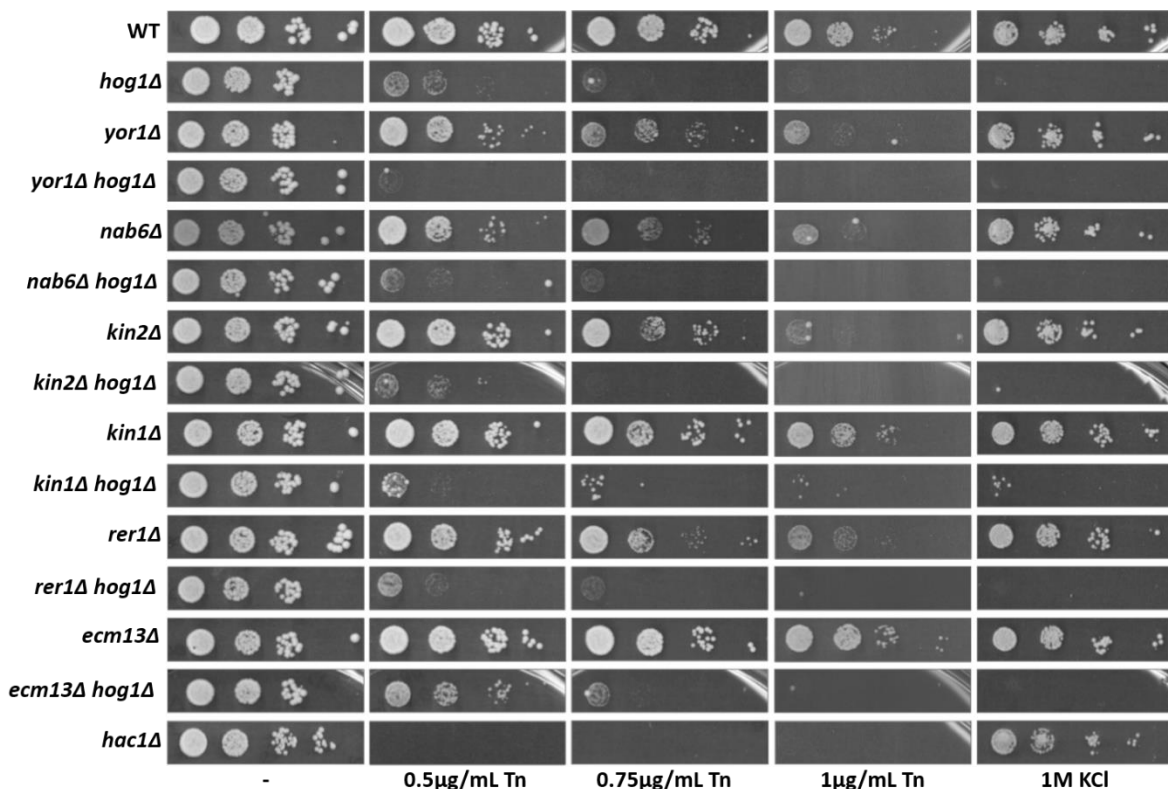


Figura 10: El efecto de la inactivación de los genes supresores en la sensibilidad a la Tn.

El crecimiento de las mutantes sencillas y dobles marcadas en la imagen se evaluó en presencia de distintas concentraciones de Tn. Las levaduras se crecieron en YPD a una $DO_{600} = 0.05$ y diluciones seriadas (1:10) se depositaron en medio sólido SD con o sin inductores de estrés marcados en la imagen. Las cajas se incubaron por 72 horas y se escanearon. Las cepas WT y *hac1Δ* se utilizaron como control de resistencia y sensibilidad a la Tn, respectivamente.

Los genes supresores no son interactores físicos de Hog1

Uno de los mecanismos probables de supresión es a través de interacciones físicas, es decir, los genes supresores pueden codificar para proteínas que interaccionan directamente con Hog1 o que forman parte de un mismo complejo de señalización. Debido a que los genes supresores encontrados no codifican para interactores conocidos

de Hog1, se propuso evaluar si existe interacción física en condiciones de estrés de RE. Para eso se realizó un ensayo de BiFC que consiste en fusionar dos proteínas de interés a cada fragmento de la proteína fluorescente Venus. Si las proteínas interactúan físicamente los fragmentos se aproximarán y esto permitirá la reconstitución de la proteína Venus y por lo tanto la emisión de fluorescencia. Las fusiones de las proteínas supresoras con VN se obtuvieron de la colección Bioneer y Hog1 se fusionó con el fragmento VC. Como se muestra en la Tabla 2, tanto en condiciones basales como en presencia de Tn no se detectó interacción entre estas proteínas, sin embargo, se pudo detectar una ligera interacción entre Hog1-Kin2 y Hog1-Rer2 en condiciones basales, por lo que sería conveniente comprobar la interacción por otros métodos experimentales ya que existe la posibilidad de que se requieran componentes intermediarios para formar complejos entre estas proteínas.

Fracción de Venus		Interacción relativa (respecto a Hog1/control)	
VC	VN	-Tn	+Tn
Hog1	-	1.00	1.00
	Ssb2	0.92	1.04
	Gis2	0.95	0.58
	Yor1	1.07	0.64
	Kin1	0.89	0.80
	Kin2	1.10	0.76
	Rer1	0.99	0.54
	Rer2	1.34	0.79
	Nab6	1.01	0.89
	Ecm13	1.05	0.69

Tabla 2: La evaluación de las interacciones físicas entre Hog1 y los supresores específicos.

La interacción física se evaluó mediante el ensayo BiFC. La interacción relativa es la intensidad de fluorescencia detectada en el ensayo de cada par de proteínas respecto a la fluorescencia detectada en la cepa Hog1-. Las células se crecieron en medio selectivo hasta $DO_{600}=0.5$ y se incubaron durante 2 horas con 1 μ g/mL de Tn o en ausencia de Tn. El ensayo se realizó de acuerdo a lo descrito en metodología, n=3.

Los supresores forman una red de interacción con Hog1

Ya que no se detectaron interacciones directas entre las proteínas supresoras y Hog1, se propuso determinar si los genes supresores participan en procesos celulares relacionados con la respuesta a estrés o si tienen interacciones reportadas con componentes de otras vías de señalización involucradas en la misma respuesta. Para hacerlo, se construyó una red de interacciones físicas a partir de datos obtenidos de

BioGRID, una base de datos con información sobre interacciones físicas recopiladas de una variedad de ensayos a baja y gran escala y a través de diferentes métodos experimentales. La red obtenida se muestra en la Figura 11A. En esta red se puede observar que los supresores Kin1, Kin2, Rer2, Gfa1 y Nab6 interactúan con Hog1 a través de un intermediario; para Kin1, Rer2 y Gfa1 el intermediario es Ssb2, una chaperona citoplásmica de la familia Hsp70 involucrada en el plegamiento de proteínas citosólicas, mientras que Rer2 interacciona con Hog1 a través de Gis2, una proteína de unión a ARN presente en gránulos de estrés y cuerpos de procesamiento. Por esta observación, se evaluó el efecto de la ausencia de Ssb2 y Gis2, nodos importantes de la red, en la respuesta a la Tn. Las mutantes *ssb2Δ* y *gis2Δ* se crecieron en presencia de Tn, como se muestra en la Figura 11A, y no se detectó sensibilidad a este inductor de estrés, sin embargo, la sobreexpresión de los genes supresores en estas mutantes causa, en todos los casos, una mayor resistencia a la Tn, lo que refuerza la relación que existe entre estos genes supresores y la respuesta a estrés de RE. También, como se observa en los ensayos de supresión en las mutantes de la vía de HOG, los supresores *RER1* y *ECM13* generan una supresión débil mientras que el resto de los genes son supresores fuertes.

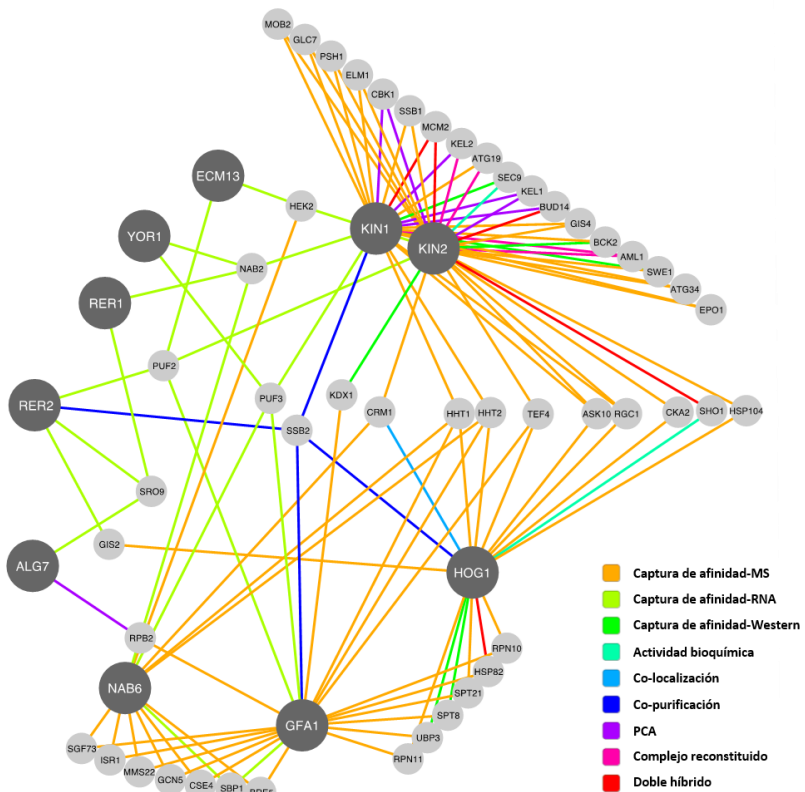
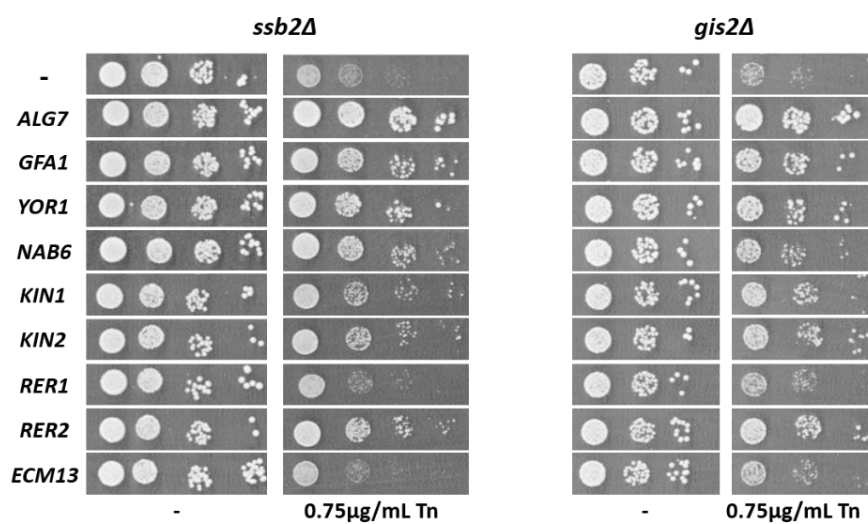
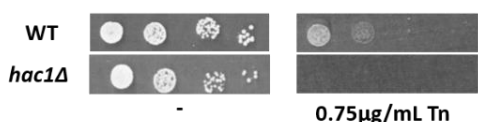
A**B**

Figura 11: La red de interacción entre Hog1 y los genes supresores

A: Los datos de las interacciones físicas de Hog1 y los supresores se obtuvieron de BioGRID y se visualizaron en Cytoscape para construir una red de interacciones. En gris oscuro se marcan los supresores y en gris claro los interactores físicos de ellos. Las proteínas con únicamente una interacción se eliminaron de la red para mejorar la visualización. Los ejes están marcados de acuerdo al método experimental empleado para obtener los datos.

B: Las mutantes nulas de los genes *SSB2* y *GIS2*, nodos centrales de la red, se evaluaron en presencia de Tn, así como el efecto que tiene la sobreexpresión de los supresores sobre estas mutantes en respuesta a la Tn. Se muestran ensayos de crecimiento en medio sólido. Las levaduras se crecieron en YPD hasta una $\text{DO}_{600}=0.05$ y diluciones seriales (1:10) se depositaron en medio sólido SD con o sin inductores de estrés marcados en la imagen. Las cajas se incubaron por 72 horas y se escanearon. Las cepas WT y *hac1Δ* se utilizaron como controles de resistencia y sensibilidad a la Tn, respectivamente.

La síntesis de dolicol es un proceso importante para responder a la Tn

El supresor Rer2 codifica para una *cis*-PT involucrada en la síntesis de dolicoles con 11 a 15 unidades de isopreno. Este es un lípido esencial en el proceso de la *N*-glicosilación, sin embargo, la sobreexpresión de este gen genera una supresión de la sensibilidad a la Tn en únicamente mutantes pertenecientes a la vía de HOG, aun cuando está involucrado en procesos directamente relacionados con la inhibición de la Tn. Debido a esto, se propuso analizar con mayor profundidad el mecanismo de supresión, para eso se evaluó el efecto de la sobreexpresión del gen *SRT1* en la sensibilidad a la Tn. Srt1 es otra *cis*-PT presente en *S. cerevisiae*, cuya función es la síntesis de dolicoles más largos por la condensación de entre 18 a 23 unidades de isopreno. Como se observa en la Figura 12A, la sobreexpresión del gen *SRT1* suprime la sensibilidad a la Tn de las mutantes *hog1Δ* y *pbs2Δ* y no la sensibilidad de la mutante *hac1Δ*, lo que confirma que la síntesis de dolicol es importante para la resistencia a la Tn.

La molécula FPP es precursor para la síntesis de dolicol, ergosterol y otras moléculas importantes en la célula. La síntesis de ergosterol comienza por la acción de la enzima Erg9. Para comprobar si la síntesis de dolicol es importante para la resistencia a la Tn, se sobreexpresó el gen *ERG9* en la mutante *hog1Δ*, con el objetivo de incrementar el uso de FPP en la síntesis de ergosterol y con esto reducir la disponibilidad de esta molécula para la síntesis de dolicol e indirectamente disminuir la cantidad de dolicol en la célula. En la Figura 12B se puede observar que la sensibilidad a la Tn de la mutante *hog1Δ* aumenta ligeramente cuando se sobreexpresa *ERG9*, lo que confirma que la resistencia a la Tn está relacionada con la producción de dolicol.

Por la observación anterior se propuso evaluar el efecto de la Tn y la ausencia de Hog1 en la producción de dolicol. Para hacerlo, se cuantificó el contenido de dolicol en las levaduras a través de cromatografía HPLC, específicamente en la cepa silvestre y en la mutante *hog1Δ*, sin y con la sobreexpresión de *RER2*, tanto en ausencia como en presencia de Tn (Figura 12C). En todas las cepas y condiciones se detectó un pico de poliprenoles en el tiempo de 1.4 minutos, así como un pico a los 3.1 minutos que corresponde al estándar Dolicol-18. Como se observa en la gráfica, en la cepa silvestre la concentración de dolicol incrementa cerca de 2 veces en respuesta Tn. En cambio, este incremento no se observa en la mutante *hog1Δ*, en la cual la concentración de dolicol es similar en ambas condiciones. Adicionalmente, la sobreexpresión de *RER2* en la mutante *hog1Δ* incrementa significativamente la concentración de dolicol en ambas condiciones. Con los datos anteriores podemos concluir que la síntesis de dolicol en la mutante *hog1Δ* no aumenta significativamente en presencia de Tn. Esto sugiere que la sensibilidad a la Tn de una mutante *hog1Δ* se puede explicar parcialmente por la deficiencia en la síntesis de dolicol, la cual puede ser revertida por la sobreexpresión de Rer2.

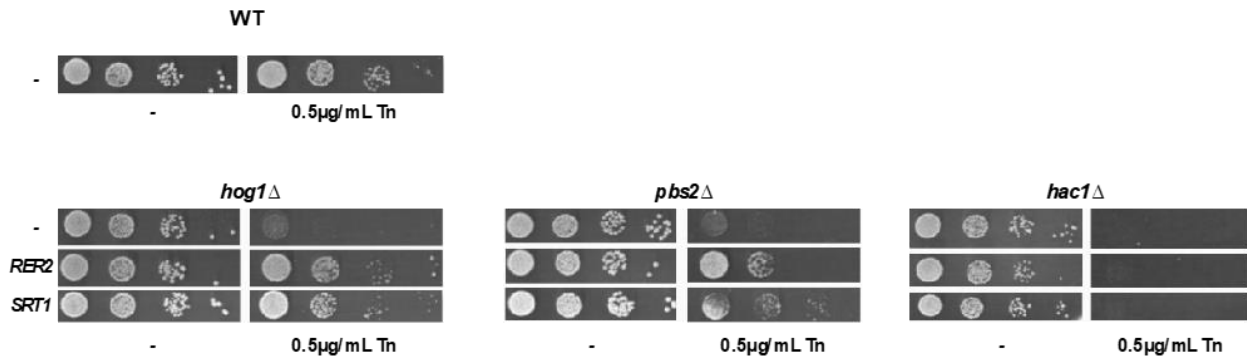
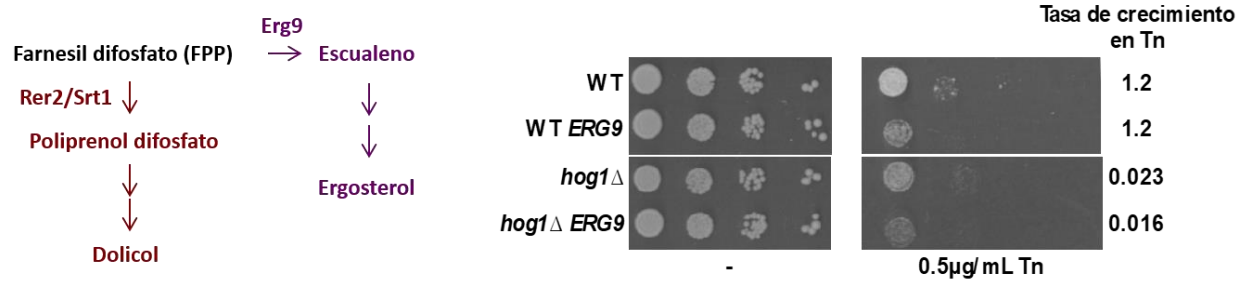
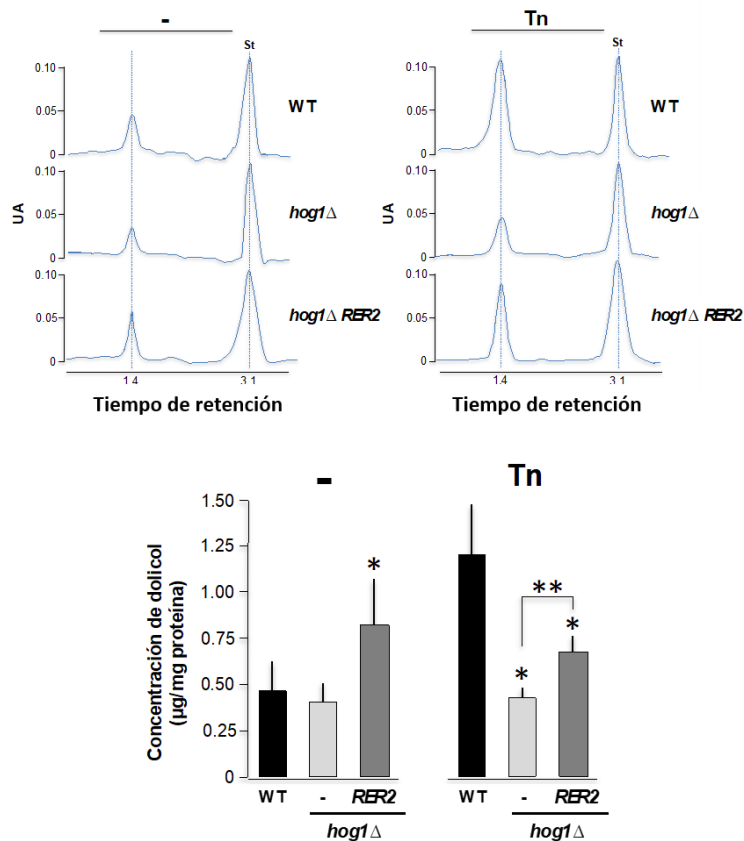
A**B****C**

Figura 12: El efecto de la modificación de la síntesis de dolicol en la resistencia a la Tn

A: Se evaluó el efecto de la sobreexpresión de las dos *cis*-preniltransferasas Rer2 y Srt1 sobre la sensibilidad a la Tn de las mutantes *hog1Δ*, *pbs2Δ* y *hac1Δ*. Se muestran ensayos de crecimiento en medio sólido. Las levaduras se crecieron en SRAF hasta una $DO_{600} = 0.05$ y diluciones seriales (1:10) se depositaron en medio sólido SGAL con o sin inductores de estrés marcados en la imagen. Las cajas se incubaron por 72 horas y se escanearon. La cepa WT se utilizó como control de resistencia a la Tn.

B: Se evaluó el efecto de la sobreexpresión del gen *ERG9* sobre la sensibilidad a la Tn de las mutantes WT y *hog1Δ*. Se muestran ensayos de crecimiento en medio sólido. Las levaduras se crecieron en SRAF hasta una $DO_{600} = 0.05$ y diluciones seriales (1:10) se depositaron en medio sólido SGAL con o sin inductores de estrés marcados en la imagen. Las cajas se incubaron por 72 horas y se escanearon. La cepa WT se utilizó como control de resistencia a la Tn.

C: Análisis del dolicol celular por HPLC. El dolicol se extrajo de las cepas WT, *hog1Δ* y *hog1Δ* sobreexpresando *RER2*, en ausencia y presencia de 1 μ g/mL de Tn, y se detectó a 210 nm por HPLC. Como estándar se empleó 1 μ g/ μ L de dolicol-18. La cuantificación del dolicol se hizo a partir del área bajo la curva del pico del tiempo 1.4 minutos respecto al área bajo la curva detectada en el estándar. La concentración se normalizó respecto a mg de proteína. Se graficó el promedio de 3 réplicas.

DISCUSIÓN

Para responder a estrés hiperosmótico Hog1 regula diversos procesos celulares como son metabolismo, expresión de genes, traducción y progresión del ciclo celular (Saito & Posas, 2012). En este trabajo se describe una estrategia que nos acerca al entendimiento de la participación de esta MAPK en el estrés de RE (Figura 13). Anteriormente se ha reportado la participación de Hog1 en la respuesta a estrés de RE (Bicknell et al., 2010; Torres-Quiroz et al., 2010), sin embargo, se desconoce el mecanismo de resistencia involucrado en este. La presencia de Hog1, así como su actividad cinasa para activar blancos parece ser importante para la resistencia a la Tn, sin embargo, no se ha detectado fosforilación de Hog1 ni su translocación al núcleo en respuesta a este antibiótico (Torres-Quiroz et al., 2010). Las mutantes de algunos componentes de la rama SLN1 son sensibles a la Tn y no a otros inductores de estrés de RE, lo que podría sugerir que además de su participación en estrés hiperosmótico, estas proteínas podrían estar relacionadas con procesos de modificación de proteínas en el citoplasma y/o en la membrana plasmática.

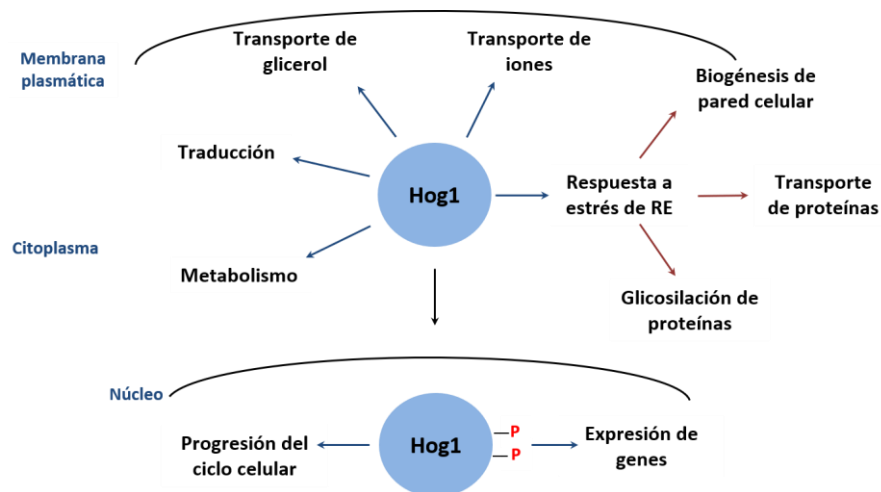


Figura 13: Las funciones celulares de Hog1 en respuesta al estrés.

La MAPK Hog1 regula procesos citosólicos y nucleares para responder a condiciones de estrés (flechas azules). En este trabajo se reportó la participación de Hog1 en procesos celulares involucrados en la respuesta a estrés de RE (flechas rojas).

Para profundizar en la participación de Hog1 en la resistencia a la Tn se buscaron supresores que por dosis génica fueran capaces de revertir la sensibilidad a la Tn de la mutante *hog1Δ*. La identificación de genes supresores de cierto fenotipo es útil en la caracterización de componentes funcionales involucrados en un proceso. Estos supresores

pueden estar relacionados con vías de señalización paralelas, complejos enzimáticos, regulación transcripcional o hasta modificar a la proteína de interés para desencadenar una respuesta (Prelich, 2012). Mediante la estrategia diseñada en este trabajo se identificaron supresores que participan en un número limitado de procesos celulares: glicosilación de proteínas (Rer2, Srt1 y Alg7), biogénesis de la pared celular (Nab6 y Ecm13), transporte de proteínas (Rer1, Kin1 y Kin2) y desintoxicación celular (Yor1). Esto sugiere que Hog1 tiene funciones pleiotrópicas y que de alguna manera regula diferentes procesos para generar una respuesta adecuada a la Tn (Figura 14).

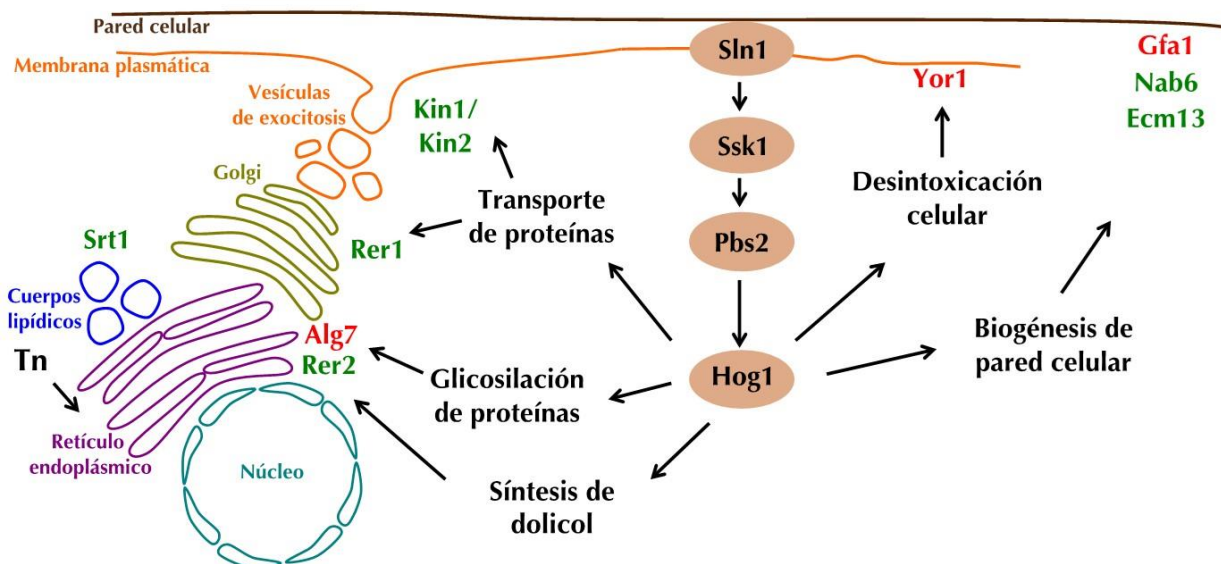


Figura 14: Los supresores de la sensibilidad a la Tn participan en limitados procesos celulares.

Resumen gráfico de los datos obtenidos en este trabajo, la resistencia a la Tn está regulada por la rama SLN1 de la vía de HOG, donde la activación de HOG regula proteínas involucradas en transporte y glicosilación de proteínas, biogénesis de pared celular y desintoxicación celular. En la imagen se resumen los supresores encontrados en el estudio y los procesos celulares en los que participan. En rojo están marcados los supresores generales y en verde se marcan los supresores específicos.

Como se mencionó anteriormente, el ensayo permitió encontrar genes involucrados en el mecanismo de acción de la Tn, estos supresores fueron los más representados, al encontrarlos en 75% de los casos. La detección de este tipo de supresores indica que la estrategia experimental fue la adecuada. Por ser supresores generales, la sobreexpresión de *ALG7*, *GFA1* y *YOR1* revierten la sensibilidad a la Tn tanto de mutantes de la vía de HOG como de mutantes de la UPR y de la homeostasis de pared celular como son, *hac1Δ* y *slt2Δ*, respectivamente. *Alg7* es la enzima UDP-N-acetilglucosamina fosfotransferasa que cataliza el primer paso de la N-glicosilación

(Barnes et al., 1984; Rine et al., 1983). La Tn es inhibidor competitivo de esta enzima ya que tiene una estructura similar al sustrato de la enzima, la *N*-acetilglucosamina (Figura 2B). La sobreexpresión de esta proteína probablemente titula a la Tn pues no existe el suficiente inhibidor para ocupar todos los sitios de las enzimas presentes. Por otro lado, Gfa1 está involucrada en la síntesis de glucosamina-6-fosfato, precursor de la *N*-acetil glucosamina (Watzele & Tanner, 1989). De la misma manera, la sobreexpresión de esta proteína genera un exceso del sustrato canónico de Alg7, el cual compite con la Tn. Finalmente, Yor1 es un transportador de xenobióticos que probablemente exporta Tn al exterior de la célula y disminuye su concentración en el interior de la célula, evitando su acción (Katzmann et al., 1995; Rogers et al., 2001).

Los supresores específicos, aquellos cuya sobreexpresión revierten exclusivamente la sensibilidad de las mutantes de la vía de HOG, están involucrados con diversos procesos celulares. Estos supresores podrían estar formando complejos extra-nucleares con las proteínas de la rama SLN1 y regular funciones citosólicas para responder a la Tn. Esta hipótesis se apoya en la observación de que una versión de Hog1 que está permanentemente anclada a la membrana plasmática genera resistencia a la Tn (García-Marqués, Randez-Gil, & Prieto, 2015). Dentro de los supresores específicos se encontraron a los genes *KIN1*, *KIN2* y *RER1*, que están involucrados en el transporte de proteínas. Los parálogos *KIN1/KIN2* son cinasas que pertenecen a la familia Snf1 del grupo de cinasas II dependientes de Ca^{2+} /calmodulina (Elbert et al., 2005). Regulan la estructura del citoesqueleto y de la pared celular durante la gemación, también están involucradas en la secreción y en la polarización celular. Estas proteínas se localizan en la membrana plasmática y en los sitios de crecimiento polar (Yuan et al., 2016). Recientemente se reportó la participación de estas cinasas en la respuesta a estrés de RE. Al parecer, tanto Kin1 como Kin2 regulan positivamente a la UPR al regular el reclutamiento del ARNm *HAC1* hacia los *foci* de Ire1 en el RE (Ghosh, Sathe, Paprocki, Raicu, & Dey, 2018). Estos genes parálogos no son totalmente redundantes ya que la mutante *kin2Δ* es más sensible a la Tn que la mutante *kin1Δ*. Como el procesamiento de *HAC1* no se ve afectado en una mutante *hog1Δ* (Torres-Quiroz et al., 2010), es probable que el mecanismo de supresión de Kin1 y Kin2 esté más relacionado con sus funciones en otros procesos como la exocitosis o el remodelamiento de la pared celular.

Otra proteína involucrada en el transporte de proteínas es Rer1, cuya función es la retención y recuperación de proteínas residentes del RE como parte del mecanismo de control de calidad. Rer1 reconoce proteínas con dominios de retención en el RE

(KDEL/HDEL) y las regresa de Golgi (K. Sato, Nishikawa, & Nakano, 1995; K. Sato et al., 1997). Durante el estrés de RE, Rer1 se localiza en Golgi, transportando proteínas mal plegadas hacia este organelo para ser eliminadas por autofagosomas (Ghavidel et al., 2015). El mecanismo de supresión también puede estar relacionado con la regulación que Rer1 ejerce sobre la localización de la proteína Mns1, una alpha-1,2-manosidasa, encargada de eliminar la última manosa del *N*-glucano de proteínas mal plegadas, etiquetándolas así para su degradación a través del ERAD (Massaad, Franzusoff, & Herscovics, 1999).

Dos genes supresores, *NAB6* y *ECM13*, codifican para proteínas relacionadas con la biogénesis de la pared celular. *NAB6* codifica para una proteína que probablemente se une a ARN mensajeros, se ha propuesto que participa en su procesamiento al interaccionar genéticamente con componentes de exosomas (Abruzzi et al., 2007). Esta proteína se localiza en gránulos de estrés y se ha copurificado con factores de regulación de la traducción (Ezeokonkwo, Ghazy, Zhelkovsky, Yeh, & Moore, 2012; Jain et al., 2016; Mitchell, Jain, She, & Parker, 2013). *Ecml3*, por su parte, se regula positivamente en respuesta a daño de ADN y se piensa que está involucrada en la síntesis de la pared celular (García et al., 2004; Lussier et al., 1997).

Finalmente, Rer2 y Srt1 son supresores que participan en el proceso de glicosilación de proteínas. Ambas proteínas son *cis*-PT, las cuales están involucradas en la síntesis de dolicol. Estas enzimas están encargadas de la condensación de unidades de isopreno para la formación de dolicoles de diferentes longitudes, de 14 a 18 unidades en el caso de Rer2 (M. Sato et al., 1999) y de 19 a 22 unidades en el caso de Srt1 (M. Sato, Fujisaki, Sato, Nishimura, & Nakano, 2001). El dolicol es esencial para los procesos de glicosilación pero también se ha reportado que tiene importancia como componente de membranas celulares y de la pared celular (Chojnacki & Dallner, 1988; Orłowski, Machula, Janik, Zdebska, & Palamarczyk, 2007). Rer2 se localiza en la membrana del RE mientras que Srt1 se ha ubicado como componente estructural de cuerpos lipídicos. Srt1 se encontró como supresor de la letalidad de la mutante *rer2Δ* (M. Sato et al., 2001) y aunque se ha determinado que los dolicoles sintetizados por Srt1 pueden ser utilizados como precursores en la *N*-glicosilación también se ha reportado su importancia en la regulación de la síntesis de la pared celular de las esporas (Hoffman, Grabińska, Guan, Sessa, & Neiman, 2017). Al parecer, la función de Rer2 es más importante que la de Srt1 ya que la mutante *rer2Δ* tiene un muy fuerte defecto de crecimiento, mientras que la mutante *srt1Δ*

crece normalmente, sin embargo, la doble mutante *rer2Δsrt1Δ* es letal, lo que indica una convergencia de funciones (Grabińska et al., 2005).

Las observaciones que se desprenden de este trabajo indican que la supresión que ejercen Rer2 y Srt1 es ocasionada por el incremento en la síntesis de dolicol ya que la sobreexpresión de cualquiera de las dos enzimas incrementa la resistencia a la Tn, sin embargo, no son completamente redundantes ya que se localizan en diferentes compartimentos y presentan diferentes patrones de expresión (M. Sato et al., 2001). En este trabajo observamos que la presencia de Tn induce un incremento en la producción de dolicol, al parecer como un mecanismo de compensación para aumentar la capacidad de glicosilación. En la mutante *hog1Δ*, sin embargo, no hay un incremento significativo de dolicol en respuesta a la Tn, lo que sugiere que la ausencia de Hog1 resulta en un defecto en la regulación de la síntesis de dolicol en condiciones de estrés de RE. Esto podría en parte explicar la sensibilidad a la Tn que presenta la mutante *hog1Δ*. Siendo así, la sobreexpresión de *RER2* incrementaría la cantidad de dolicol en el RE revirtiendo la sensibilidad a la Tn de la cepa *hog1Δ*.

Alternativamente, para comprobar que la producción de dolicol es importante para la resistencia a la Tn, se sobreexpresó el gen *ERG9*, cuyo producto comparte el sustrato FPP con las cis-PT Rer2 y Srt1. En estas condiciones, indirectamente se disminuye la cantidad de dolicol celular al emplear al FPP exclusivamente en la producción de ergosterol. Una mutante *hog1Δ* sobreexpresando *ERG9* es más sensible a la Tn, apoyando la hipótesis de que se requiere un incremento en la síntesis de dolicol para generar una resistencia a este antibiótico. Se ha reportado que la síntesis *de novo* de dolicol es defectuosa en mutantes de la vía de ergosterol. Particularmente, la mutante *erg9Δ* tiene una mayor poza de dolicol (Szkopińska, Rytka, Karst, & Palamarczyk, 1993), así como únicamente sintetiza dolicóles a partir de FPP y no otras moléculas como ergosterol, ubiquinona, etc (Grabowska, Karst, & Szkopińska, 1998).

En la naturaleza se encuentran mezclas de dolicóles de 4 o 5 longitudes diferentes. Los poliprenoles tienen funciones celulares diversas; en bacterias se utilizan como acarreadores de azúcares para la síntesis de la pared celular (Manat et al., 2014) y en levaduras participan en la regulación de las enzimas que participan en la síntesis de componentes de la pared celular (Hoffman et al., 2017; Orłowski et al., 2007). El dolicol también es importante para promover la fluidez de las membranas celulares (Valtersson et al., 1985), en la fusión de vesículas (van Duijn et al., 1986) y en el tráfico de membranas

y vesículas (Belgareh-Touzé et al., 2003). Se ha propuesto también que el dolicol puede actuar como “*scavenger*” de radicales libres y regular así especies reactivas de oxígeno producidas por UV, por agentes químicos o por envejecimiento (Bergamini et al., 2004; Bizzarri et al., 2003; Sgarbossa et al., 2003). Todo esto sugiere que el dolicol puede tener actividades importantes adicionales a su función canónica de acarreador de polisacáridos en la *N*-glicosilación, por lo que resultaría interesante explorar con detalle el papel de Hog1 en la regulación de la producción del dolicol celular, y definir así si el mecanismo de supresión está restringido a un incremento en la *N*-glicosilación o involucra algún otro proceso.

Es importante resaltar que en este estudio no se detectaron interactores físicos de Hog1, sin embargo, los datos disponibles de sus interacciones físicas se han realizado en condiciones de hiperosmolaridad, y no en otros tipos de estrés. por lo que es probable que los supresores sean activados a través de intermediarios de Hog1. Nuestra red de interacciones y nuestros ensayos de interacción sugieren que las proteínas supresoras requieren intermediarios para asociarse con Hog1, sin embargo, no se puede descartar completamente que algunas de ellas interactúen directamente con Hog1. Esto porque las proteínas Kin1, Kin2, Nab6 tienen motivos S/T-P que son potenciales sitios de fosforilación mediada por MAPK. Esto se apoya además en el hecho de que la actividad de cinasa de Hog1 es esencial para generar resistencia a estrés de RE inducido por Tn. Notoriamente, todos los supresores que se aislaron tienen actividades extra-nucleares, ninguno de ellos se ha reportado como activador transcripcional, lo que refuerza la observación de que Hog1 no se transloca al núcleo durante un estímulo con agentes inductores de estrés de RE.

En conclusión, este trabajo nos ha permitido conocer proteínas involucradas en la respuesta a la Tn y que tienen una relación funcional con Hog1, y nos ofrece un panorama en el cual la célula tiene una gran capacidad para generar vías de respuesta a una gran variedad de estímulos con un repertorio limitado de proteínas.

CONCLUSIONES

1. Los supresores por sobreexpresión de la sensibilidad de la mutante *hog1Δ* a la Tn están involucrados en procesos celulares extra nucleares de transporte y glicosilación de proteínas, biogénesis de pared celular y desintoxicación celular.
2. Los genes *NAB6*, *KIN1* y *KIN2* tienen un efecto aditivo a *HOG1* en la resistencia a la Tn, indicando que participan en vías independientes a Hog1. Mientras que *RER1* y *ECM13* participan en la misma vía de señalización que Hog1.
3. La Tn induce un incremento en la concentración de dolicol y este proceso es dependiente de Hog1.

REFERENCIAS

- Abruzzi, K., Denome, S., Olsen, J. R., Assenholt, J., Haaning, L. L., Jensen, T. H., & Rosbash, M. (2007). A Novel Plasmid-Based Microarray Screen Identifies Suppressors of *rrp6* in *Saccharomyces cerevisiae*. *Molecular and Cellular Biology*, 27(3), 1044-1055. <https://doi.org/10.1128/MCB.01299-06>
- Araki, K., & Nagata, K. (2011). Protein Folding and Quality Control in the ER. *Cold Spring Harbor Perspectives in Biology*, 3(11), a007526-a007526. <https://doi.org/10.1101/cshperspect.a007526>
- Barnes, G., Hansen, W. J., Holcomb, C. L., & Rine, J. (1984). Asparagine-linked glycosylation in *Saccharomyces cerevisiae*: Genetic analysis of an early step. *Molecular and Cellular Biology*, 4(11), 2381-2388. <https://doi.org/10.1128/mcb.4.11.2381>
- Belgareh-Touzé, N., Corral-Debrinski, M., Launhardt, H., Galan, J.-M., Munder, T., Le Panse, S., & Haguenauer-Tsapis, R. (2003). Yeast functional analysis: Identification of two essential genes involved in ER to Golgi trafficking. *Traffic (Copenhagen, Denmark)*, 4(9), 607-617.
- Bergamini, E., Bizzarri, R., Cavallini, G., Cerbai, B., Chiellini, E., Donati, A., ... Tamburini, I. (2004). Ageing and oxidative stress: A role for dolichol in the antioxidant machinery of cell membranes? *Journal of Alzheimer's Disease: JAD*, 6(2), 129-135.
- Bicknell, A. A., Tourtellotte, J., & Niwa, M. (2010). Late Phase of the Endoplasmic Reticulum Stress Response Pathway Is Regulated by Hog1 MAP Kinase. *Journal of Biological Chemistry*, 285(23), 17545-17555. <https://doi.org/10.1074/jbc.M109.084681>
- Bizzarri, R., Cerbai, B., Signori, F., Solaro, R., Bergamini, E., Tamburini, I., & Chiellini, E. (2003). New perspectives for (S)-dolichol and (S)-nordolichol synthesis and biological functions. *Biogerontology*, 4(6), 353-363. <https://doi.org/10.1023/B:BGEN.0000006555.87407.04>
- Bowman, S. M., & Free, S. J. (2006). The structure and synthesis of the fungal cell wall. *BioEssays*, 28(8), 799-808. <https://doi.org/10.1002/bies.20441>
- Braakman, I., & Hebert, D. N. (2013). Protein Folding in the Endoplasmic Reticulum. *Cold Spring Harbor Perspectives in Biology*, 5(5), a013201-a013201. <https://doi.org/10.1101/cshperspect.a013201>
- Breitling, J., & Aebi, M. (2013). N-Linked Protein Glycosylation in the Endoplasmic Reticulum. *Cold Spring Harbor Perspectives in Biology*, 5(8), a013359-a013359. <https://doi.org/10.1101/cshperspect.a013359>
- Cantagrel, V., & Lefeber, D. J. (2011). From glycosylation disorders to dolichol biosynthesis defects: A new class of metabolic diseases. *Journal of Inherited Metabolic Disease*, 34(1), 1-10. <https://doi.org/10.1007/s10545-010-9371-0>

Disease, 34(4), 859-867. <https://doi.org/10.1007/s10545-011-9301-0>

Chakrabarti, A., Chen, A. W., & Varner, J. D. (2011). A review of the mammalian unfolded protein response. *Biotechnology and Bioengineering*, 108(12), 2777-2793. <https://doi.org/10.1002/bit.23282>

Chen, Y. (2005). Identification of Mitogen-Activated Protein Kinase Signaling Pathways That Confer Resistance to Endoplasmic Reticulum Stress in *Saccharomyces cerevisiae*. *Molecular Cancer Research*, 3(12), 669-677. <https://doi.org/10.1158/1541-7786.MCR-05-0181>

Chojnacki, T., & Dallner, G. (1988). The biological role of dolichol. *Biochemical Journal*, 251(1), 1-9. <https://doi.org/10.1042/bj2510001>

Cox, J. S., & Walter, P. (1996). A novel mechanism for regulating activity of a transcription factor that controls the unfolded protein response. *Cell*, 87(3), 391-404. [https://doi.org/10.1016/0168-9525\(97\)90082-2](https://doi.org/10.1016/0168-9525(97)90082-2)

Cox, Jeffery S., Shamu, C. E., & Walter, P. (1993). Transcriptional induction of genes encoding endoplasmic reticulum resident proteins requires a transmembrane protein kinase. *Cell*, 73(6), 1197-1206. [https://doi.org/10.1016/0092-8674\(93\)90648-A](https://doi.org/10.1016/0092-8674(93)90648-A)

Cyr, D. M., & Hebert, D. N. (2009). Protein quality control—Linking the unfolded protein response to disease. *EMBO reports*, 10(11), 1206-1210. <https://doi.org/10.1038/embor.2009.224>

Elbert, M., Rossi, G., & Brennwald, P. (2005). The Yeast Par-1 Homologs Kin1 and Kin2 Show Genetic and Physical Interactions with Components of the Exocytic Machinery. *Molecular Biology of the Cell*, 16(2), 532-549. <https://doi.org/10.1091/mbc.e04-07-0549>

Ezeokonkwo, C., Ghazy, M. A., Zhelkovsky, A., Yeh, P.-C., & Moore, C. (2012). Novel interactions at the essential N-terminus of poly(A) polymerase that could regulate poly(A) addition in *Saccharomyces cerevisiae*. *FEBS Letters*, 586(8), 1173-1178. <https://doi.org/10.1016/j.febslet.2012.03.036>

García, R., Bermejo, C., Grau, C., Pérez, R., Rodríguez-Peña, J. M., Francois, J., ... Arroyo, J. (2004). The Global Transcriptional Response to Transient Cell Wall Damage in *Saccharomyces cerevisiae* and Its Regulation by the Cell Integrity Signaling Pathway. *Journal of Biological Chemistry*, 279(15), 15183-15195. <https://doi.org/10.1074/jbc.M312954200>

García-Marqués, S., Randez-Gil, F., & Prieto, J. A. (2015). Nuclear versus cytosolic activity of the yeast Hog1 MAP kinase in response to osmotic and tunicamycin-induced ER stress. *FEBS Letters*, 589(16), 2163-2168. <https://doi.org/10.1016/j.febslet.2015.06.021>

Ghavidel, A., Baxi, K., Ignatchenko, V., Prusinkiewicz, M., Arnason, T. G., Kislinger, T., ... Harkness, T. A. A. (2015). A Genome Scale Screen for Mutants with Delayed Exit from

Mitosis: Ire1-Independent Induction of Autophagy Integrates ER Homeostasis into Mitotic Lifespan. *PLOS Genetics*, 11(8), e1005429. <https://doi.org/10.1371/journal.pgen.1005429>

Ghosh, C., Sathe, L., Paprocki, J. D., Raicu, V., & Dey, M. (2018). Adaptation to Endoplasmic Reticulum Stress Requires Transphosphorylation within the Activation Loop of Protein Kinases Kin1 and Kin2, Orthologs of Human Microtubule Affinity-Regulating Kinase. *Molecular and Cellular Biology*, 38(23), e00266-18, /mcb/38/23/e00266-18.atom. <https://doi.org/10.1128/MCB.00266-18>

Grabińska, K., Sosińska, G., Orłowski, J., Swiezewska, E., Berges, T., Karst, F., & Palamarczyk, G. (2005). Functional relationships between the *Saccharomyces cerevisiae* cis-prenyltransferases required for dolichol biosynthesis. *Acta Biochimica Polonica*, 52(1), 221-232. <https://doi.org/055201221>

Grabiska, K., & Palamarczyk, G. (2002). Dolichol biosynthesis in the yeast: An insight into the regulatory role of farnesyl diphosphate synthase. *FEMS Yeast Research*, 2(3), 259-265. [https://doi.org/10.1016/S1567-1356\(02\)00110-1](https://doi.org/10.1016/S1567-1356(02)00110-1)

Grabowska, D., Karst, F., & Szkopińska, A. (1998). Effect of squalene synthase gene disruption on synthesis of polyprenols in *Saccharomyces cerevisiae*. *FEBS Letters*, 434(3), 406-408. [https://doi.org/10.1016/S0014-5793\(98\)01019-9](https://doi.org/10.1016/S0014-5793(98)01019-9)

Harrison, K. D., Park, E. J., Gao, N., Kuo, A., Rush, J. S., Waechter, C. J., ... Sessa, W. C. (2011). Nogo-B receptor is necessary for cellular dolichol biosynthesis and protein *N*-glycosylation: NgBR is necessary for cellular dolichol biosynthesis. *The EMBO Journal*, 30(12), 2490-2500. <https://doi.org/10.1038/emboj.2011.147>

Hoffman, R., Grabińska, K., Guan, Z., Sessa, W. C., & Neiman, A. M. (2017). Long-Chain Polyprenols Promote Spore Wall Formation in *Saccharomyces cerevisiae*. *Genetics*, genetics.300322.2017. <https://doi.org/10.1534/genetics.117.300322>

Jain, S., Wheeler, J. R., Walters, R. W., Agrawal, A., Barsic, A., & Parker, R. (2016). ATPase-Modulated Stress Granules Contain a Diverse Proteome and Substructure. *Cell*, 164(3), 487-498. <https://doi.org/10.1016/j.cell.2015.12.038>

Jones, G. M., Stalker, J., Humphray, S., West, A., Cox, T., Rogers, J., ... Prelich, G. (2008). A systematic library for comprehensive overexpression screens in *Saccharomyces cerevisiae*. *Nature Methods*, 5(3), 239-241. <https://doi.org/10.1038/nmeth.1181>

Katzmann, D. J., Hallstrom, T. C., Voet, M., Wysock, W., Golin, J., Volckaert, G., & Moye-Rowley, W. S. (1995). Expression of an ATP-binding cassette transporter-encoding gene (YOR1) is required for oligomycin resistance in *Saccharomyces cerevisiae*. *Molecular and Cellular Biology*, 15(12), 6875-6883. <https://doi.org/10.1128/MCB.15.12.6875>

Kaufman, R. J. (2002). Orchestrating the unfolded protein response in health and disease. *Journal of Clinical Investigation*, 110(10), 1389-1398.

<https://doi.org/10.1172/JCI0216886>

- Lodish, H. F. (Ed.). (2000). *Molecular cell biology* (4th ed). New York: W.H. Freeman.
- Lussier, M., White, A. M., Sheraton, J., di Paolo, T., Treadwell, J., Southard, S. B., ... Bussey, H. (1997). Large scale identification of genes involved in cell surface biosynthesis and architecture in *Saccharomyces cerevisiae*. *Genetics*, 147(2), 435-450.
- Manat, G., Roure, S., Auger, R., Bouhss, A., Barreteau, H., Mengin-Lecreux, D., & Touzé, T. (2014). Deciphering the metabolism of undecaprenyl-phosphate: The bacterial cell-wall unit carrier at the membrane frontier. *Microbial Drug Resistance (Larchmont, N.Y.)*, 20(3), 199-214. <https://doi.org/10.1089/mdr.2014.0035>
- Massaad, M. J., Franzusoff, A., & Herscovics, A. (1999). The processing α 1,2-mannosidase of *Saccharomyces cerevisiae* depends on Rer1p for its localization in the endoplasmic reticulum. *European Journal of Cell Biology*, 78(7), 435-440. [https://doi.org/10.1016/S0171-9335\(99\)80070-3](https://doi.org/10.1016/S0171-9335(99)80070-3)
- McCaffrey, K., & Braakman, I. (2016). Protein quality control at the endoplasmic reticulum. *Essays In Biochemistry*, 60(2), 227-235. <https://doi.org/10.1042/EBC20160003>
- Mitchell, S. F., Jain, S., She, M., & Parker, R. (2013). Global analysis of yeast mRNPs. *Nature Structural & Molecular Biology*, 20(1), 127-133. <https://doi.org/10.1038/nsmb.2468>
- Mori, K., Ogawa, N., Kawahara, T., Yanagi, H., & Yura, T. (1998). Palindrome with Spacer of One Nucleotide Is Characteristic of the *cis*-Acting Unfolded Protein Response Element in *Saccharomyces cerevisiae*. *Journal of Biological Chemistry*, 273(16), 9912-9920. <https://doi.org/10.1074/jbc.273.16.9912>
- Nishikawa, S., & Nakano, A. (1993). Identification of a gene required for membrane protein retention in the early secretory pathway. *Proceedings of the National Academy of Sciences*, 90(17), 8179-8183. <https://doi.org/10.1073/pnas.90.17.8179>
- Orłowski, J., Machula, K., Janik, A., Zdebska, E., & Palamarczyk, G. (2007). Dissecting the role of dolichol in cell wall assembly in the yeast mutants impaired in early glycosylation reactions. *Yeast*, 24(4), 239-252. <https://doi.org/10.1002/yea.1479>
- Prelich, G. (2012). Gene Overexpression: Uses, Mechanisms, and Interpretation. *Genetics*, 190(3), 841-854. <https://doi.org/10.1534/genetics.111.136911>
- Rauthan, M., & Pilon, M. (2011). The mevalonate pathway in *C. elegans*. *Lipids in Health and Disease*, 10(1), 243. <https://doi.org/10.1186/1476-511X-10-243>
- Rine, J., Hansen, W., Hardeman, E., & Davis, R. W. (1983). Targeted selection of recombinant clones through gene dosage effects. *Proceedings of the National Academy of Sciences*, 80(22), 6750-6754. <https://doi.org/10.1073/pnas.80.22.6750>
- Rogers, B., Decottignies, A., Kolaczkowski, M., Carvajal, E., Balzi, E., & Goffeau, A. (2001). The pleitropic drug ABC transporters from *Saccharomyces cerevisiae*. *Journal of*

Molecular Microbiology and Biotechnology, 3(2), 207-214.

Saito, H., & Posas, F. (2012). Response to Hyperosmotic Stress. *Genetics*, 192(2), 289-318. <https://doi.org/10.1534/genetics.112.140863>

Sato, K., Nishikawa, S., & Nakano, A. (1995). Membrane protein retrieval from the Golgi apparatus to the endoplasmic reticulum (ER): Characterization of the RER1 gene product as a component involved in ER localization of Sec12p. *Molecular Biology of the Cell*, 6(11), 1459-1477. <https://doi.org/10.1091/mbc.6.11.1459>

Sato, K., Sato, M., & Nakano, A. (1997). Rer1p as common machinery for the endoplasmic reticulum localization of membrane proteins. *Proceedings of the National Academy of Sciences*, 94(18), 9693-9698. <https://doi.org/10.1073/pnas.94.18.9693>

Sato, M., Fujisaki, S., Sato, K., Nishimura, Y., & Nakano, A. (2001). Yeast *Saccharomyces cerevisiae* has two cis-prenyltransferases with different properties and localizations. Implication for their distinct physiological roles in dolichol synthesis. *Genes to Cells*, 6(6), 495-506. <https://doi.org/10.1046/j.1365-2443.2001.00438.x>

Sato, M., Sato, K., Nishikawa, S., Hirata, A., Kato, J., & Nakano, A. (1999). The Yeast *RER2* Gene, Identified by Endoplasmic Reticulum Protein Localization Mutations, Encodes *cis*-Prenyltransferase, a Key Enzyme in Dolichol Synthesis. *Molecular and Cellular Biology*, 19(1), 471-483. <https://doi.org/10.1128/MCB.19.1.471>

Schenk, B., Rush, J. S., Waechter, C. J., & Aeby, M. (2001). An alternative *cis*-isoprenyltransferase activity in yeast that produces polyisoprenols with chain lengths similar to mammalian dolichols. *Glycobiology*, 11(1), 89-98. <https://doi.org/10.1093/glycob/11.1.89>

Sgarbossa, A., Lenci, F., Bergamini, E., Bizzarri, R., Cerbai, B., Signori, F., ... Maccheroni, M. (2003). Dolichol: A solar filter with UV-absorbing properties which can be photoenhanced. *Biogerontology*, 4(6), 379-386. <https://doi.org/10.1023/B:BGEN.0000006558.44482.a4>

Shamu, C. E., & Walter, P. (1996). Oligomerization and phosphorylation of the Ire1p kinase during intracellular signaling from the endoplasmic reticulum to the nucleus. *The EMBO Journal*, 15(12), 3028-3039.

Shamu, Caroline E., Cox, J. S., & Walter, P. (1994). The unfolded-protein-response pathway in yeast. *Trends in Cell Biology*, 4(2), 56-60. [https://doi.org/10.1016/0962-8924\(94\)90011-6](https://doi.org/10.1016/0962-8924(94)90011-6)

Sidrauski, C. (1998). The unfolded protein response: An intracellular signalling pathway with many surprising features. *Trends in Cell Biology*, 8(6), 245-249. [https://doi.org/10.1016/S0962-8924\(98\)01267-7](https://doi.org/10.1016/S0962-8924(98)01267-7)

Storm, M., Sheng, X., Arnoldussen, Y. J., & Saatcioglu, F. (2016). Prostate cancer and

the unfolded protein response. *Oncotarget*, 7(33).
<https://doi.org/10.18632/oncotarget.9912>

Szkopińska, A., Rytka, J., Karst, F., & Palamarczyk, G. (1993). The deficiency of sterol biosynthesis in *Saccharomyces cerevisiae* affects the synthesis of glycosyl derivatives of dolichyl phosphates. *FEMS Microbiology Letters*, 112(3), 325-328.
<https://doi.org/10.1111/j.1574-6968.1993.tb06470.x>

Thibault, G., & Ng, D. T. W. (2012). The Endoplasmic Reticulum-Associated Degradation Pathways of Budding Yeast. *Cold Spring Harbor Perspectives in Biology*, 4(12), a013193-a013193. <https://doi.org/10.1101/cshperspect.a013193>

Torres-Quiroz, F., García-Marqués, S., Coria, R., Randez-Gil, F., & Prieto, J. A. (2010). The Activity of Yeast Hog1 MAPK Is Required during Endoplasmic Reticulum Stress Induced by Tunicamycin Exposure. *Journal of Biological Chemistry*, 285(26), 20088-20096.
<https://doi.org/10.1074/jbc.M109.063578>

Valtersson, C., van Duyn, G., Verkleij, A. J., Chojnacki, T., de Kruijff, B., & Dallner, G. (1985). The influence of dolichol, dolichol esters, and dolichyl phosphate on phospholipid polymorphism and fluidity in model membranes. *The Journal of Biological Chemistry*, 260(5), 2742-2751.

van Duijn, G., Valtersson, C., Chojnacki, T., Verkleij, A. J., Dallner, G., & de Kruijff, B. (1986). Dolichyl phosphate induces non-bilayer structures, vesicle fusion and transbilayer movement of lipids: A model membrane study. *Biochimica et Biophysica Acta (BBA) - Biomembranes*, 861, 211-223. [https://doi.org/10.1016/0005-2736\(86\)90423-2](https://doi.org/10.1016/0005-2736(86)90423-2)

Watzele, G., & Tanner, W. (1989). Cloning of the glutamine: fructose-6-phosphate amidotransferase gene from yeast. Pheromonal regulation of its transcription. *The Journal of Biological Chemistry*, 264(15), 8753-8758.

Welihinda, A. A., & Kaufman, R. J. (1996). The Unfolded Protein Response Pathway in *Saccharomyces cerevisiae*: OLIGOMERIZATION AND TRANS-PHOSPHORYLATION OF Ire1p (Ern1p) ARE REQUIRED FOR KINASE ACTIVATION. *Journal of Biological Chemistry*, 271(30), 18181-18187. [Https://doi.org/10.1074/jbc.271.30.18181](https://doi.org/10.1074/jbc.271.30.18181)

Yuan, S.-M., Nie, W.-C., He, F., Jia, Z.-W., & Gao, X.-D. (2016). Kin2, the Budding Yeast Ortholog of Animal MARK/PAR-1 Kinases, Localizes to the Sites of Polarized Growth and May Regulate Septin Organization and the Cell Wall. *PLOS ONE*, 11(4), e0153992.
<https://doi.org/10.1371/journal.pone.0153992>

ANEXOS

1. Lista de cepas

Cepa	Genotipo
BY4742 WT	MAT α <i>his3Δ1 leu2Δ0 lys2Δ0 ura3Δ0</i>
BY4741 WT	MAT α <i>his3Δ1 leu2Δ0 met15Δ0 ura3Δ0</i>
<i>hog1Δ</i>	BY4742 <i>hog1:KANMX4</i>
<i>pbs2Δ</i>	BY4742 <i>pbs2:KANMX4</i>
<i>ssk1Δ</i>	BY4742 <i>ssk1:KANMX4</i>
<i>hac1Δ</i>	BY4742 <i>hac1:KANMX4</i>
<i>slt2Δ</i>	BY4742 <i>slt2:KANMX4</i>
<i>yor1Δ</i>	BY4742 <i>yor1:KANMX4</i>
<i>nab6Δ</i>	BY4742 <i>nab6:KANMX4</i>
<i>kin2Δ</i>	BY4742 <i>kin2:KANMX4</i>
<i>kin1Δ</i>	BY4742 <i>kin1:KANMX4</i>
<i>rer1Δ</i>	BY4742 <i>rer1:KANMX4</i>
<i>ecm13Δ</i>	BY4742 <i>ecm13:KANMX4</i>
<i>yor1Δ hog1Δ</i>	BY4742 <i>yor1:KANMX4 hog1:NATMX4</i>
<i>nab6Δ hog1Δ</i>	BY4742 <i>nab6:KANMX4 hog1:NATMX4</i>
<i>kin2Δ hog1Δ</i>	BY4742 <i>kin2:KANMX4 hog1:NATMX4</i>
<i>kin1Δ hog1Δ</i>	BY4742 <i>kin1:KANMX4 hog1:NATMX4</i>
<i>rer1Δ hog1Δ</i>	BY4742 <i>rer1:KANMX4 hog1:NATMX4</i>
<i>ecm13Δ hog1Δ</i>	BY4742 <i>ecm13:KANMX4 hog1:NATMX4</i>
<i>ssb2Δ</i>	BY4742 <i>ssb2:KANMX4</i>
<i>gis2Δ</i>	BY4742 <i>gis2:KANMX4</i>
<i>Kin1 VN</i>	BY4741 <i>KIN1-VN URA3</i>
<i>Kin2 VN</i>	BY4741 <i>KIN2-VN URA3</i>
<i>Rer1 VN</i>	BY4741 <i>RER1-VN URA3</i>
<i>Rer2 VN</i>	BY4741 <i>RER2-VN URA3</i>
<i>Ecm13 VN</i>	BY4741 <i>ECM13-VN URA3</i>
<i>Nab6 VN</i>	BY4741 <i>NAB6-VN URA3</i>
<i>Hog1 VC</i>	BY4742 <i>HOG1-VC KANMX4</i>

2. Lista de oligonucleótidos

Nombre	Secuencia (5' - 3')	Sitio de anclaje
T3	ATTAACCCTCACTAAAGGGA	4976
M13(-50)F	TTGGGTAACGCCAGGG	5201
T7	TAATACGACTCACTATAGGG	2999
SP6	CTATAGTGTACCTAAAT	158
ALG7F	GGATCCACGCCATAATTCAAC	-1000
ALG7R	AAGCTTGAGAGGGAATACAAA	+1543
GFA1F	GAACACCAATGTGGG	-530
GFA1R	AGCTTGTAGTGCGCA	+2255
YOR1F	GCATGCCGCCTCTTAGTTG	-572
YOR1R	CCCGGGAATGAAAAAGGACCG	+4643
NAB6F	GGATCCGGTGAATGCTCACT	-947
NAB6R	TCTAGACCGCCTTAGGCTTCC	+3467
KIN2F	TGATTCACCGCTTG	-467
KIN2R	AGCAGATCTCAGCTT	+3537
KIN1F	GAAGGGTCCGGTTAG	-795
KIN1R	GTGTCTGCTTAGGTCC	+3322
RER2F	TCGACAAGATTG	-1000
RER2R	GGTTAGTTCCCTGC	+2840
RER1F	GGATCCCAGAGATGAATA	-499
RER1R	AAGCTTCTCCATTATAAATG	+753
ECM13F	GCAGTAACGCACGGC	-548
ECM13R	TCTAGAAAGTGGTGTGACT	+876
DHOG1F	AAAGGGAAAACAGGGAAAACTACAACATCGTATATAAGCTTGCCT TGTCCCCGCCGG	-40
DHOG1R	GAAGTAAGAATGAGTGGTTAGGGACATTAAAAAAACACGTTCGACACT GGATGGCGGGCGTTAG	+1309
HOG1VCF	CGGTAAACCAGGCCATACAGTACGCTAATGAGTCCAACAGGGTCGACG GATCCCCGGGTT	+1266
HOG1VCR	GAAGTAAGAATGAGTGGTTAGGGACATTAAAAAAACACGTTCGATGAAT TCGAGCTCGTT	+1309
SRT1F	ATGAAAATGCCAGT	+1
SRT1R	TTATTCATCTCCTGT	+1032
ERG9F	ATGGGAAAGCTATTA	+1
ERG9R	TCACGCTCTGTGTA	+1335

Article

Tunicamycin Sensitivity-Suppression by High Gene Dosage Reveals New Functions of the Yeast Hog1 MAP Kinase

Mariana Hernández-Elvira ¹, Ricardo Martínez-Gómez ¹, Eunice Domínguez-Martin ¹, Akram Méndez ¹, Laura Kawasaki ¹, Laura Ongay-Larios ² and Roberto Coria ^{1,*}

¹ Departamento de Genética Molecular, Instituto de Fisiología Celular, Universidad Nacional Autónoma de México, CP 04510 Cd., Mexico

² Unidad de Biología Molecular, Instituto de Fisiología Celular, Universidad Nacional Autónoma de México, CP 04510 Cd., Mexico

* Correspondence: rcoria@ifc.unam.mx; Tel.: +52-55-56-22-56-52

Received: 8 April 2019; Accepted: 9 July 2019; Published: 12 July 2019



Abstract: In the yeast *Saccharomyces cerevisiae*, components of the High Osmolarity Glycerol (HOG) pathway are important for the response to diverse stresses including response to endoplasmic reticulum stress (ER stress), which is produced by the accumulation of unfolded proteins in the lumen of this organelle. Accumulation of unfolded proteins may be due to the inhibition of protein N-glycosylation, which can be achieved by treatment with the antibiotic tunicamycin (Tn). In this work we were interested in finding proteins involved in the ER stress response regulated by Hog1, the mitogen activated protein kinase (MAPK) of the HOG pathway. A high gene dosage suppression screening allowed us to identify genes that suppressed the sensitivity to Tn shown by a *hog1Δ* mutant. The suppressors participate in a limited number of cellular processes, including lipid/carbohydrate biosynthesis and protein glycosylation, vesicle-mediated transport and exocytosis, cell wall organization and biogenesis, and cell detoxification processes. The finding of suppressors Rer2 and Srt1, which participate in the dolichol biosynthesis pathway revealed that the *hog1Δ* strain has a defective polyprenol metabolism. This work uncovers new genetic and functional interactors of Hog1 and contributes to a better understanding of the participation of this MAPK in the ER stress response.

Keywords: yeast; Hog1; MAP kinase; endoplasmic reticulum; stress; suppression; unfolded protein response (UPR)

1. Introduction

The synthesis of transmembrane and secreted proteins occurs in ribosomes attached to the endoplasmic reticulum (ER) membrane. In the ER lumen such proteins are subjected to different modifications such as N-glycosylation, formation of disulphur bonds and protein folding. Properly processed proteins continue through the secretion pathway in order to be transported to their final location. All organisms are exposed to adverse conditions that decrease the capacity of the ER to fulfill these processes, leading to the production and accumulation of misfolded proteins, inducing a condition known as endoplasmic reticulum stress (ER stress). ER stress triggers a cellular response that includes the unfolded protein response (UPR), which is a conserved signaling pathway present in all eukaryotic cells, including yeast [1], *Dictyostelium discoideum* [2], plants [3], and mammals [4]. In the yeast *Saccharomyces cerevisiae* the UPR consists of an endoplasmic reticulum membrane sensor named Ire1 [5], which in the presence of misfolded proteins oligomerises and autophosphorylates [6,7]; this in turn triggers its cytoplasmic endonuclease activity, which processes the *HAC1* pre-mRNA [8].

The spliced mRNA is efficiently translated to produce the transcription factor Hac1 [8,9], which regulates transcription of several target genes, such as those encoding chaperones, glycosylation enzymes and proteases among others [10] in order to alleviate the accumulation of unfolded proteins.

It has been proposed that the UPR is not the only cellular pathway needed to cope with the ER stress [11]. Components of other pathways appear to be required to produce a full cellular response to ER stress inducers; particularly, some components of the high osmolarity glycerol (HOG) pathway have been implicated in the response to ER stress induced by the antibiotic tunicamycin (Tn). This antibiotic is a nucleoside structurally similar to the UDP-N-acetylglucosamine and blocks the first step of the N-glycosylation catalyzed by the Glucosamine-N-acetyl phosphotransferase enzyme [12,13]. The HOG pathway is a signaling system involved in survival under hyperosmotic conditions and it consists of two mechanistically different branches connected to a MAPK module, the SLN1 branch and the SHO1 branch, which converge on the scaffold MAPKK Pbs2, which in turn activates the MAPK Hog1 [14–16]. Once activated, Hog1 is translocated into the nucleus [17,18] where it regulates expression of genes whose products are involved in cell cycle arrest and adaptation to high osmolarity conditions.

In order to respond to ER stress induced by Tn, the cell requires the presence of both Pbs2 and Hog1. Additionally, Ssk1, the phosphorelay response regulator of the SLN1 branch, appears to be required for Tn response; however, components of the SHO1 branch seem to be dispensable [12,13]. As mentioned above, the presence of Hog1 is required for a proper response to Tn, but it appears that it does not need to be phosphorylated in order to produce resistance to the ER stress inducer. Indeed, a strain expressing an unphosphorylated form of Hog1 is able to grow in Tn, although not at the wild type level, but clearly above the growth shown by the *HOG1* null mutant [13]. Additionally, treatment with high Tn concentrations for an extended period of time only produces a very weak level of Hog1 phosphorylation that does not trigger its nuclear import [13]. Interestingly, a full cellular response to Tn requires the kinase activity of Hog1, since a point mutation that eliminates its kinase activity produces high sensitivity to Tn [13]. In addition to its participation in the ER stress response, several reports suggest that Hog1 has cytoplasmic activities, for example in the general stress response system [19,20] and in regulation of mitophagy [21,22].

With the aim of increasing knowledge regarding the participation of Hog1 in the ER stress response, we searched for genes whose products can suppress the sensitivity to Tn displayed by a Hog1-deficient strain but not its sensitivity to hyperosmotic stress. With this screening, we not only detected genes that were able to specifically suppress the Tn sensitivity of the *hog1Δ* mutant, but we also found genes that reverted the sensitivity shown by the *hog1Δ* mutant and by the *hac1Δ* mutant.

2. Materials and Methods

2.1. Yeast Strains, Gene Disruptions, and Culture Conditions

The *S. cerevisiae* strains used in this work are shown in Supplementary Table S1. All of them are isogenic to BY4742 or BY4741. The wild type and the single null mutants were obtained from the EUROSCARF collection. Double mutants were constructed by integration of the *NATMX4* cassette (which provides nourseothricin resistance) into the *HOG1* locus of single mutants. The integrating cassette was constructed by PCR using the oligonucleotides DHOG1F and DHOG1R (Supplementary Table S2) and contained the *NATMX4* gene flanked by *HOG1* 5' and 3' UTR fragments of 40 base pairs respectively. Integrations of the cassette were performed by homologous recombination. All deletions were confirmed by PCR.

Yeast cells were grown at 30 °C in YPD medium (1% yeast extract, 2% peptone, and 2% glucose) or SD medium (0.67% yeast nitrogen base without amino acids and 2% glucose, supplemented with the required amino acids for plasmid selection). Glucose was substituted by 2% raffinose (Sraf) or 2% galactose (Sgal) according to the requirements of the experiments. When needed, nourseothricin (100 µg/mL) was added to the media. YPGAL was the same as YPD except for the substitution of glucose by galactose.

Escherichia coli DH5 α strain was used to propagate plasmids. Bacteria were grown at 37 °C in LB medium (1% tryptone, 0.5% yeast extract, and 0.5% NaCl) containing 100 μ g/mL ampicillin or 50 μ g/mL kanamycin (for library-plasmid selection).

2.2. Stress Assays

Stress sensitivity assays were done by dropping aliquots of 10-fold serial dilutions of early-logarithmic YPD-cell cultures (OD_{600} adjusted to 0.05) on Tn and KCl plates. Plates were incubated at 30 °C for 72 h and scanned. For liquid cultures, cells with the same density were inoculated in triplicate in Honeycomb 2 plates (100 wells). Density readings were recorded every hour during 48 h of incubation at 30 °C in a BioScreen C microplate spectrophotometer (Oy Growth Curves Ab Ltd, Helsinki, Finland). The relative growth rate is the slope value of the linear regression of three independent liquid cultures.

2.3. High Dosage Suppression Screening

A diagram representing the suppression-screening assay is shown in Figure 1. The *hog1 Δ* mutant was transformed with a genomic library constructed to specifically perform overexpression screenings in *S. cerevisiae* [23]. The library contains a collection of more than 1000 overlapping genome fragments from the FY4 *S. cerevisiae* strain, cloned into the multicopy pGP564 plasmid. Transformants were plated in selective medium containing 1 μ g/mL Tn. Tn resistant clones were streaked on 1 M KCl and those sensitive to high osmolarity were selected. Plasmids from Tn resistant/KCl sensitive cells were extracted and propagated in *E. coli*. The selected plasmids were re-introduced into *hog1 Δ* yeast cells for a second round of selection. Ends of the yeast genome inserts were sequenced in order to map the Tn suppressor genome fragments. Standard yeast genetics protocols were used [24].

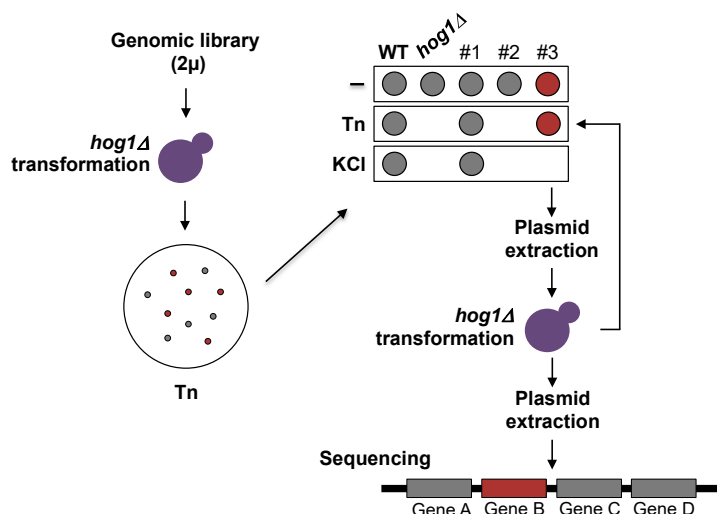


Figure 1. Dosage suppression screening protocol. The *hog1 Δ* strain was transformed with a genomic library constructed in a 2 μ plasmid. Yeast cells were plated on selective medium (SD + 25 μ g/mL of the required amino acids and nitrogen bases) containing 1 μ g/mL Tn. Plates were incubated for 48 h at 30 °C. Colonies that appeared were grown to early-logarithmic phase in liquid selective medium and adjusted to 0.5 OD_{600} . An aliquot of each transformant was dropped onto selective medium containing either 0.5 μ g/mL Tn or 1M KCl. Plasmids were purified from the Tn-resistant and KCl-sensitive clones and reintroduced into the *hog1 Δ* strain for a second round of selection. Suppressor plasmids were extracted, and the genomic inserts were sequenced.

2.4. Gene Expression

Each ORF contained in the suppression plasmids was cloned with its respective promoter in order to be expressed in yeast cells. Subcloning was done by PCR using oligonucleotides shown in

Supplementary Table S2 (only the oligonucleotides for suppressor genes are shown). The PCR products were obtained using genomic DNA of the BY4742 wild type strain as template. The PCR products were cloned into the pGEM-T-Easy vector and then subcloned into the yeast YEp352 vector [25]. The YEp352 clones were used for yeast transformation. All PCR products were sequenced in full.

2.5. Physical Interactions and Construction of the Interaction Network

Physical protein interactions between Hog1 and suppressor proteins were determined by the Bimolecular Fluorescence Complementation (BiFC) assay [26]. Proteins fused to the amino-end (VN) of the fluorescent protein Venus were obtained from the VN-fusion library (Bioneer, Daejeon, Republic of Corea) that is constructed in the BY4741 (*Mata*) strain. Hog1-VC (carboxyl-end of the Venus protein) was constructed by fusing the *HOG1* ORF in frame with the gene encoding VC. The fused gene was integrated into the *HOG1* locus of the BY4742 (*Mata*) strain by homologous recombination. Co-expression of VN and VC fusion constructs was achieved in diploid cells after mating BY4741 and BY4742 recombinant strains. Protein interactions were detected by flow cytometry using the Attune Acoustic Focusing Cytometer. Fluorescence statistics were calculated with the Attune software (version 2.1) and the statistical significance was determined with a Welch *t*-test.

Data of the known interactors for each suppressor gene and *HOG1* were obtained from the BioGRID database (<https://thebiogrid.org/>) (version 3.4.144), which is a repository of available physical and genetic interactions determined by different low- and high-throughput experimental assays and compiled through comprehensive curation [27]. The physical interaction data were extracted and visualized with Cytoscape [28] according to the protocol previously described [29]. The output interactors, i.e., the proteins that interact with only one node of the network, were eliminated in order to select the proteins connected with at least two other interactors. The network obtained after this reduction was clustered with the force directed layout with default parameters in Cytoscape and the visualization (separation of the nodes) was improved manually. The edges were colored according to the experimental assay that supports each interaction in the database.

2.6. Polyprenol Determination

Yeast cells were grown to mid-logarithmic phase in YPGAL (OD₆₀₀ adjusted to 0.5) and incubated during 2 h with either 1 µg/mL Tn or DMSO (Tn dissolvent). Yeast cells were centrifuged and the pellet was washed with water. Polyprenols extraction was performed as previously described [30] with modifications. Yeast cells were resuspended in water and disrupted with glass beads. The lipids were extracted by shaking during 2 h with chloroform/methanol (2:1 *v/v*) at RT. The organic phase was collected washed three times with 1/5 volume of 10mM EDTA in 0.9% NaCl and evaporated to dryness. Lipids were resuspended in methanol/water (10:1 *v/v*) containing 15% KOH and alkaline hydrolysis was performed during 2 h at 95 °C. Lipophylic products were extracted twice with diethyl ether and evaporated to dryness. The lipids obtained were dissolved in hexane and applied to a silica column equilibrated with hexane. The column was washed with 3% diethyl ether in hexane and the polyprenol fraction was eluted with 17% diethyl ether in hexane. The fraction was evaporated to dryness, resuspended in hexane and subjected to HPLC analysis. Polyprenols detection was performed with a reverse phase Symmetry C18 Waters column (3.5 µm, 4.6 × 75 mm) using a HPLC Waters Alliance e2695/2489/2414 equipment (Milford, MA, USA). Samples were run at 25 °C at a flow rate of 1.2 mL/min in isocratic elution with 55% methanol, 23% isopropanol, and 22% hexane and detected with UV light (210 nm). We used 1 µg/µL of C-90 Dolichol (Dolichol-18) from Larodan Research Grade Lipids (Solna, Sweden) as a standard. Polyprenol concentration corresponded to the area under the curve of each peak, referred to the area under the curve of the internal standard peak and expressed by mg of protein. Mean values, standard deviation, and significance were graphed and analyzed from three independent experiments. Statistical significance was tested with Student *t* test.

3. Results

3.1. Isolation of High Dosage-Gene Suppressors of *Hog1Δ* Tunicamycin Sensitivity

In order to shed light onto the way in which Hog1 participates in the response to ER stress inducers, we designed a dosage-suppression screening to identify genes required for the Hog1-Tn response. For the screening the *hog1Δ* mutant was transformed with a genome library constructed in a high copy plasmid [23] selecting clones resistant to Tn but sensitive to KCl. To this end, yeast transformants were plated in medium containing Tn to isolate cells resistant to the antibiotic; then, the transformants were dropped on plates containing KCl in order to identify the clones that were sensitive to hyperosmotic stress (Figure 1). The suppressor plasmids were extracted from the selected transformants and were reintroduced into the *hog1Δ* mutant to confirm Tn resistance and KCl sensitivity (Figure 1).

With this strategy, we isolated 40 plasmids that conferred resistance to Tn but not to hyperosmotic stress. These plasmids were sequenced to determine the chromosomal region responsible for the suppression. Among these 40 plasmids only 8 different regions were represented (Figure 2A). The regions are distributed in 6 different chromosomes and their size range is from 9 Kb to 12 Kb. Figure 2A summarizes the characteristics of the 40 suppressor plasmids; suppressor 8 was the most represented (14 times), while suppressors 70, 86, and 87 were isolated only one time. The level of Tn sensitivity suppression varied between strains. Sup 11 showed the weakest suppressor level while suppressors 8, 39, and 70 showed the strongest (Figure 2A,B). In our assays we included as a control the *hac1Δ* mutant, which lacks the basic leucine zipper (b-Zip) transcription factor, which regulates the gene transcription in the UPR pathway. This mutant is highly sensitive to Tn (Figure 2B).

Since each chromosomal region contained several ORFs (Figure 2A), we subcloned each of them independently in order to identify the ORF responsible for the suppression. From this assay we identified 8 genes (colored in brown in Figure 2A) that conferred resistance to Tn but not to hyperosmotic stress upon the *hog1Δ* mutant (Figure 2C). The level of suppression varied among the genes. We found differences in sensitivity to Tn and therefore in the growth rate of the *hog1Δ* mutant transformed with the different genes (Figure 2C). The highest growth rate of the *hog1Δ* mutant in Tn was observed with *ALG7*, while the lowest was obtained with *ECM13*. Although *KIN1* was not found as a suppressor in this screening, it was included in this study since it has been reported to be paralogous to *KIN2* [31]. As can be observed, *KIN1* and *KIN2* had the same level of suppression (Figure 2C).

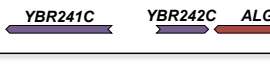
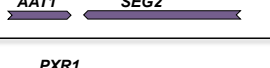
Name	Chromosome coordinates	Size (bp)	Chromosome region	No. of times isolated	Relative suppression level*
Sup8	II 702,406- 712,203	9797		14	+++++
Sup39	XI 238,339- 250,650	12311		13	+++++
Sup47	VII 1,050,372- 1,061,331	10959		3	+++
Sup11	XIII 28,455- 38,857	10402		5	++
Sup31	XII 330,854- 341,765	10911		2	+++
Sup70	II 239,720- 249,439	9719		1	++++
Sup86	II 133,290- 141,740	8450		1	+++
Sup87	III 111,555- 122,059	10504		1	+++

Figure 2. Cont.

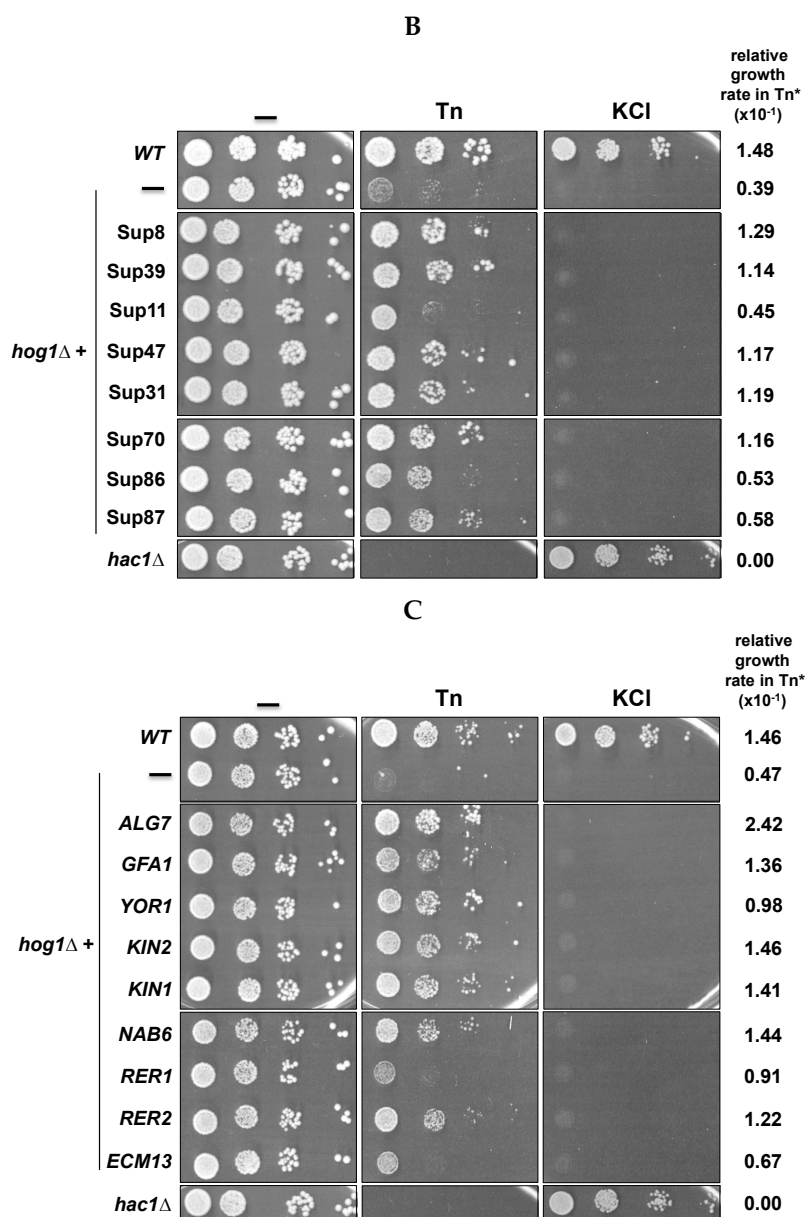


Figure 2. Suppression of the *hog1 Δ* Tn sensitivity. (A) Schematic representation of the genomic region contained in each suppressor plasmid. Chromosome number and insert coordinates and size are shown. Number of isolated times that each suppressor plasmid was isolated along with its relative suppression level (according to Figure 2B) are indicated. ORF orientation is depicted by the colored arrows. ORFs that show suppressor activity are marked in brown. (B) Serial dilution dropping assay of the *hog1 Δ* strain transformed with suppressor plasmids. Yeast cells were grown in YPD to early-logarithmic phase and adjusted to 0.5 OD₆₀₀ in fresh YPD. 10-fold serial dilutions were spotted on selective medium (see legend of Figure 1) containing either 0.5 μ g/mL Tn or 1 M KCl. The *hac1 Δ* mutant was used as Tn sensitivity control. Plates were incubated at 30 °C for 72 h and scanned. (C) Genes colored in brown in Figure 2A were subcloned into the multicopy plasmid YEpl352 and expressed in the *hog1 Δ* strain under the control of their own promoter. A serial dilution assay was performed as described in Figure legend 2B. (*) The relative growth rate is the slope value of the linear regression of liquid cultures made in triplicate and grown in YPD containing 0.5 μ g/mL Tn. Liquid cultures were performed in a microplate spectrophotometer at 30 °C with constant shaking. The OD₆₀₀ readings were determined at 1 h intervals during 48 h. *KIN1*, which was not detected in the screening was included in this assay since it is paralogous to *KIN2* (see text).

3.2. Genes Can Be Divided into General and HOG-Specific Suppressors of Tn Sensitivity

In order to determine whether the isolated genes were specific suppressors of the Tn-sensitivity observed in the *hog1Δ* mutant, we tested their suppressor activity in mutants of other components of the HOG pathway that have been implicated in the response to ER stress induced by Tn, specifically *PBS2* and *SSK1* [13]. We also introduced the suppressor genes in the *hac1Δ* in order to ascertain whether suppression is or is not restricted to the components of the HOG pathway. We observed that all suppressor genes did confer resistance, to different degrees, upon the *pbs2Δ* and *ssk1Δ* mutants. Interestingly, three genes, *ALG7*, *GFA1* and *YOR1*, also conferred resistance upon the *hac1Δ* mutant (Figure 3). This indicates that *ALG7*, *GFA1* and *YOR1* are general suppressors of Tn sensitivity, while *NAB6*, *KIN1*, *KIN2*, *RER1*, *RER2* and *ECM13* can be considered specific suppressors of the deficiency shown by the mutants of the HOG pathway. The general suppressors were the most represented in the isolated plasmids (30 of 40) (Figure 2B). In contrast, the specific suppressors were represented in only 10 of 40 isolated plasmids (excluding *KIN1*), suggesting that these suppressors can be found more rarely in this kind of screening. Table 1 summarizes the main characteristics of the general and specific suppressors including the proved or putative cellular process where they can be participating (Saccharomyces Genome Database (SGD): www.yeastgenome.org; Gene Ontology (GO) database: www.geneontology.org). Regarding the general suppressors, *ALG7* encodes the UDP-N-acetyl-glucosamine-1-P-transferase which catalyzes the first step of N-glycosylation and is a direct target of Tn [32,33]; *GFA1* encodes the glutamine-fructose-6-phosphate amidotransferase which participates in the synthesis of chitin, a constituent of the yeast cell wall, and in the synthesis of N-acetylglucosamine [34,35]; and *YOR1* codes for an ATP-binding cassette (ABC) transporter located in the plasma membrane [36,37] which participates in cell detoxification processes. Regarding the specific *hog1Δ* suppressors, these include genes that code for proteins with a variety of functions. *NAB6* encodes a protein that binds polyadenylated RNAs which mainly encode proteins destined to the cell wall [38]; *KIN2* and its paralogous *KIN1* encode serine/threonine protein kinases that have been implicated in exocytosis and may also play a role in septin cytoskeleton and cell wall organization [39,40]; *RER2* encodes the *cis*-prenyltransferase involved in the production of dolichol from the isoprenoid lipid farnesyl diphosphate [41]. Dolichol is the acceptor and carrier of oligosaccharides that are transferred to proteins during the folding process. *RER1* encodes a protein known as Retention in the Endoplasmic Reticulum which participates in protein retention in the ER lumen and in retrograde vesicle-mediated transport from Golgi to ER [42,43]; and *ECM13* encodes a protein of unknown function that is upregulated by cell wall damage and appears to be involved in cell wall biosynthesis and architecture [44,45].

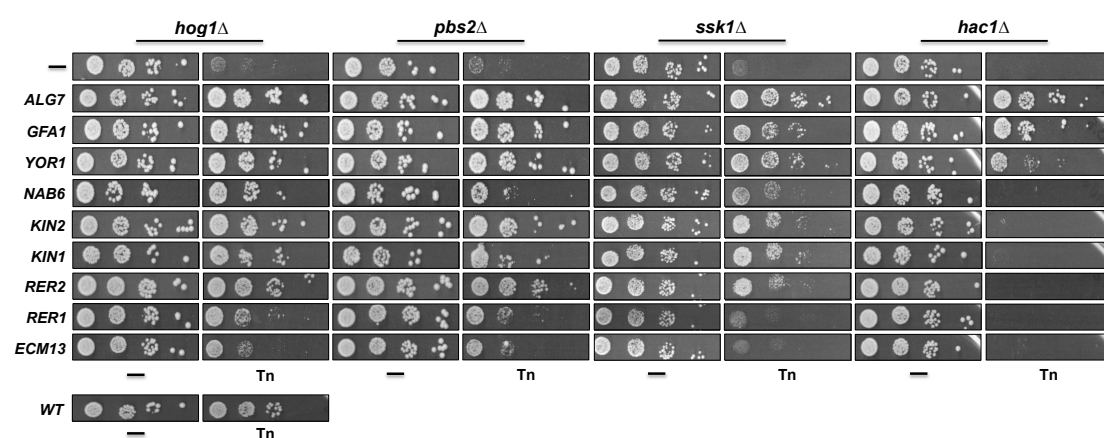


Figure 3. Effect of expression of suppressor genes in the Tn sensitivity of different strains. The suppressor genes were overexpressed in the indicated strains as described in Figure legend 2C. A serial dilution assay was performed as described (Figure legend 2B). Plates were incubated at 30 °C for 72 h and scanned.

Table 1. General and specific suppressors and the cellular process where they participate.

Gene	Protein Name	Biological Process	Cellular Component
<i>ALG7</i>	UDP-N-acetyl-glycosamine-1-P-transferase	Protein N-linked glycosylation	Endoplasmic reticulum
<i>GFA1</i>	Glutamine-fructose-6-phosphate amidotransferase	Cell wall biosynthesis	Unknown
<i>YOR1</i>	Plasma membrane ATP-binding cassette (ABC) transporter	Xenobiotic transport	Plasma membrane
<i>NAB6</i>	Putative RNA binding protein	Binds to poliA RNAs	Cytoplasm
<i>KIN2</i>	Serine/threonine protein kinase	Exocytosis	Plasma membrane
<i>KIN1</i>	Serine/threonine protein kinase	Exocytosis	Plasma membrane
<i>RER2</i>	Cis-prenyltransferase	ER to Golgi vesicle-mediated transport. Protein glycosilation	Endoplasmic reticulum
<i>RER1</i>	Retention in the endoplasmic reticulum	ER to Golgi vesicle-mediated transport. Protein retention in the ER lumen. Retrograde vesiclemediated transport, Golgi to ER	COPI-coated vesicle vacuole
<i>ECM13</i>	Protein induced by treatment with methoxysoralen and UVA irradiation	Cell wall biosynthesis?	Unknown

3.3. Inactivation of Some Suppressor Genes Confers Sensitivity to Tn

We next evaluated whether the inactivation of some of the suppressor genes affects cell growth in Tn and KCl. In this assay we did not include *ALG7*, *GFA1*, and *RER2* null mutants since *ALG7* and *GFA1* are essential genes and the *rer2Δ* mutant has a severe growth impairment. It was evident that disruption of *YOR1*, *NAB6*, and *KIN2* induced sensitivity to Tn at the highest concentration tested (1 µg/mL), while sensitivity was barely detected at lower concentrations (Figure 4). Disruption of *RER1* also induced sensitivity to Tn but to a lesser extent compared to disruption of *YOR1*, *NAB6*, and *KIN2*, while inactivation of the *ECM13* gene did not affect growth in Tn. In contrast to the *kin2Δ* mutant, the *kin1Δ* mutant showed very low sensitivity to Tn. As expected, none of the null mutants of the suppressor genes showed growth defects when they were plated on 1M KCl (Figure 4). Additionally, we detected that inactivation of *YOR1*, *NAB6*, *KIN2*, and *KIN1* in a *hog1Δ* background increased the sensitivity to Tn shown by the *hog1Δ* mutant (Figure 4), suggesting that they might participate in Hog1 independent pathways during the Tn response. In contrast, inactivation of *RER1* and *ECM13* did not affect the Tn sensitivity of the *hog1Δ* mutant, suggesting that they may be components of the same pathway.

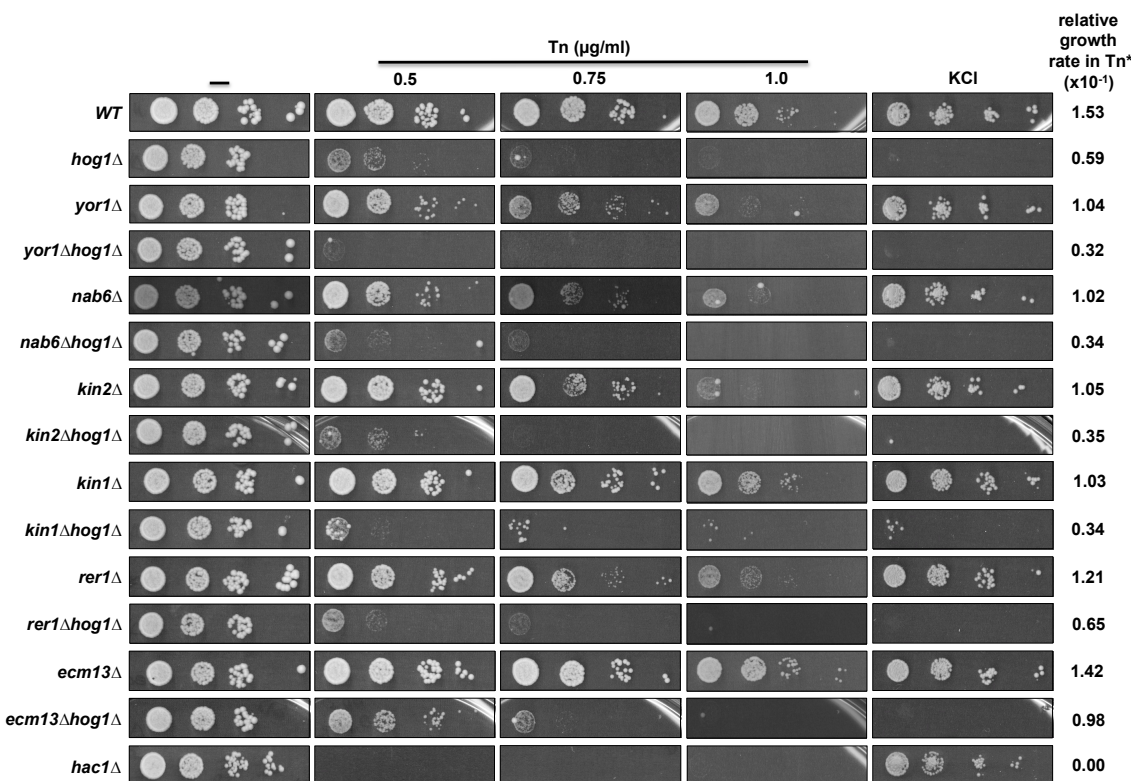


Figure 4. Effect of the inactivation of the suppressor genes on Tn sensitivity and their epistatic interaction with *HOG1*. Single mutants of each suppressor ORF (obtained from the EUROSCARF collection) and the double mutants (constructed as described in the methods section), were tested in different concentrations of Tn or 1M KCl. Yeast cells were grown in YPD and plated as described in Figure legend 2B. Plates were incubated at 30 °C for 72 h and scanned. (*) Relative growth rate was determined from growth at 0.5 µg/mL Tn as described in Figure legend 2.

3.4. Suppressor Genes may Form an Interaction Network with HOG1

The genes that suppress the Tn sensitivity of the *hog1Δ* strain do not appear to encode canonical interactors of Hog1. However, it could be that a putative interaction with one or more suppressor proteins would occur in conditions that induce ER stress. Therefore, we looked for physical interactions between Hog1 and the specific suppressor proteins in the presence of Tn. Using Hog1 as bait and the specific suppressor proteins Nab6, Kin1, Kin2, Rer1, Rer2, and Ecm13 as preys we performed a Bimolecular Fluorescence Complementation (BiFC) assay to detect physical interactions. As expected, none of the suppressor proteins tested appeared to interact physically with Hog1 with and without Tn exposure (Supplementary Table S3), although the fluorescence displayed by the Kin2-Hog1 and Rer2-Hog1 pairs under un-induced conditions was slightly higher than the negative control (Supplementary Table S3). This observation suggests that the suppressors could require one or more intermediates to associate physically with Hog1.

In order to determine whether or not the suppressor genes could participate in functional processes required to cope with the ER stress induced by Tn, we constructed a physical interaction network based on available data from the BioGRID database (Figure 5). This analysis showed that five suppressors, namely Kin1, Kin2, Rer2, Gfa1, and Nab6 may indeed interact with Hog1 through one intermediate. For Kin1, Rer2, and Gfa1, the intermediate protein is Ssb2, a cytoplasmic chaperon of the Hsp70 family that is involved in protein folding processes [46]. Interestingly, Rer2 may also have a physical interaction with Hog1 through Gis2, a RNA binding protein present in processing bodies and stress granules, which contain translationally repressed RNAs [47]. Although the suppression mechanism cannot be deducted from the structure of the interaction network, it provides relevant information

regarding proteins that belong to pathways linked with the ER stress response and not previously associated with Hog1.

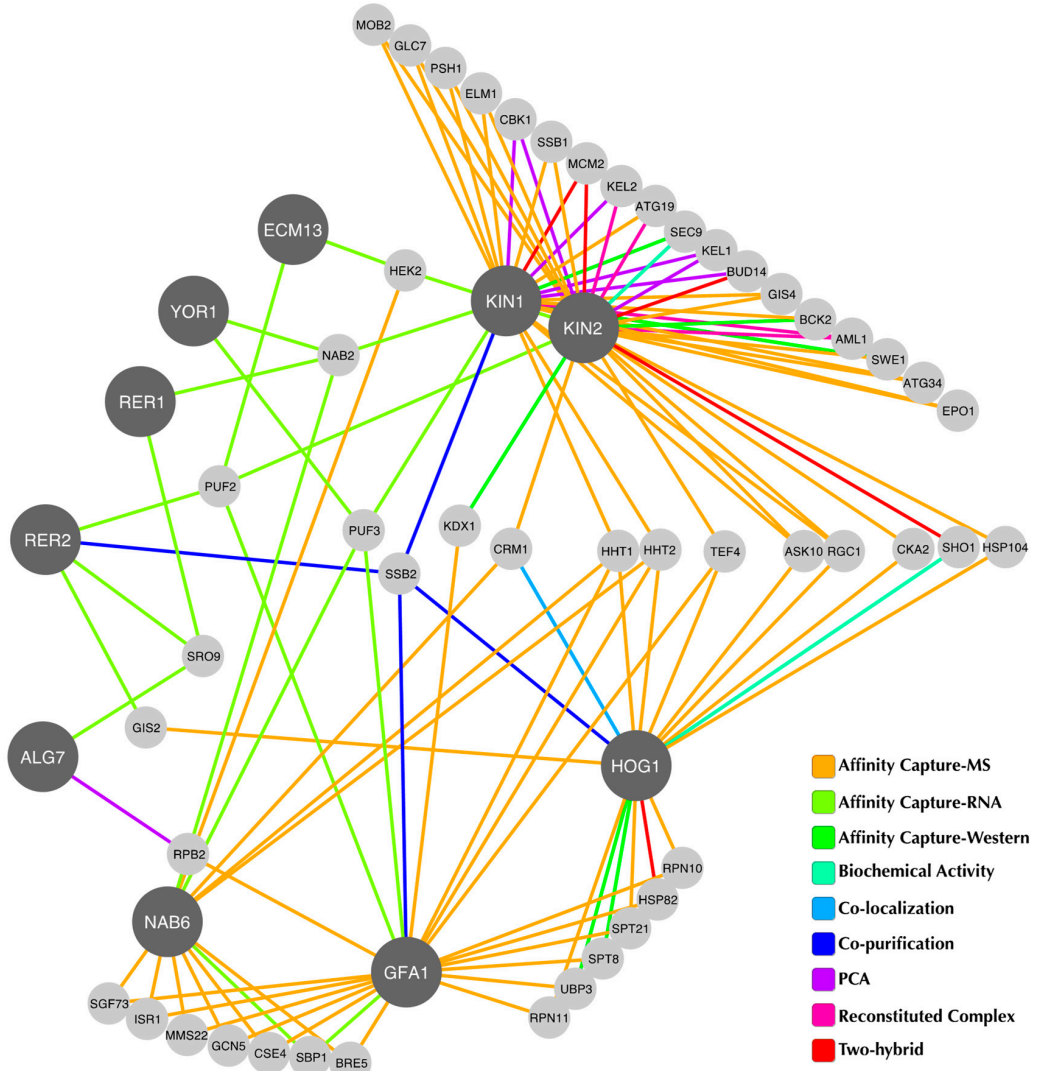


Figure 5. Physical interaction network. Physical interactions of suppressor proteins and Hog1 as deduced from the BioGRID database and visualised with Cytoscape. The network was constructed according to the criteria described in the methods section. Hog1 and suppressor proteins are depicted with dark grey circles. The connecting lines represent the physical interactions and are colored according to the experimental assay that supports each interaction. Known interactors found in the database are colored in light grey.

Since *SSB2* encodes a chaperon of the Hsp70 family that participates in protein folding and appears to be an important interaction node for *Rer2* and *Kin1* we evaluated its involvement in the ER stress response. We observed that the mutant lacking *Ssb2* showed resistance to Tn at the same level as the wild type strain (Figure 6), however overexpression of *RER2*, *KIN1*, and its paralog *KIN2* in the *ssb2Δ* mutant increased its resistance to Tn, while overexpression of *RER1* and *ECM13* did not (Figure 6). This observation indicates that *RER2*, *KIN1*, and *KIN2* interact genetically with *SSB2*, and also validates the proposed physical interaction network.

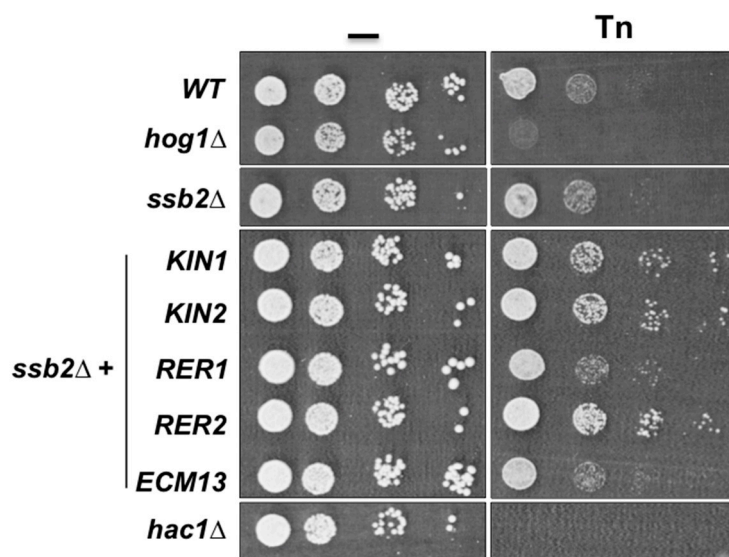


Figure 6. Effect of the inactivation of *SSB2* and overexpression of suppressor genes on Tn sensitivity. The single *ssb2Δ* mutant and transformants carrying the indicated genes were tested in 1.0 $\mu\text{g}/\text{mL}$ of Tn as indicated in figure legend 2B. Overexpression was achieved by cloning the indicated genes in the multicopy plasmid YEp352 under the control of their own promoter. Serial dilution assay was performed as indicated in figure legend 2B. Plates were incubated at 30 °C for 72 h and scanned.

3.5. The Cis-Prenyltransferase Srt1 also Suppresses the Tn Sensitivity of the Hog1Δ Mutant

Tn is a protein glycosylation inhibitor that blocks the activity of the UDP-*N*-acetylglucosamine phosphate transferase (Alg7). This enzyme catalyzes the addition of *N*-acetylglucosamine to dolichol-phosphate, located in the ER membrane. Production of dolichol from farnesyl diphosphate is dependent on the activity of the *cis*-prenyltransferase Rer2 which synthesizes dolichols of 14–18 isoprene units. Yeast cells express a second *cis*-prenyltransferase known as Srt1 (Figure 7A), located mainly in lipid droplets, which synthesizes dolichols of 18–23 isoprene units [41,48]. We tested whether overexpression of *SRT1* would suppress the Tn sensitivity displayed by the *hog1Δ* mutant. We found that *hog1Δ* cells overexpressing *SRT1* grow as well as those expressing *RER2* in a medium containing 0.75 $\mu\text{g}/\text{mL}$ Tn (Figure 7B). Accordingly, overexpression of *SRT1* was able to revert the sensitivity of a *pbs2Δ* mutant but not that of the *hac1Δ* mutant, indicating that the suppression process is specific to the HOG1 pathway (not shown). These results suggest that an increase in the cellular concentration of dolichol may revert the Tn sensitivity displayed by the *hog1Δ* mutant.

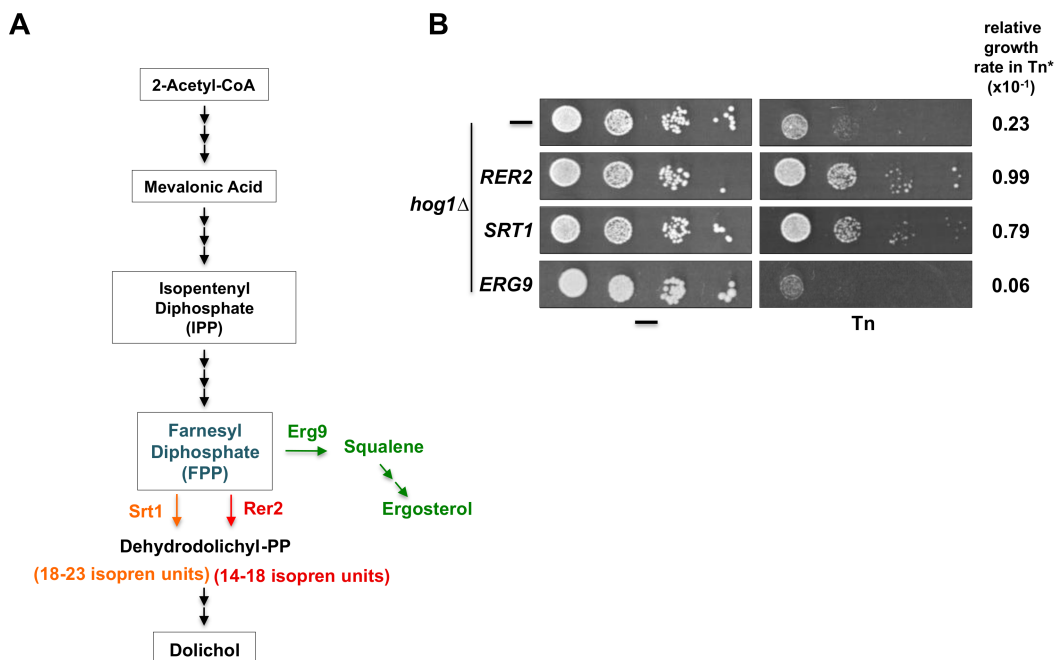


Figure 7. Effects of overexpression of proteins involved in the dolichol and ergosterol synthesis pathways on *hog1Δ* Tn sensitivity. (A) Schematic representation of the dolichol and ergosterol synthesis pathways. Farnesyl diphosphate (FPP) is synthesized from 2-Acetyl-CoA through the mevalonic acid pathway. FPP is a shared substrate of Rer2 (and Srt1) and Erg9 to synthesize either dolichol or ergosterol respectively. (B) Serial dilution assay of the *hog1Δ* strain transformed with the pYES2 vector or with pYES2 carrying *RER2*, *SRT1*, or *ERG9* genes. A spot dilution assay was performed as described above (Figure legend 2B) except that the cells were grown in SRaf medium and then spotted onto SGal or SGal containing 0.5 µg/mL Tn. Plates were incubated at 30 °C for 72 h and scanned. (*) The growth rate in Tn was measured as described in Figure legend 2C.

3.6. Hog1-Tn Sensitivity Is Enhanced by Overexpression of ERG9

Farnesyl diphosphate (FPP) is not only a precursor of dolichol but also of ergosterol through a series of reactions initiated by the farnesyl-diphosphate farnesyl transferase encoded by the essential *ERG9* gene (Figure 7A). We set out to determine whether the over-utilization of farnesyl diphosphate for the production of ergosterol would affect growth of the *hog1Δ* mutant in Tn. We found that the sensitivity to 0.5 µg/mL Tn of the *hog1Δ* mutant was enhanced when *ERG9* was overexpressed (Figure 7B). Taking this result together with the observation of the effect of *RER2* and *SRT1* overexpression indicated that the effect of Tn on the *hog1Δ* mutant may in part be dependent on the cellular concentration of dolichol.

3.7. The *hog1Δ* Strain Has Reduced Polyprenols Concentration

Based on the previous observations, we hypothesized that the deficient growth of the *hog1Δ* mutant in media containing Tn could be due to an impairment in the dolichol synthesis. We determined the polyprenol content by liquid chromatography (HPLC) in wild type, *hog1Δ*, and the *hog1Δ* overexpressing *RER2* strains treated or not treated with Tn. It was possible to detect in the three strains an enriched polyprenol that may range from 12 to 15 isopren units (Figure 8A). In the wild type strain, the Tn treatment induced approximately a two-fold increase in dolichol concentration (Figure 8B). The same treatment however was unable to induce an increment of dolichol in the *hog1Δ* strain. Overexpression of *RER2* in the *hog1Δ* mutant produced an increment of dolichol, which was statistically significant in both treatments (Figure 8B). Taking together, these results suggest that the *hog1Δ* strain has a strong defect in the polyprenol metabolism under stressful conditions and that this defect is partially compensated with the *RER2* overexpression.

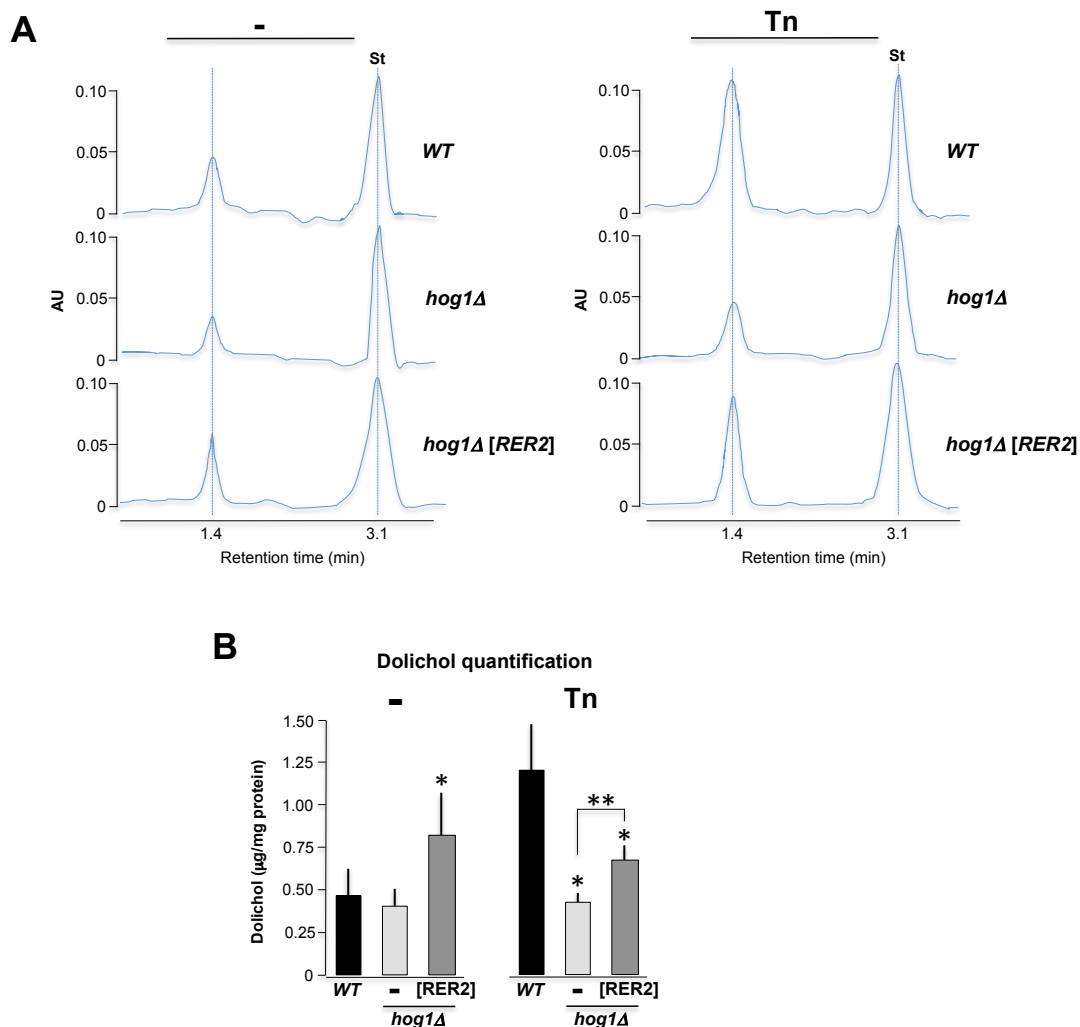


Figure 8. Effect of Hog1 inactivation and Tn treatment on the polyisoprenols concentration. (A) HPLC analysis of dolichols isolated from the wild type, *hog1Δ* and *hog1Δ[RER2]* strains, with or without 1 µg/mL Tn. Dolichol detection was performed by reverse phase HPLC analysis. One representative profile out of three is depicted. 1 µg/µL of standard dolichol (18 isoprene units) was included as internal control (St). (B) Dolichol concentration was calculated by determining the area under the curve of the dolichol peak relative to the area under the curve of the standard peak (St) and adjusted by protein concentration (See supplemental Table S4). Mean values (\pm SD) were calculated from three independent experiments. One asterisk indicates statistical significance regarding the WT strain. Two asterisks indicate statistical significance between *hog1Δ* and *hog1Δ[RER2]* strains.

4. Discussion

The isolated suppressors of Hog1 Tn sensitivity allowed us to identify genes whose products participate in a restricted number of cellular processes. According to the SGD and GO geneontology databases, these include protein glycosylation (Rer2 and Alg7); vesicle transport and exocytosis (Rer1, Rer2, Kin1, and Kin2); cell wall organization or biogenesis (Gfa1, Nab6, and Ecm13); and cell detoxification processes (Yor1). The limited number of specific suppressors that were detected indicates that the mechanisms by which Hog1 participates in a protective response to ER stress may be limited to very few pathways. It is interesting that with this screening we did not detect proven physical interactors of Hog1. This can be explained by the fact that most interaction assays with Hog1 are carried out under hyperosmotic conditions. This observation suggests that the suppressor proteins may not be phosphorylation targets of Hog1 and that Hog1 may play a regulatory role in the Tn response through one or more intermediates with the suppressor proteins. Several of these intermediates participate

in cellular processes related to stress conditions. However, it has been demonstrated that the kinase activity of Hog1 is essential to trigger a protective response to ER stress inducers [13,49]. Accordingly, we found putative Hog1 phosphorylation motifs (S/T-P) [50,51] in some suppressor proteins except Rer1, Rer2, and Alg7. Kin1 and Kin2 have 3 and 5 putative S/T-P phosphorylation sites respectively, while Nab6, Yor1 and Gfa1 contain one site each [52] (<https://phosphogrid.org/>). Although we cannot rule out that Hog1 may phosphorylate some suppressor proteins our interaction assay disregard this possibility, however a more extensive interaction study would be suitable.

It is interesting that none of the suppressors found plays a role in gene transcription and that all of them have extra-nuclear activities, which is in agreement with the observation that Hog1 is not transported into the nucleus in response to Tn stress [13,49]. Additionally, the specific suppressors found in this study were able to revert the Tn sensitivity shown by the *pbs2Δ* and the *ssk1Δ* mutants. This indicates that these suppressors may participate in one or several pathways made up of extra-nuclear proteins, including components of the phosphorelay pathway. Accordingly, a version of Hog1 that has been anchored to the plasma membrane by means of a CAAX motif was able to provide full ER stress protection [49]. All these observations support a model in which Hog1 shows regulatory cytoplasmic activity in order to counteract the stress caused by Tn.

The functions that Alg7, Gfa1 and Yor1 have in the cell make them logical candidates to provide cellular protection against Tn. In fact, they revert the Tn sensitivity not only of the *hog1Δ* mutant but also that of the *hac1* mutant. The increased concentration of Alg7, the UDP-N-acetylglucosamine phosphate transferase that catalyzes the addition of N-acetylglucosamine to dolichyl-phosphate [32], would titrate the drug due to the fact that Tn and the enzyme substrate UDP-GlcNAc have a similar structure and compete for the enzyme's active site. Similarly, the overexpression of Gfa1, an amidotransferase that participates in the formation of glucosamine 6-P, which is a precursor of UDP-GlcNAc [34], would increase the concentration of UDP-GlcNAc, counteracting the inhibitory effect of Tn on Alg7. Finally, the overactivity of the ABC transporter Yor1 would help to eliminate the Tn from the cell as it does with different organic compounds and xenobiotics [36,53]. The finding of these suppressors is an indication that the screening has been performed properly since their function is related to the action mode of Tn.

Within the specific suppressors, *KIN1* and *KIN2* encode serine/threonine kinases. They are part of the Snf1 kinase family of the Ca^{2+} /calmodulin-dependent kinase II (CaMK), involved in the regulation of cell polarity and exocytosis, as well as in the regulation of the septin cytoskeleton and cell wall [39,40]. Their *hog1Δ*-suppression activity may be related to one of those functions; however, it has been recently assigned a new role for the Kin kinases. It appears that Kin1 and Kin2 may have a role in the Ire1-mediated targeting and processing of *HAC1* mRNA, thus positively regulating the UPR [54]. Interestingly, as detected by Anshu et al. [54] and in our assays, Kin1 and Kin2 are not totally redundant since a lack of Kin2 produced high sensitivity to Tn; in contrast, a lack of Kin1 barely affected the cellular response to Tn. Since the *HAC1* processing appears to be normal in a *hog1Δ* mutant [13], it is interesting to have found Kin1 and Kin2 as specific suppressors of Hog1. Our epistatic experiments suggest that Hog1 and at least Kin2 act in parallel pathways regarding ER stress. Taken together, these observations suggest that the suppression activity of Kin2 (and perhaps that of Kin1) is more closely related to its function in cell wall regulation and exocytosis, than to its role in regulating the UPR [40,54].

Rer1 and Rer2 were also found as specific Hog1-suppressors. Unlike Kin1 and Kin2, these proteins do not contain putative Hog1 phosphorylation motifs. Rer1 is localized in the early region of the Golgi apparatus and is involved in the retrieval of proteins from the Golgi and is also essential for the proper localization of proteins in the ER [42,43]. Its suppressor activity could be related to its participation in the ER localization of type II membrane proteins, including Mns1, which is the alpha-1,2-mannosidase that catalyzes the last step in glycoprotein maturation in the ER and is required for the ER-associated protein degradation [55–57]. In our assays, disruption of *RER1* moderately impaired the cell in its response to Tn and apparently it is not additive to *HOG1*. The functional relationship between the two proteins in the Tn response requires a more detailed study.

RER2 encodes the *cis*-prenyltransferase enzyme, which catalyzes the conversion of farnesyl diphosphate (FPP) to dehydrololichyl diphosphate, the precursor of dolichol, which is the ER lipid where the oligosaccharide required for the *N*-glycosylation is assembled [41]. The suppression activity of Rer2 could be related mainly to its role in increasing dolichol concentration. This observation is supported by the fact that the *cis*-prenyltransferase Srt1, which catalyzes the same reaction, also suppresses the Tn sensitivity of a *hog1Δ* mutant. Rer2 is localized in dots associated with the ER and in lipid particles, while Srt1 appears to be localized only in lipid particles [48,58]. Nevertheless, Rer2 is expressed in early logarithmic phase and Srt1 is expressed in stationary phase, and the products of Srt1 are apparently not converted totally to dolichol and dolichyl phosphate; Srt1 behaves as a multicopy suppressor of *rer2Δ* mutant [48] indicating that in the absence of Rer2, Srt1 may adequately supplement the dolichol pool. The *rer2Δ* mutant has a severe growth defect while the *srt1Δ* mutant grows normally [41]. All of these characteristics imply that Rer2 and Srt1 are not redundant, and that they play different roles in the cell physiology; interestingly, they suppress the Tn sensitivity of the *hog1Δ* mutant almost to the same level. Here we found evidence that in the presence of Tn the dolichol content in a wild type strain increases significantly. This suggests that one mechanism to partially counteract the Tn effect is by overproducing dolichol. This protective mechanism is defective in the absence of Hog1 and is partially compensated by the overexpression of *RER2*. For the *hog1Δ* mutant the increased production of dolichol by *RER2* overexpression will partially suppress the Tn sensitivity. This finding is interesting since it has been observed that a *Trypanosoma brucei* mutant with defects in the *N*-glycosylation pathway accumulates larger amounts of polypropenols compared to its parental strain [59]. The involvement of Hog1 in lipid metabolism has been observed previously, for example, inhibition of sphingolipids and ergosterol biosynthesis activates the Hog1 pathway [60] and stress-mediated activation of Hog1 represses the synthesis of ergosterol [61]. An alternative approach to test that the suppression activity of Rer2 (and Srt1) is related to its function in the synthesis of dolichol was by overexpressing, in the *hog1Δ* mutant, the *ERG9* gene, which encodes the farnesyl-diphosphate farnesyl transferase [62]. FPP is precursor of squalene, which is eventually converted to ergosterol [63,64]. Indeed, here we found that Erg9 may act as a diverter, converting FPP into squalene and enhancing the Tn sensitivity of the *hog1Δ* mutant. All these evidences indicate that the Hog1 role in the ER stress response could be related in part to its involvement in lipid metabolism including the polypropenol pathway.

The Nab6 and Ecm13 suppression mechanism is at present difficult to deduce since their function remains undefined. Nab6 appears to bind RNAs that encode proteins for the cell wall [38]. It is present in stress granules and co-purifies with Cap-binding proteins and other translation factors [38,65]. It could be that Nab6 regulates translation of this sort of mRNA in response to stress conditions since we detected that the *nab6Δ* mutant is moderately sensitive to Tn. *ECM13* encodes a protein of unknown function that is upregulated by cell wall damage and it may be involved in cell wall biosynthesis and architecture [44,45]; however the null mutant is as resistant to Tn as the wild type strain.

In summary, the screening of high dosage gene suppressors allowed us to conclude that Hog1 may be performing pleiotropic functions in order to regulate the cellular response to ER stress inducers. To counteract the effects of tunicamycin, the cell requires a number of cellular proteins to act in concert with Hog1. It is of the highest interest to study in detail the functional relationship between the suppressor proteins and Hog1. This study opens the field to the investigation of new functions of this MAP kinase in yeast.

Supplementary Materials: The following are available online at <http://www.mdpi.com/2073-4409/8/7/710/s1>, Table S1: Yeast strains used in this work, Table S2: List of oligonucleotides used in this work; Table S3: Relative interaction of Hog1 with suppressor proteins, Table S4: Dolichol concentration determined from HPLC profiles.

Author Contributions: Investigation, M.H.-E., R.M.-G., and E.D.-M.; Methodology, M.H.-E. and A.M.; Writing—original draft, M.H.-E., E.D.-M., A.M., L.K., L.O.-L., and R.C.; Writing—review and editing, M.H.-E., L.K., L.O.-L., and R.C.

Funding: This work was supported by grant numbers CONACyT: CB-254078; and PAPIIT, DAGAPA, UNAM: IN210616.

Acknowledgments: M.H.-E. is a PhD student in the Doctorate program in Biochemical Sciences, Universidad Nacional Autónoma de México (UNAM), and received fellowship 366635 from CONACYT; E.D.-M. is a PhD candidate in the Doctorate program in Biomedical Sciences, Universidad Nacional Autónoma de México (UNAM), and received fellowship 380127 from CONACYT. We wish to acknowledge the technical support provided by the Molecular Biology and Computer Facilities, IFC, UNAM. We acknowledge David Eduardo Meza Sánchez from the Metabolic and Proteomic Unit (RAI) for his technical assistance in the HPLC analysis. We also acknowledge the technical assistance of Ma. Teresa Lara Ortiz, Francisco Torres-Quiroz, Georgina Garza, Juliana Rojo, Norma Sánchez and Martha Calahorra. We acknowledge Patrick Weill for the revision of the English language.

Conflicts of Interest: The authors declare no conflict of interest.

References

1. Hernández-Elvira, M.; Torres-Quiroz, F.; Escamilla-Ayala, A.; Domínguez-Martin, E.; Escalante, R.; Kawasaki, L.; Ongay-Larios, L.; Coria, R. The unfolded protein response pathway in the yeast *Kluyveromyces lactis*. A comparative view among yeast species. *Cells* **2018**, *7*, 106. [[CrossRef](#)] [[PubMed](#)]
2. Domínguez-Martín, E.; Hernández-Elvira, M.; Vincent, O.; Coria, R.; Escalante, R. Unfolding the endoplasmic reticulum of a social amoeba: *Dictyostelium discoideum* as a new model for the study of endoplasmic reticulum stress. *Cells* **2018**, *7*, 56. [[CrossRef](#)] [[PubMed](#)]
3. Fanata, W.I.D.; Lee, S.Y.; Lee, K.O. The unfolded protein response in plants: A fundamental adaptive cellular response to internal and external stresses. *J. Proteom.* **2013**, *93*, 356–368. [[CrossRef](#)] [[PubMed](#)]
4. Chakrabarti, A.; Chen, A.W.; Varner, J.D. A review of the mammalian unfolded protein response. *Biotechnol. Bioeng.* **2011**, *108*, 2777–2793. [[CrossRef](#)] [[PubMed](#)]
5. Cox, J.S.; Shamu, C.E.; Walter, P. Transcriptional induction of genes encoding endoplasmic reticulum resident proteins requires a transmembrane protein kinase. *Cell* **1993**, *73*, 1197–1206. [[CrossRef](#)]
6. Shamu, C.E.; Walter, P. Oligomerization and phosphorylation of the Ire1p kinase during intracellular signaling from the endoplasmic reticulum to the nucleus. *EMBO J.* **1996**, *15*, 3028–3039. [[CrossRef](#)] [[PubMed](#)]
7. Welihinda, A.A.; Kaufman, R.J. The Unfolded Protein Response Pathway in *Saccharomyces cerevisiae*: Oligomerization and trans-phosphorylation of Ire1p (Ern1p) are required for kinase activation. *J. Biol. Chem.* **1996**, *271*, 18181–18187. [[CrossRef](#)] [[PubMed](#)]
8. Sidrauski, C. The unfolded protein response: An intracellular signaling pathway with many surprising features. *Trends Cell Biol.* **1998**, *8*, 245–249. [[CrossRef](#)]
9. Cox, J.S.; Walter, P. A novel mechanism for regulating activity of a transcription factor that controls the unfolded protein response. *Cell* **1996**, *87*, 391–404. [[CrossRef](#)]
10. Mori, K.; Ogawa, N.; Kawahara, T.; Yanagi, H.; Yura, T. Palindrome with spacer of one nucleotide is characteristic of the *cis*-acting unfolded protein response element in *Saccharomyces cerevisiae*. *J. Biol. Chem.* **1998**, *273*, 9912–9920. [[CrossRef](#)]
11. Chen, Y.; Feldman, D.E.; Deng, C.; Brown, J.A.; De Giacomo, A.F.; Gaw, A.F.; Shi, G.; Le, Q.T.; Brown, J.M.; Koong, A.C. Identification of mitogen-activated protein kinase signaling pathways that confer resistance to endoplasmic reticulum stress in *Saccharomyces cerevisiae*. *Mol. Cancer Res.* **2005**, *3*, 669–677. [[CrossRef](#)] [[PubMed](#)]
12. Bicknell, A.A.; Tourtellotte, J.; Niwa, M. Late phase of the endoplasmic reticulum stress response pathway is regulated by Hog1 MAP kinase. *J. Biol. Chem.* **2010**, *285*, 17545–17555. [[CrossRef](#)] [[PubMed](#)]
13. Torres-Quiroz, F.; García-Marqués, S.; Coria, R.; Randez-Gil, F.; Prieto, J.A. The activity of yeast Hog1 MAPK is required during endoplasmic reticulum stress induced by tunicamycin exposure. *J. Biol. Chem.* **2010**, *285*, 20088–20096. [[CrossRef](#)] [[PubMed](#)]
14. Brewster, J.; de Valoir, T.; Dwyer, N.; Winter, E.; Gustin, M. An osmosensing signal transduction pathway in yeast. *Science* **1993**, *259*, 1760–1763. [[CrossRef](#)] [[PubMed](#)]
15. Maeda, T.; Wurgler-Murphy, S.M.; Saito, H. A two-component system that regulates an osmosensing MAP kinase cascade in yeast. *Nature* **1994**, *369*, 242–245. [[CrossRef](#)] [[PubMed](#)]
16. Posas, F. Osmotic activation of the HOG MAPK pathway via Ste11p MAPKKK: Scaffold role of Pbs2p MAPKK. *Science* **1997**, *276*, 1702–1705. [[CrossRef](#)]

17. Ferrigno, P. Regulated nucleo/cytoplasmic exchange of HOG1 MAPK requires the importin beta homologs NMD5 and XPO1. *EMBO J.* **1998**, *17*, 5606–5614. [[CrossRef](#)]
18. Reiser, V.; Salah, S.M.; Ammerer, G. Polarized localization of yeast Pbs2 depends on osmostress, the membrane protein Sho1 and Cdc42. *Nat. Cell Biol.* **2000**, *2*, 620–627. [[CrossRef](#)]
19. de Nadal, E.; Posas, F. Multilayered control of gene expression by stress-activated protein kinases. *EMBO J.* **2010**, *29*, 4–13. [[CrossRef](#)]
20. Martínez-Montaños, F.; Pascual-Ahuir, A.; Proft, M. Toward a genomic view of the gene expression program regulated by osmostress in yeast. *OMICS J. Integr. Biol.* **2010**, *14*, 619–627. [[CrossRef](#)]
21. Aoki, Y.; Kanki, T.; Hirota, Y.; Kurihara, Y.; Saigusa, T.; Uchiumi, T.; Kang, D. Phosphorylation of Serine 114 on Atg32 mediates mitophagy. *Mol. Biol. Cell* **2011**, *22*, 3206–3217. [[CrossRef](#)] [[PubMed](#)]
22. Mao, K.; Klionsky, D.J. MAPKs regulate mitophagy in *Saccharomyces cerevisiae*. *Autophagy* **2011**, *7*, 1564–1565. [[CrossRef](#)] [[PubMed](#)]
23. Jones, G.M.; Stalker, J.; Humphray, S.; West, A.; Cox, T.; Rogers, J.; Dunham, I.; Prelich, G. A systematic library for comprehensive overexpression screens in *Saccharomyces cerevisiae*. *Nat. Methods* **2008**, *5*, 239–241. [[CrossRef](#)] [[PubMed](#)]
24. Amberg, D.C.; Burke, D.; Strathern, J.N.; Burke, D. *Methods in Yeast Genetics: A Cold Spring Harbor Laboratory Course Manual*, 2005 ed.; Cold Spring Harbor Laboratory Press: Cold Spring Harbor, NY, USA, 2005; ISBN 978-0-87969-728-0.
25. Hill, J.E.; Myers, A.M.; Koerner, T.J.; Tzagoloff, A. Yeast/*E. coli* shuttle vectors with multiple unique restriction sites. *Yeast* **1986**, *2*, 163–167. [[CrossRef](#)] [[PubMed](#)]
26. Sung, M.-K.; Huh, W.-K. Bimolecular fluorescence complementation analysis system for in vivo detection of protein-protein interaction in *Saccharomyces cerevisiae*. *Yeast* **2007**, *24*, 767–775. [[CrossRef](#)]
27. Stark, C. BioGRID: A general repository for interaction datasets. *Nucleic Acids Res.* **2006**, *34*, D535–D539. [[CrossRef](#)]
28. Shannon, P. Cytoscape: A software environment for integrated models of biomolecular interaction networks. *Genome Res.* **2003**, *13*, 2498–2504. [[CrossRef](#)]
29. Baryshnikova, A. Exploratory analysis of biological networks through visualization, clustering, and functional annotation in cytoscape. *Cold Spring Harb. Protoc.* **2016**, *2016*. [[CrossRef](#)]
30. Grabińska, K.; Sosińska, G.; Orłowski, J.; Swiezewska, E.; Berges, T.; Karst, F.; Palamarczyk, G. Functional relationships between the *Saccharomyces cerevisiae* cis-prenyltransferases required for dolichol biosynthesis. *Acta Biochim. Pol.* **2005**, *52*, 221–232.
31. Levin, D.E.; Hammond, C.I.; Ralston, R.O.; Bishop, J.M. Two yeast genes that encode unusual protein kinases. *Proc. Natl. Acad. Sci. USA* **1987**, *84*, 6035–6039. [[CrossRef](#)]
32. Rine, J.; Hansen, W.; Hardeman, E.; Davis, R.W. Targeted selection of recombinant clones through gene dosage effects. *Proc. Natl. Acad. Sci. USA* **1983**, *80*, 6750–6754. [[CrossRef](#)] [[PubMed](#)]
33. Barnes, G.; Hansen, W.J.; Holcomb, C.L.; Rine, J. Asparagine-linked glycosylation in *Saccharomyces cerevisiae*: Genetic analysis of an early step. *Mol. Cell. Biol.* **1984**, *4*, 2381–2388. [[CrossRef](#)] [[PubMed](#)]
34. Watzele, G.; Tanner, W. Cloning of the glutamine: Fructose-6-phosphate amidotransferase gene from yeast. Pheromonal regulation of its transcription. *J. Biol. Chem.* **1989**, *264*, 8753–8758. [[PubMed](#)]
35. Bowman, S.M.; Free, S.J. The structure and synthesis of the fungal cell wall. *BioEssays* **2006**, *28*, 799–808. [[CrossRef](#)] [[PubMed](#)]
36. Katzmann, D.J.; Hallstrom, T.C.; Voet, M.; Wysock, W.; Golin, J.; Volckaert, G.; Moye-Rowley, W.S. Expression of an ATP-binding cassette transporter-encoding gene (YOR1) is required for oligomycin resistance in *Saccharomyces cerevisiae*. *Mol. Cell. Biol.* **1995**, *15*, 6875–6883. [[CrossRef](#)] [[PubMed](#)]
37. Rogers, B.; Decottignies, A.; Kolaczkowski, M.; Carvajal, E.; Balzi, E.; Goffeau, A. The pleitropic drug ABC transporters from *Saccharomyces cerevisiae*. *J. Mol. Microbiol. Biotechnol.* **2001**, *3*, 207–214. [[PubMed](#)]
38. Abruzzi, K.; Denome, S.; Olsen, J.R.; Assenholt, J.; Haaning, L.L.; Jensen, T.H.; Rosbash, M. A novel plasmid-based microarray screen identifies suppressors of rrp6 in *Saccharomyces cerevisiae*. *Mol. Cell. Biol.* **2007**, *27*, 1044–1055. [[CrossRef](#)]
39. Elbert, M.; Rossi, G.; Brennwald, P. The yeast Par-1 homologs Kin1 and Kin2 show genetic and physical interactions with components of the exocytic machinery. *Mol. Biol. Cell* **2005**, *16*, 532–549. [[CrossRef](#)]

40. Yuan, S.-M.; Nie, W.-C.; He, F.; Jia, Z.-W.; Gao, X.-D. Kin2, the budding yeast ortholog of animal MARK/PAR-1 kinases, localizes to the sites of polarized growth and may regulate septin organization and the cell wall. *PLoS ONE* **2016**, *11*, e0153992. [[CrossRef](#)]
41. Sato, M.; Sato, K.; Nishikawa, S.; Hirata, A.; Kato, J.; Nakano, A. The yeast *RER2* gene, identified by endoplasmic reticulum protein localization mutations, encodes *cis*-Prenyltransferase, a key enzyme in dolichol synthesis. *Mol. Cell. Biol.* **1999**, *19*, 471–483. [[CrossRef](#)]
42. Nishikawa, S.; Nakano, A. Identification of a gene required for membrane protein retention in the early secretory pathway. *Proc. Natl. Acad. Sci. USA* **1993**, *90*, 8179–8183. [[CrossRef](#)] [[PubMed](#)]
43. Sato, K.; Sato, M.; Nakano, A. Rer1p as common machinery for the endoplasmic reticulum localization of membrane proteins. *Proc. Natl. Acad. Sci. USA* **1997**, *94*, 9693–9698. [[CrossRef](#)] [[PubMed](#)]
44. Lussier, M.; White, A.M.; Sheraton, J.; di Paolo, T.; Treadwell, J.; Southard, S.B.; Horenstein, C.I.; Chen-Weiner, J.; Ram, A.F.; Kapteyn, J.C.; et al. Large scale identification of genes involved in cell surface biosynthesis and architecture in *Saccharomyces cerevisiae*. *Genetics* **1997**, *147*, 435–450.
45. García, R.; Bermejo, C.; Grau, C.; Pérez, R.; Rodríguez-Peña, J.M.; Francois, J.; Nombela, C.; Arroyo, J. The global transcriptional response to transient cell wall damage in *Saccharomyces cerevisiae* and its regulation by the cell integrity signaling pathway. *J. Biol. Chem.* **2004**, *279*, 15183–15195. [[CrossRef](#)]
46. Pfund, C.; Lopez-Hoyo, N.; Ziegelhoffer, T.; Schilke, B.A.; Lopez-Buesa, P.; Walter, W.A.; Wiedmann, M.; Craig, E.A. The molecular chaperone Ssb from *Saccharomyces cerevisiae* is a component of the ribosome—Nascent chain complex. *EMBO J.* **1998**, *17*, 3981–3989. [[CrossRef](#)] [[PubMed](#)]
47. Rojas, M.; Farr, G.W.; Fernandez, C.F.; Lauden, L.; McCormack, J.C.; Wolin, S.L. Yeast Gis2 and its human ortholog CNBP are novel components of stress-induced RNP granules. *PLoS ONE* **2012**, *7*, e52824. [[CrossRef](#)] [[PubMed](#)]
48. Sato, M.; Fujisaki, S.; Sato, K.; Nishimura, Y.; Nakano, A. Yeast *Saccharomyces cerevisiae* has two *cis*-prenyltransferases with different properties and localizations. Implication for their distinct physiological roles in dolichol synthesis. *Genes Cells* **2001**, *6*, 495–506. [[CrossRef](#)]
49. García-Marqués, S.; Randez-Gil, F.; Prieto, J.A. Nuclear versus cytosolic activity of the yeast Hog1 MAP kinase in response to osmotic and tunicamycin-induced ER stress. *FEBS Lett.* **2015**, *589*, 2163–2168. [[CrossRef](#)]
50. Songyang, Z.; Lu, K.P.; Kwon, Y.T.; Tsai, L.H.; Filhol, O.; Cochet, C.; Brickey, D.A.; Soderling, T.R.; Bartleson, C.; Graves, D.J.; et al. A structural basis for substrate specificities of protein Ser/Thr kinases: Primary sequence preference of casein kinases I and II, NIMA, phosphorylase kinase, calmodulin-dependent kinase II, CDK5, and Erk1. *Mol. Cell. Biol.* **1996**, *16*, 6486–6493. [[CrossRef](#)]
51. Bardwell, L. Mechanisms of MAPK signaling specificity. *Biochem. Soc. Trans.* **2006**, *34*, 837–841. [[CrossRef](#)]
52. Ledesma, L.; Sandoval, E.; Cruz-Martínez, U.; Escalante, A.M.; Mejía, S.; Moreno-Álvarez, P.; Ávila, E.; García, E.; Coello, G.; Torres-Quiroz, F. YAAM: Yeast Amino Acid Modifications Database. *Database* **2018**, *2018*. [[CrossRef](#)] [[PubMed](#)]
53. Cui, Z.; Hirata, D.; Tsuchiya, E.; Osada, H.; Miyakawa, T. The Multidrug Resistance-associated Protein (MRP) Subfamily (Yrs1/Yor1) of *Saccharomyces cerevisiae* is important for the tolerance to a broad range of organic anions. *J. Biol. Chem.* **1996**, *271*, 14712–14716. [[CrossRef](#)] [[PubMed](#)]
54. Anshu, A.; Mannan, M.A.; Chakraborty, A.; Chakrabarti, S.; Dey, M. A novel role for protein kinase Kin2 in regulating *HAC1* mRNA translocation, splicing, and translation. *Mol. Cell. Biol.* **2015**, *35*, 199–210. [[CrossRef](#)] [[PubMed](#)]
55. Camirand, A.; Heysen, A.; Grondin, B.; Herscovics, A. Glycoprotein biosynthesis in *Saccharomyces cerevisiae*. Isolation and characterization of the gene encoding a specific processing alpha-mannosidase. *J. Biol. Chem.* **1991**, *266*, 15120–15127. [[PubMed](#)]
56. Massaad, M.J.; Franzusoff, A.; Herscovics, A. The processing α 1,2-mannosidase of *Saccharomyces cerevisiae* depends on Rer1p for its localization in the endoplasmic reticulum. *Eur. J. Cell Biol.* **1999**, *78*, 435–440. [[CrossRef](#)]
57. Sato, K.; Sato, M.; Nakano, A. Rer1p, a retrieval receptor for ER membrane proteins, recognizes transmembrane domains in multiple modes. *Mol. Biol. Cell* **2003**, *14*, 3605–3616. [[CrossRef](#)] [[PubMed](#)]
58. Currie, E.; Guo, X.; Christiano, R.; Chitraju, C.; Kory, N.; Harrison, K.; Haas, J.; Walther, T.C.; Farese, R.V. High confidence proteomic analysis of yeast LDs identifies additional droplet proteins and reveals connections to dolichol synthesis and sterol acetylation. *J. Lipid Res.* **2014**, *55*, 1465–1477. [[CrossRef](#)] [[PubMed](#)]

59. Acosta-Serrano, A.; O'Rear, J.; Quellhorst, G.; Lee, S.H.; Hwa, K.-Y.; Krag, S.S.; Englund, P.T. Defects in the N-linked oligosaccharide biosynthetic pathway in a *Trypanosoma brucei* glycosylation mutant. *Eukaryot. Cell* **2004**, *3*, 255–263. [[CrossRef](#)] [[PubMed](#)]
60. Tanigawa, M.; Kihara, A.; Terashima, M.; Takahara, T.; Maeda, T. Sphingolipids regulate the yeast high-osmolarity glycerol response pathway. *Mol. Cell. Biol.* **2012**, *32*, 2861–2870. [[CrossRef](#)]
61. Montañés, F.M.; Pascual-Ahuir, A.; Proft, M. Repression of ergosterol biosynthesis is essential for stress resistance and is mediated by the Hog1 MAP kinase and the Mot3 and Rox1 transcription factors. *Mol. Microbiol.* **2011**, *79*, 1008–1023. [[CrossRef](#)]
62. Jennings, S.M.; Tsay, Y.H.; Fisch, T.M.; Robinson, G.W. Molecular cloning and characterization of the yeast gene for squalene synthetase. *Proc. Natl. Acad. Sci. USA* **1991**, *88*, 6038–6042. [[CrossRef](#)] [[PubMed](#)]
63. Janik, A.; Juchimiuk, M.; Kruszewska, J.; Orowski, J.; Pasikowska, M.; Palamarczyk, G. Impact of yeast glycosylation pathway on cell integrity and morphology. In *Glycosylation*; Petrescu, S., Ed.; InTech: London, UK, 2012; ISBN 978-953-51-0771-2.
64. Ma, B.-X.; Ke, X.; Tang, X.-L.; Zheng, R.-C.; Zheng, Y.-G. Rate-limiting steps in the *Saccharomyces cerevisiae* ergosterol pathway: Towards improved ergosta-5,7-dien-3 β -ol accumulation by metabolic engineering. *World J. Microbiol. Biotechnol.* **2018**, *34*, 55. [[CrossRef](#)] [[PubMed](#)]
65. Mitchell, S.F.; Jain, S.; She, M.; Parker, R. Global analysis of yeast mRNPs. *Nat. Struct. Mol. Biol.* **2013**, *20*, 127–133. [[CrossRef](#)] [[PubMed](#)]



© 2019 by the authors. Licensee MDPI, Basel, Switzerland. This article is an open access article distributed under the terms and conditions of the Creative Commons Attribution (CC BY) license (<http://creativecommons.org/licenses/by/4.0/>).

Review

The Unfolded Protein Response Pathway in the Yeast *Kluyveromyces lactis*. A Comparative View among Yeast Species

Mariana Hernández-Elvira ¹ , Francisco Torres-Quiroz ² , Abril Escamilla-Ayala ³, Eunice Domínguez-Martin ¹ , Ricardo Escalante ⁴, Laura Kawasaki ¹, Laura Ongay-Larios ⁵ and Roberto Coria ^{1,*}

¹ Departamento de Genética Molecular, Instituto de Fisiología Celular, Universidad Nacional Autónoma de México, 04510 Mexico City, Mexico; melvira@email.ifc.unam.mx (M.H.-E.); edominguez@email.ifc.unam.mx (E.D.-M.); lkawasaki@ifc.unam.mx (L.K.)

² Departamento de Bioquímica y Biología Estructural, Instituto de Fisiología Celular, Universidad Nacional Autónoma de México, 04510 Mexico City, Mexico; ftq@ifc.unam.mx

³ Laboratory for Membrane Trafficking, VIB-KU Leuven Center for Brain & Disease Research and Department of Neurosciences, KU Leuven, 3000 Leuven, Belgium; abril.escamillaayala@kuleuven.vib.be

⁴ Instituto de Investigaciones Biomédicas “Alberto Sols” (CSIC-UAM), Arturo Duperier 4, 28029 Madrid, Spain; rescalante@iib.uam.es

⁵ Unidad de Biología Molecular, Instituto de Fisiología Celular, Universidad Nacional Autónoma de México, 04510 Mexico City, Mexico; longay@ifc.unam.mx

* Correspondence: rcoria@ifc.unam.mx; Tel.: +52-55-56-22-56-52

Received: 30 June 2018; Accepted: 8 August 2018; Published: 14 August 2018



Abstract: Eukaryotic cells have evolved signalling pathways that allow adaptation to harmful conditions that disrupt endoplasmic reticulum (ER) homeostasis. When the function of the ER is compromised in a condition known as ER stress, the cell triggers the unfolded protein response (UPR) in order to restore ER homeostasis. Accumulation of misfolded proteins due to stress conditions activates the UPR pathway. In mammalian cells, the UPR is composed of three branches, each containing an ER sensor (PERK, ATF6 and IRE1). However, in yeast species, the only sensor present is the inositol-requiring enzyme Ire1. To cope with unfolded protein accumulation, Ire1 triggers either a transcriptional response mediated by a transcriptional factor that belongs to the bZIP transcription factor family or an mRNA degradation process. In this review, we address the current knowledge of the UPR pathway in several yeast species: *Saccharomyces cerevisiae*, *Schizosaccharomyces pombe*, *Candida glabrata*, *Cryptococcus neoformans*, and *Candida albicans*. We also include unpublished data on the UPR pathway of the budding yeast *Kluyveromyces lactis*. We describe the basic components of the UPR pathway along with similarities and differences in the UPR mechanism that are present in these yeast species.

Keywords: yeast; endoplasmic reticulum; stress; UPR; Ire1; Hac1; Kar2

1. Introduction

Secreted and transmembrane proteins are synthesised in ribosomes that are attached to the endoplasmic reticulum (ER) membrane and are co-translationally processed and folded in the lumen of this organelle. Protein folding is accomplished by chemical modification, including the addition of oligosaccharides (N-glycosylation) and formation of disulphide bonds. These modifications are essential for the proper function of the proteins. Certain physiological, environmental, or pathogenic conditions can cause the accumulation of unfolded proteins, generating a condition known as ER stress.

Experimentally, ER stress is induced by treatment with agents that either inhibit N-glycosylation, such as tunicamycin (Tn) or 2-deoxyglucose (2-DOG), or agents that disrupt the formation of disulphide bonds such as dithiothreitol (DTT) and β -mercaptoethanol (β -ME). In order to respond to these harmful conditions, eukaryotic organisms activate a conserved signalling pathway termed the unfolded protein response (UPR). Many components and mechanisms of this pathway are conserved between species and they are dedicated to restoring ER homeostasis by increasing protein folding capacity and by decreasing the load of new proteins arriving to the ER. In metazoans, the UPR has three branches, each one named after the protein involved in sensing the ER stress stimulus. They are known as IRE1 (inositol-requiring enzyme 1), PERK (protein kinase RNA-like endoplasmic reticulum kinase) and ATF6 (activating transcription factor 6). The presence of these branches is species-dependent; however, the most conserved component of the UPR is the IRE1 branch, which is present in all eukaryotes including yeasts and the social amoeba *Dictyostelium discoideum* [1,2].

The IRE1 branch is composed by Ire1, that acts as a sensor of the ER stress. Under ER stress, Ire1 processes the mRNA of a bZIP transcription factor (in most cases known as Hac1). Once synthesised, the transcription factor is transported into the nucleus where it regulates transcription of a variety of genes such as those that encode chaperones, post-translational modification enzymes and proteins for proteolytic degradation. This pathway was initially described in *Saccharomyces cerevisiae*, and it was later detected in other yeast species, but it is not universally conserved among yeasts. For instance, the fission yeast *Schizosaccharomyces pombe* lacks a Hac1 orthologue and the UPR does not consist of a transcriptional response; instead, Ire1 triggers an ER-targeted mRNAs decay pathway. In this review, we describe the current knowledge regarding the UPR in several yeast species, namely *S. cerevisiae*, *S. pombe*, *Candida glabrata*, *Cryptococcus neoformans* and *Candida albicans*. In the third section, we present original data (obtained in our group) regarding the UPR in *Kluyveromyces lactis*. To our knowledge, this is the first review that describes the UPR of these six yeast species and we expect that it will be of great interest to researchers in the field.

2. The UPR in *Saccharomyces cerevisiae*

The IRE1 pathway was initially described in *S. cerevisiae*. In this system the ScIre1 protein has been extensively characterised. In this work we do not intend to describe in detail all the information accumulated regarding ScIre1, due to space limitations; we will simply refer to the general characteristics that are relevant to this review. ScIre1 is a 1115 amino acid residue transmembrane protein (Figure 1). This protein has a sensor domain at its N-terminus that lies inside the lumen and interacts with unfolded proteins, while its C-terminus lies in the cytosol and contains a serine-threonine kinase domain and an endoribonuclease domain [3,4]. A single transmembrane segment that lies in a region with very low similarity to the Ire1 of other yeast species connects the luminal N-terminal sensor domain with the cytoplasmic kinase and endoribonuclease domains (Figure 1). The activity of ScIre1 is regulated by the ER-luminal resident chaperone ScKar2 (BiP) (see below). Briefly, ScKar2 is bound to the N-terminus of ScIre1 under normal conditions and dissociates in response to ER stress [5,6]. Dissociation of ScKar2 leads to ScIre1 dimerisation and ultimately to its oligomerisation by binding to unfolded proteins through its core stress-sensing region (CSSR) located in the sensor domain [7–9]. The crystal structure of the *S. cerevisiae* CSSR suggests that it is able to form a groove similar to that present in the histocompatibility complex where the unfolded proteins may be captured [7]. The interaction with unfolded proteins may be essential for ScIre1 activation [10].

ScIre1 was initially isolated as essential for growth in the absence of inositol [11]. It was later determined that the null mutant was lethal in the presence of ER stress inducers [12]. An *S. cerevisiae* mutant lacking Ire1 is auxotrophic for inositol because it is unable to induce adequate expression of Ino1, the inositol-1-phosphate synthase that constitutes the rate-limiting step in the *de novo* inositol biosynthesis pathway [11,13]. The absence of inositol induces the UPR in wild-type yeast cells, and treatment with Tn induces *INO1* expression in an ScIre1-dependent manner [14]. ScIre1 is not required

for cell growth in normal conditions but it is essential for growth in the presence of ER stress inducers such as Tn and β -ME [14,15].

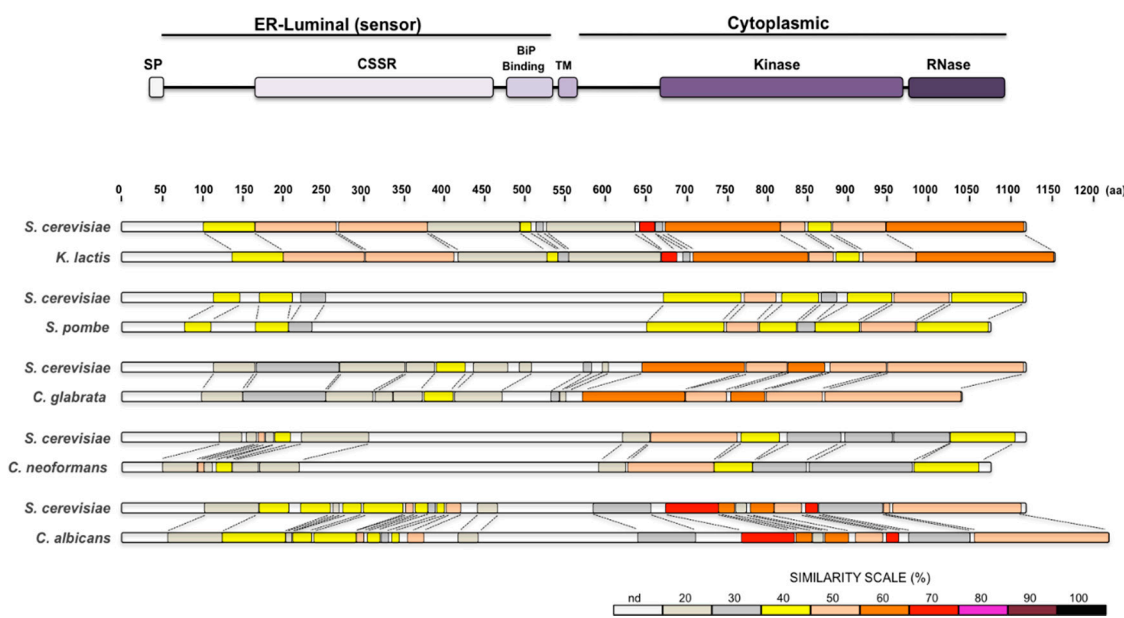


Figure 1. (Top) Diagram of the Ire1 protein structure. Signal Peptide (SP), Core Stress Sensing Region (CSSR), BiP Binding domain, Transmembrane segment (TM), and the Kinase and RNase domains were deduced from the *S. cerevisiae* Ire1 protein. (Bottom) Pairwise alignments between the *S. cerevisiae*, *K. lactis*, *S. pombe*, *C. glabrata*, *C. neoformans* and *C. albicans*, Ire1 orthologues. The Ire1 protein of each species is compared to the *S. cerevisiae* one. Protein sequences were analysed with SIM local alignment tool and results were visualized with LALNVIEW. Protein schemes are drawn to scale.

Mutations that affect either the groove where unfolded peptides bind ($M^{229}A$, $F^{285}A$, $Y^{301}A$) or those that affect oligomerisation and clustering ($F^{247}A$, $W^{426}A$) affect the response to ER stress-inducing agents [9,10]. Additionally, mutations that substitute K^{702} and N^{1057} abolish kinase and RNase activities respectively and also affect growth in ER stress inducers [3,16–18]. These data indicate that in *S. cerevisiae* all three Ire1 activities, i.e., the unfolded protein sensor, the kinase activity and the RNase activity, are essential for Ire1 function in the UPR pathway and required for proper ER stress response.

Once *ScIre1* is active, it, in turn, activates the transcription factor *Hac1p*, which comprises 238 amino acids and belongs to the basic-leucine zipper (bZIP) family. It contains a basic DNA binding region of 21 amino acids followed by a leucine zipper motif of 20 amino acids (Figure 2) [19]. In the presence of ER stress, *ScHac1* binds as a homodimer to promoters of UPR targets [19,20] in sequences known as UPRE (unfolded protein response element) motifs. It has been proposed that *ScHac1* binds to long and short UPREs (see below) through at least two different mechanisms, allowing a wide regulation of UPR gene transcription [20]. Conserved N and R residues within the basic DNA binding region of *ScHac1* are essential for recognition of palindromic or semi-palindromic UPRE DNA target sites (Figure 2). These residues make direct contact with the major groove of DNA [21,22]. A lack of *Hac1* does not compromise cell growth in normal conditions but it does cause sensitivity to ER-stress-inducing drugs such as Tn and DTT, and also to caffeine [23], and as in the case of an *ScIre1* null mutant, a lack of *ScHac1* causes inositol auxotrophy [13,24].

Although the *ScHAC1* precursor mRNA (*HAC1^u*, for uninduced *HAC1*) is constitutively produced, the *ScHac1* protein is not detected [25]. *ScHAC1* mRNA contains an unconventional 252 nucleotide intron near its 3' end (Figure 3) that is specifically processed only by the RNase domain of *ScIre1* [4,26,27]. *ScHAC1* pre-mRNA contains a translational attenuator that is located near the 5' end of the intron [26]. The attenuation of translation is exerted by base pairing between the intron

and the 5' untranslated region, forming a loop structure where the ribosomes are stalled [28,29] (see the analogous mechanism of *K. lactis* attenuation depicted in Section 3). After splicing, the two exons are joined together by the RNA ligase Rlg1, leading to the formation of a mature mRNA (*HAC1ⁱ*, for induced *HAC1*) [13]. This splicing allows the substitution of the last 10 amino acid residues of *ScHac1^u* by 18 residues, rendering a protein of 238 amino acids (*ScHac1ⁱ*) [25,27]. The novel 18 amino acids at the C-terminus tail of Hac1 function as the transcription transactivation domain [30]. *ScHAC1* mRNA splicing by *ScIre1* is a highly selective and efficient process that is promoted by the binding of pre-mRNA to a docking site formed by a positively charged motif located in the cytosolic linker domain of Ire1. The R⁶⁴⁷ and R⁶⁵⁰ residues located within this basic motif appear to play an important role in the binding of *HAC1* pre-mRNA [17]. Additionally, *ScHAC1* mRNA forms a stem-loop structure at its 3' UTR that contains an important component, the 3' UTR bipartite element (3'BE), which consists of two juxtaposed short motifs located at the distal end of the loop. This stem structure cooperates with the intron stalling structure to target the *ScHAC1* mRNA to the Ire1 oligomer foci in order to allow efficient splicing of the mRNA. The two short motifs are highly conserved in several yeast *HAC1* orthologues [29].

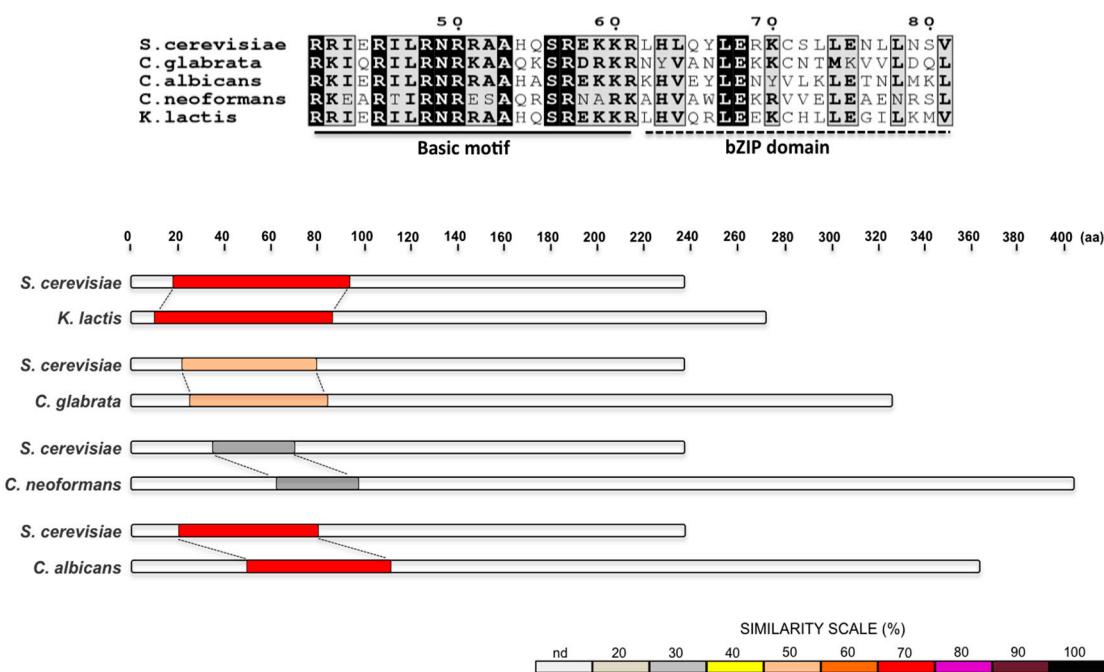


Figure 2. (Top) Alignment of the basic motif and the bZIP domain of Hac1 (or Hxl1) of yeast species. Amino acids fully conserved are depicted in black boxes. Amino acid coordinates correspond to the *S. cerevisiae* protein. **(Bottom)** Pairwise alignments between the *S. cerevisiae*, *K. lactis*, *S. pombe*, *C. glabrata*, *C. neoformans* and *C. albicans*, Ire1 orthologues. The Ire1 protein of each species is compared to the *S. cerevisiae* one. Protein sequences were analyzed with SIM local alignment tool and results were visualized with LALNVIEW.

Dissection of promoter sequences in the *ScKAR2* gene allows the identification of a 22-bp unfolded protein response element [31,32] to which *ScHac1* binds directly [19,25]. Within the 22-bp element a central semi-palindromic core of 7 bp (5'-CAGNGTG-3') known as UPRE-1 motif, is essential for the transcriptional activity of *ScKAR2* under ER stress [19]. The UPRE-1 motif, later determined to comprise from 11 to 13 bp [20], is present in several genes that are UPR targets [33,34]. Genes that are *ScHac1* targets lacking the UPRE-1 motif contain a distinct sequence called UPRE-2 [35]. This sequence is 6 to 7 bp long (5'-TACGTGT-3') and binds *ScHac1* with high affinity [20].

ScKar2 is an ER-resident chaperone that belongs to the Hsp70 family. It has an ATPase domain near its N-terminus adjacent to the substrate-binding domain [36]. ATPase activity is required for its

participation in the translocation of proteins across the ER membrane [37]. ScKar2 also participates in ER-associated protein degradation by maintaining luminal substrates in a retrotranslocation-competent state [38]. ScKar2 negatively regulates the UPR through its interaction with ScIre1. Under ER stress conditions, binding of unfolded proteins to ScKar2 induces its dissociation from ScIre1, leading to the activation of the UPR pathway [6,39]. ScKar2 is an essential and abundant protein, the synthesis of which is further induced by the presence of unfolded proteins [32,40].

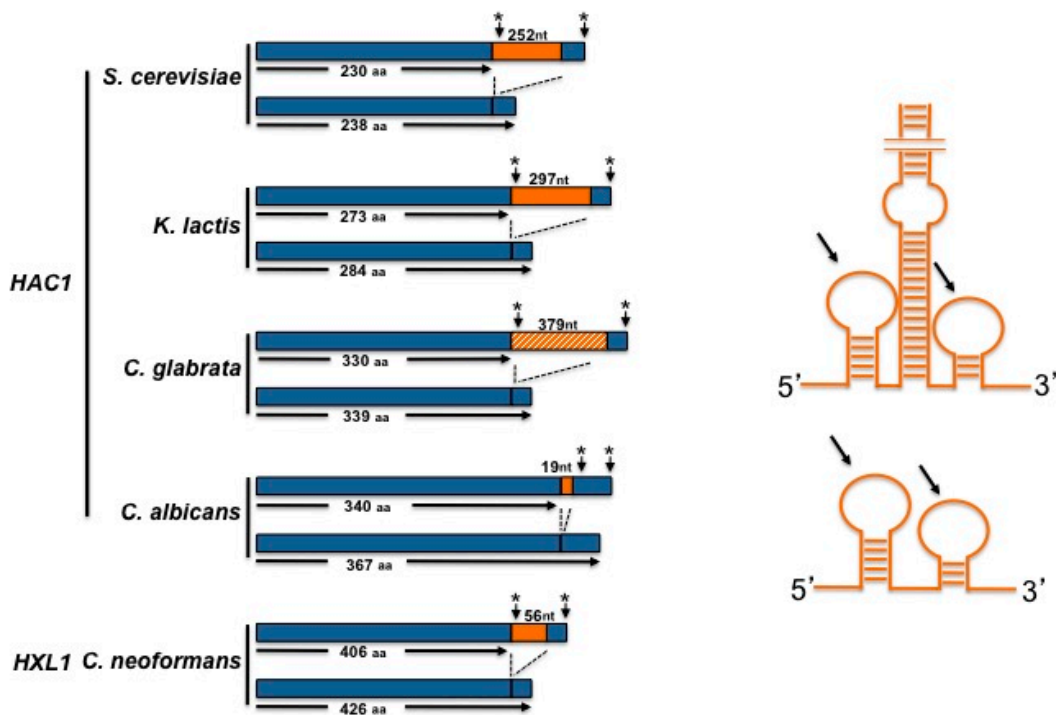


Figure 3. (Left) Scheme of un-spliced and spliced *HAC1* (or *HXL1*) RNAs. Sizes of putative protein products from un-spliced and spliced RNAs are depicted. Introns (and their sizes in nucleotides) are shown by the orange boxes. The putative *HAC1* intron of *C. glabrata*, that appears not to be processed is indicated by the slashed box. Stop codons are indicated by asterisk. (Right) Scheme of putative stem-loop structures of large and small introns. Arrows indicate 5' and 3' exon-intron boundaries. Structures are not drawn to scale.

3. The UPR in *Kluyveromyces lactis*

K. lactis is a biotechnologically important yeast which diverged before the genome duplication that gave rise to the *Saccharomyces* species [41]; thus, it represents a suitable organism for making evolutionary comparisons with *S. cerevisiae*.

The *K. lactis* genome encodes orthologue proteins of the IRE1 branch of the UPR signalling pathway, namely Ire1, Hac1, and Kar2. The KLLA0D13266g ORF of *K. lactis* has been identified as putative homologue of the *IRE1* gene of *S. cerevisiae*. It comprises 3459 nucleotides including the stop codon and codes for a protein of 1152 amino acids. Comparative analysis shows that the putative protein has 48% identity with ScIre1, and exhibits a structure similar to that of *S. cerevisiae* (Figure 1). From the sequence analysis of *KlIre1*, a luminal dimerisation domain at the N-terminal region, a serine/threonine protein kinase catalytic domain, and an endoribonuclease domain located at the C-terminus can be predicted. *KlIre1* conserves the K⁷³⁷ and N¹⁰⁹⁶ residues, which are essential for the kinase and RNase activities in *S. cerevisiae*. Additionally, *KlIre1* conserves the R residues (673 and 676) that in *S. cerevisiae* participate in the binding of *HAC1* RNA.

Experimental data from our group showed that *KlIre1* is involved in the UPR pathway in *K. lactis*; a *Klire1* mutant is sensitive to ER stress induced by Tn or 2-DOG (Figure 4). However, unlike *S. cerevisiae*,

in *K. lactis* *IRE1* is not essential for growth in the absence of inositol (Figure 4), indicating that in this species the *Ire1* function may differ, or that *K. lactis* may synthesise inositol in the absence of *KIire1*.

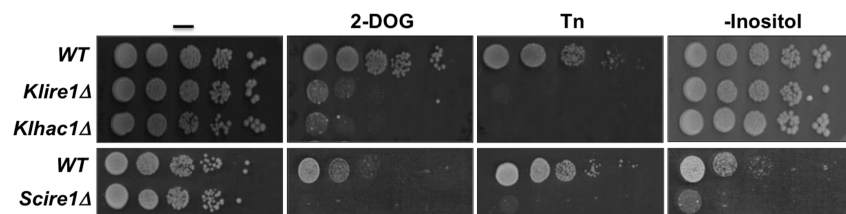


Figure 4. Effect of *IRE1* and *HAC1* inactivation on the *K. lactis* growth properties. *K. lactis* null mutants were obtained by standard homologous recombination introducing in both cases the *URA3* selective cassette. *K. lactis* cells were grown in YPD (1% yeast extract, 2% peptone, and 2% Glucose) until 0.5 OD₆₀₀ then were washed and suspended in fresh YPD. Cells were spotted as 10 fold serial dilutions on YPD plates containing 15 mM 2-DOG or 50 ng/mL Tn and on plates of 2% glucose, 0.5% ammonium sulfate, 0.17% yeast nitrogen base w/o amino acids and w/o inositol. *S. cerevisiae* wild type and *ire1Δ* strains were included as controls. Cells were plated on the same media except that the 2-DOG concentration was 20 mM and the Tn concentration was 500 ng/mL. Plates were incubated at 30 °C and photographed 48 h later.

A *K. lactis* *HAC1* gene has been identified in the *K. lactis* genome database. *KIHAC1* is a 1152 nucleotide gene that encodes a pre-mRNA formed by two exons of 805 and 50 nucleotides respectively and a long intron of 297 nucleotides (Figure 3), which has been identified as characteristic in several *Saccharomyces* species and some other yeasts [42]. Transcription of the *KIHAC1* gene produces an mRNA that is processed upon ER stress induction. After 30 min of exposure of *K. lactis* cells to 2-DOG, the presence of two forms of the transcript are evident (Figure 5), the larger form corresponds to the unprocessed *KIHAC1* mRNA (*HAC1^u* mRNA), and the second to the mature form (*HAC1ⁱ* mRNA). In *K. lactis*, the sequence of the *HAC1ⁱ* mRNA predicts a 284 amino acids protein that has the features of a bZIP transcriptional factor; namely, a conserved DNA binding domain and a basic leucine zipper domain (Figure 2).

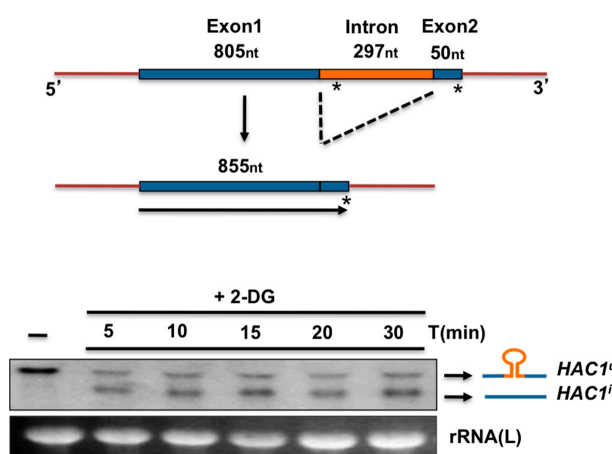


Figure 5. (Top) Diagram of the precursor and processed forms of *K. lactis* *HAC1* RNA. Exon and intron sizes (nucleotides) were determined by sequence analysis. Size of the induced *HAC1* (*HAC1ⁱ*) includes the stop codon. (Bottom) Northern blot analysis of *HAC1* processing. *K. lactis* cells were grown in YPD (1% yeast extract, 2% peptone, and 2% Glucose) until 0.5 OD₆₀₀. Cells were treated with 20 mM 2-DOG for the indicated times. Total RNA was extracted with the conventional Trizol protocol. Boiled RNA was loaded in a 1% agarose gel, electrophoresed, and transferred to a nylon membrane. The RNA was probed with a fragment containing the first 500 nt of the *HAC1* ORF labelled with ³²P and visualized in a phosphorimager. The large rRNA was used as a load control.

Sequence analysis of both the *KIHAC1^u* and *KIHAC1ⁱ* revealed that the pre-mRNA contains conserved cleavage motifs at the 5' and 3' intron-exon boundaries. Secondary structure analysis showed that these regions are capable of folding in a stem-loop structure (Figure 6). This sort of structure together with the 5' and 3' motifs is essential for the recognition and further cleavage of the pre-mRNA. We also found that there is a region in the intron (+909 to +936) that can base-pair with a region in the 5'UTR (−52 to −28) of the mRNA (Figure 6), allowing the formation of a translation attenuation structure like that of the *S. cerevisiae* mRNA and other *HAC1* RNAs with long introns [42,43]. Another interesting feature of the *K. lactis HAC1* mRNA is the presence of a conserved bipartite element, located in the 3'UTR, which in *S. cerevisiae* appears to be important in targeting the mRNA to Ire1 oligomers [29].

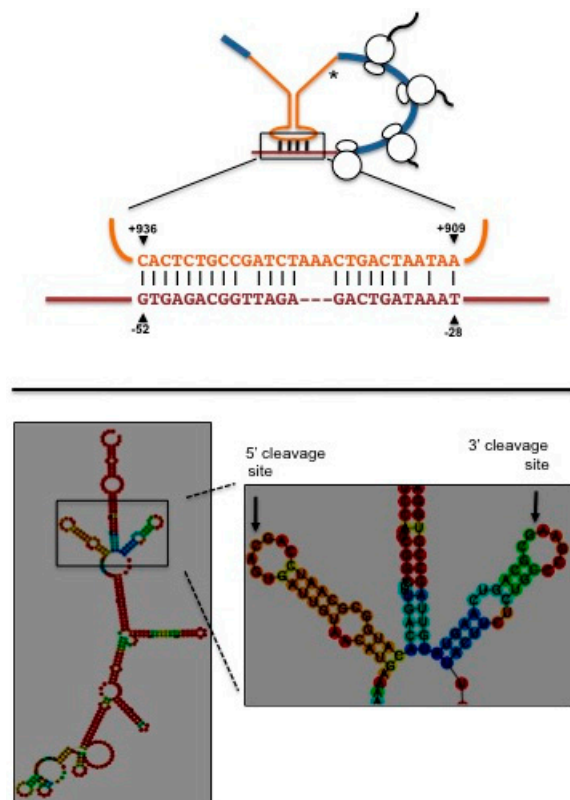


Figure 6. (Top) Diagram of a predicted translation attenuation structure formed in the *K. lactis HAC1* pre-mRNA. Exons are indicated in blue, intron is indicated in orange and 5' untranslated region in brown. Coordinates are relative to the first nucleotide of the translation start codon. Asterisk indicates an in-frame stop codon located within the intron. (Bottom) Predicted stem-loop secondary structure of the exon-intron boundaries of *K. lactis HAC1* pre-mRNA. Arrows pinpoint the 5' and 3' cleavage sites. The predicted secondary structure was obtained using the RNAfold web server from the ViennaRNA Web Services.

The aforementioned characteristics suggest that *K. lactis HAC1* mRNA is regulated and activated in a similar manner as that of *S. cerevisiae*, and that its translation may be modulated by the regulatory intron which upon ER stress is cleaved by the endonuclease activity of *KlIre1* at the 5' and 3' specific splicing sites, and the exons are joined. This would render the *KIHAC1* mRNA translatable, and the active transcriptional factor Hac1 would be produced.

Like *KlIre1*, *KlHac1* is also a key element in the ER stress response pathway of *K. lactis*. A null mutant of *KIHAC1* is sensitive to agents that induce ER stress, such as Tn or 2-DOG (Figure 4). Additionally, as in the case of *KlIRE1*, this gene is dispensable for growth in the absence of inositol (Figure 4).

The *K. lactis* *KAR2* gene codes for the major ER chaperone, Kar2. The gene was identified by its high similarity with the *S. cerevisiae* gene. It has 2040 nucleotides and predicts a 679 amino acid protein, with 77.3% identity with the *S. cerevisiae* Kar2 [44].

*Kl*Kar2 displays characteristics typical of the Hsp70 type of chaperones such as a hydrophobic leader sequence, and an ER retention signal at its C-terminus, which is important in order to prevent its secretion. In *K. lactis* the retention signal of Kar2 is the tetrapeptide DDLE, while in *S. cerevisiae* it is HDEL; this difference seems to be important for the specificity of the retention system [44,45]. The *K. lactis* Kar2 sequence contains a potential N-glycosylation site at the C-terminal region, although it is not known whether it is functional in this budding yeast [45]. Additionally, the *Kl*Kar2 C-terminus shows some sequence conservation with that of *S. pombe* and cross-reacts with an antibody raised against the BiP of this latter species [46].

We found that the *K. lactis* *KAR2* gene is upregulated under ER stress. Treatment of *K. lactis* cells with 2-DOG induced over-expression of a GFP reporter gene fused to the *KAR2* promoter (Figure 7). By deletion analyses, we also identified a 211 nucleotide region with promoter activity that responded to 2-DOG induction (from −291 to −479). Within this region, we detected a 22 nucleotide motif (Figure 7) with some identity to the *S. cerevisiae* UPRE [20,31]. Furthermore, inside this motif the heptanucleotide TGACGTG was detected, which exhibits high similarity to UPRE-1 of *S. cerevisiae*. This motif was searched in promoter regions of several *K. lactis* genes that in *S. cerevisiae* have been identified as UPR-responsive genes. This analysis allowed us to identify the consensus sequence T/GG/CANG/CTG/C which may represent the *K. lactis* UPRE responsive element (Figure 8).

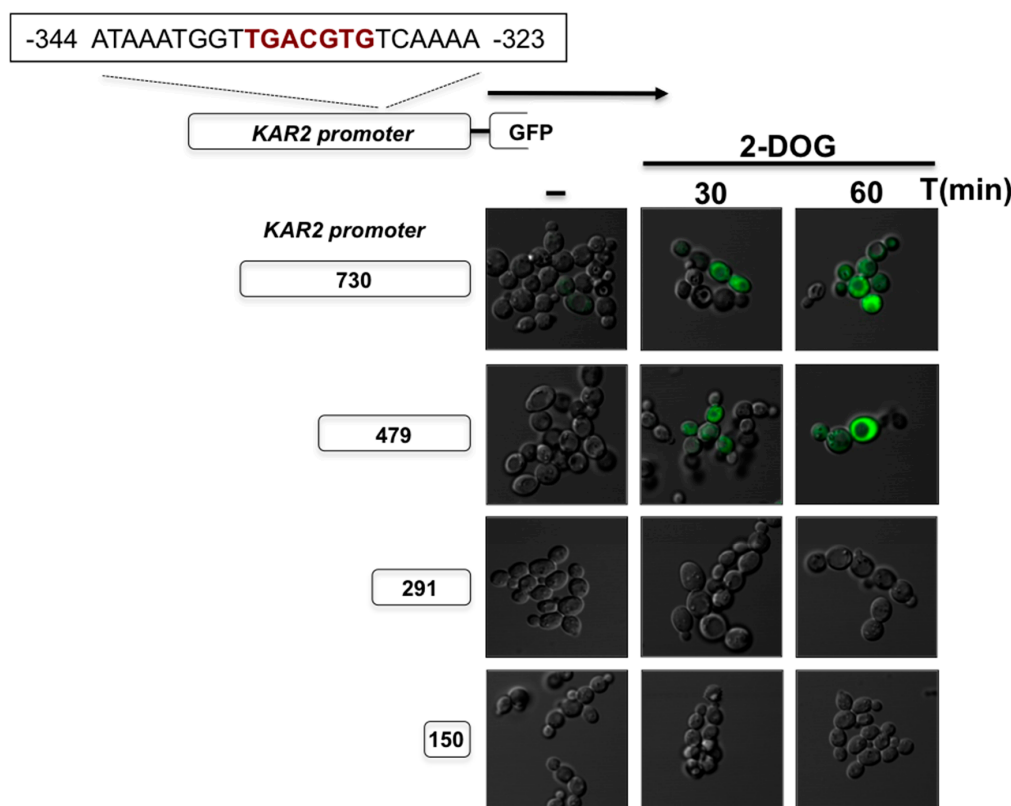


Figure 7. Detection of *K. lactis* *KAR2* promoter activity upon ER stress. The putative *KlKAR2* promoter (730 nucleotides of the upstream start codon region) and the indicated serial deletions fragments were fused to the GFP reporter gene. Constructions were cloned in an episomal multicopy *K. lactis* plasmid and used to transfet wild type cells. Cells were grown in YPD until 0.5 OD₆₀₀ and treated with 2-DOG for the indicated times. Cells were visualized under epi-fluorescence microscopy and photographed.

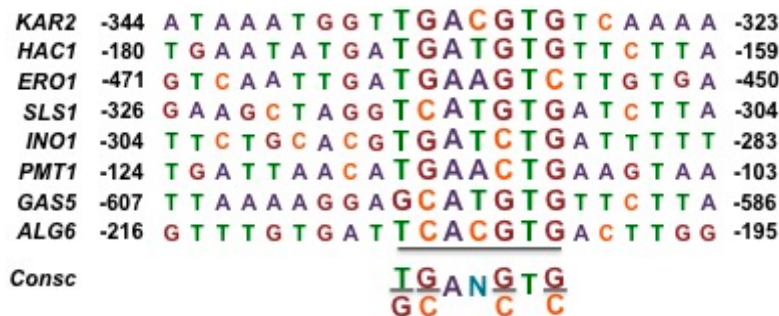


Figure 8. Blast search of the putative *K. lactis* UPRE motif (shown in brown in Figure 7) in putative ER stress-responsive genes. The search was directed to the indicated 5' untranslated regions of the indicated genes. Coordinates are relative to the first nucleotide of the respective translation start codon.

4. The UPR in *Schizosaccharomyces pombe*

S. pombe, the fission yeast, is a model organism used to analyse different aspects of cellular physiology. Interestingly, this yeast species lacks *HAC1* and the ER stress response is mediated by an Ire1-dependent mRNA degradation.

The Ire1 of *S. pombe* has the same structural features as *ScIre1* (Figure 1). It has a luminal domain and a cytosolic portion that contains the kinase and endoribonuclease domains. The full length *SpIre1* sequence shows only 24% identity with *ScIre1*, which indicates a wide evolutionary distance between the two proteins. *SpIre1* contains the K⁶⁸² and N¹⁰¹⁴ residues, which have been shown to be essential for kinase and RNase activities in *S. cerevisiae* respectively [3,16,17]. However, the R residues that may form the basic motif of the putative RNA docking site [17,18], and that are well conserved in other yeast species are not present in *SpIre1*, suggesting that it might not bind a specific RNA molecule.

S. pombe Ire1 null mutants are sensitive to ER stress inducers such as DTT and Tn [47] and since *S. pombe* is a natural auxotroph for inositol due to the absence of the inositol-1-phosphate synthase, the lack of inositol in the medium is lethal to *S. pombe* [48,49]. In this yeast, inositol is essential for mating and sporulation [50]. Although the mechanism remains unknown, it has been proposed that the effect of inositol may be indirect, possibly through regulation of membrane and cell wall composition [51].

Unlike *S. cerevisiae* and other yeast species, no specific substrate has been identified for *SpIre1*, suggesting that *S. pombe* lacks a *Hac1* orthologue. In contrast to *S. cerevisiae* and other yeast species the UPR in *S. pombe* is not mediated by a transcriptional reprogramming; instead, it has been observed that the *SpIre1* RNase activity is involved in a mechanism termed Regulated Ire-Dependent De^cay (RIDD) [52]. This process was first described in *Drosophila* [53] but it has also been observed in plants [54] and mammalian cells [55,56]. In *S. pombe* upon ER-stress, *SpIre1* cleaves ER-localised mRNAs at consensus sites, leading to free 5' and 3' end-containing mRNA fragments that are rapidly degraded by exoribonucleases in a 5'-3' direction [57] and by the exosome in the 3'-5' direction [53], thus alleviating the ER-protein load. The *SpIre1* mRNA substrates contain a consensus UG/CU sequence flanking the cleavage sites. These cleavage sites reside within the coding sequences of mRNAs, resulting in the stalling of ribosomes engaged in translation. Those ribosomes are then liberated by a ribosome/mRNA decay pathway known as 'no-go decay', which consists of the endonucleolytic cleavage of the RNA and the Dom34/Hbs1-dependent recycling of the ribosome [58].

Approximately 31% of the mRNAs regulated by *SpIre1* code for proteins involved in lipid metabolism, and particularly in sterol metabolism. Sterol has also been shown to induce ER stress and to trigger UPR in *S. cerevisiae* [59]. Despite the fact that it is not known how the reduction in sterol synthesis regulates the toxicity associated with ER stress, it has been suggested that this kind of stress affects vesicular sterol transport and that therefore, when sterol biosynthesis is reduced, ER membrane fluidity may be stabilised [52].

One of the RIDD substrates is the mRNA that codes for the Grp78 chaperone orthologue BiP1 [52,60]. *SpIre1* cleaves the *BiP1* mRNA within the consensus UG/CU sequence located in its 3'-UTR, leading to the loss of the polyA tail. Paradoxically, *SpIre1* activity does not increase the *SpBiP1* mRNA degradation rate; instead, it makes it more stable, possibly due to the elimination of an RNA degradation sequence without affecting its translation efficiency.

In *S. pombe*, Bip1 is a 663 amino acid protein essential for cell viability and its expression is induced by various stresses, such as heat shock and Tn. It contains an ER retention signal [60] and a predicted N-glycosylation site [46]. Indeed, a small portion (10%) of *SpBiP1* is rapidly N-glycosylated upon synthesis and this glycosylation does not change with time. As one might expect, Tn prevents the appearance of the glycosylated form of BiP1 [46]. Although the synthesis of the mRNA of *SpBiP1* is not increased upon ER stress, its extended stability after *SpIre1*-dependent cleavage following ER stress results in an increase of the *SpBip1* protein [52]. Finally, it appears that elimination of the 3'-UTR mRNA processing site in *SpBiP1* induces a significant impairment in the response to ER stress conditions [52].

5. The UPR in *Candida glabrata*

C. glabrata is one of the most common human pathogenic yeasts. It is phylogenetically related to *S. cerevisiae*, and it has the canonical Ire1 kinase and the transcriptional factor Hac1. However, the ER stress response mechanism in this yeast is very different; particularly, *CgHAC1* mRNA is not spliced by *CgIre1*, and *CgIre1* regulates the response in an Hac1-independent manner.

C. glabrata Ire1 is a 1036 amino acid protein that conserves the typical Ire1 domains: the N-terminal hydrophobic signal sequence, an ER luminal domain, a transmembrane segment, a serine/threonine kinase domain and a nuclease domain. Overall, *CgIre1* displays 49% similarity and 33% identity with *ScIre1* (Figure 1). *CgIre1* is required for cellular response to ER stress inducers such as Tn and DTT, and this function requires its kinase and the ribonuclease activities [61]. However, the ribonuclease activity of *CgIre1* does not seem to be required for the *CgHAC1* RNA splicing (see below); instead it appears to participate in the degradation of ER-associated mRNAs through a RIDD pathway similar to that of *S. pombe* [61]. Accordingly, *CgIre1* does not trigger a transcriptional response to ER stress; instead, transcription is regulated by the calcium signalling pathway which depends on calcineurin phosphatase [61] (see below).

C. glabrata has a single *HAC1* orthologue containing a highly conserved bZIP domain and a conserved DNA binding region [61] (Figure 2). Overall, the *CgHac1* transcription factor shows low similarity and low identity with *ScHac1*. The *CgHAC1* pre-mRNA contains a predicted intron of 379 nucleotides (Figure 3), which may potentially form a stem-loop structure, but it apparently lacks the consensus Ire1 splicing recognition sequences [61]. Unlike *CgIre1*, a lack of *CgHac1* does not induce sensitivity to ER stress inducers and *CgHac1* remains un-spliced in both stressed and non-stressed conditions. A lack of *HAC1* pre-mRNA splicing under ER stress conditions supports the notion that in *C. glabrata* there is a RIDD pathway that is *CgIre1*-dependent but *CgHac1*-independent [62]. Nevertheless, un-spliced *CgHac1* is able to induce transcription of UPR genes in *S. cerevisiae*, indicating that it has conserved its structure and function [61].

The transcriptional response to ER stress in *C. glabrata* depends on calcineurin signalling and on the Slt2 MAPK pathway [61]. In this yeast, calcineurin prevents cell death upon ER stress by regulating calcium influx through the Crz1 transcription factor [61]. The calcineurin-Crz1 pathway is also required for the response of *C. glabrata* to various stress stimuli and for virulence [63]. The Slt2 MAPK may also exert an ER stress surveillance function to ensure transmission of healthy ER to daughter cells, as it does in *S. cerevisiae* [62,64]. In *C. glabrata*, the gene transcription program triggered by ER stress appears to be more closely related to calcineurin-Crz1 regulated genes than to increasing the folding capacity of the ER [61,65]. In fact the *CgKAR2* promoter lacks a consensus UPRE sequence and its expression depends on the Crz1 transcription factor [61]. In summary, *C. glabrata* monitors ER stress by means of three pathways acting in parallel: the Ire1-RIDD pathway, the calcineurin-Crz1 pathway and

the Stl2-surveillance pathway. *CgIre1* is also required for virulence, although its role in the infectious process remains unknown [61].

6. The UPR in *Cryptococcus neoformans*

C. neoformans is a basidiomycetous yeast. It is the most common cause of severe pulmonary infections and meningoencephalitis in immunocompromised patients. This yeast has an unfolded protein response pathway involved in ER stress response and virulence [66–68].

C. neoformans has a conserved Ire1 protein. Overall *CnIre1* displays 25% identity with *ScIre1*. It contains the typical Ire1 domains, a sensor-luminal domain, a Ser/Thr protein kinase, and a ribonuclease domain (Figure 1). It also contains the catalytic sites (Lys⁶⁴¹ and Arg¹⁰¹⁰) for kinase and ribonuclease activities. A lack of Ire1 in *C. neoformans* generates sensitivity to ER stress inducers like Tn and DTT, and the *ire1* mutant also shows a variety of pleiotropic effects such as thermosensitivity and sensitivity to cell wall damaging agents [69]. The mutant lacking *CnIre1* is avirulent since it is defective in forming the antiphagocytic capsule that is essential for evading the host immune response [69,70]. Inositol is required for mating and virulence and *C. neoformans* can use myo-inositol as a sole carbon source [71]; but there is no report that *CnIre1* is required for its synthesis.

CnIre1 processes the *HXL1* pre-mRNA (the *HAC1* orthologue), which encodes a bZIP transcription factor that appears to be phylogenetically distant from *ScHac1* (Figure 2). *Hxl1* shows the lowest sequence conservation on the basic DNA binding domain compared to the other bZIP factors described in this work (Figure 2). However, like other *HACs*, *HXL1* contains an unconventional intron of 56 nucleotides whose splicing sites are well conserved with *basidiomycetes* and *ascomycetes* fungi (Figure 3) [70]. Although a small proportion of spliced *HXL1* mRNA coexists with the unspliced molecule in unstressed conditions, most pre-RNA is spliced by *CnIre1* under ER stress conditions [69]. In contrast to *S. cerevisiae* and *K. lactis*, the *CnHXL1* intron does not seem to contain sequences complementary to the 5'-UTR region, disregarding an attenuation mechanism for negative regulation of translation. This suggests that the unspliced mRNA can be translated, yielding a 406 amino acid protein in contrast to the 426 amino acids of the induced *Hxl1* protein [70]. In *C. neoformans*, an alternative mechanism of post-transcriptional regulation has been described. Splicing and stability of the *HXL1* mRNA is regulated through binding of Puf4, a component of the pumilio-FBF family of mRNA binding proteins that facilitates splicing under ER-stress conditions and attenuates mRNA degradation during ER stress attenuation [72].

A Kar2/BiP chaperone has been identified in *C. neoformans*, whose expression under ER stress conditions is regulated by the Ire1-Hxl1 pathway [69,73]. *CnKar2* is an essential protein with 679 amino acid residues that displays an Hsp70 domain and an ER retention signal [73,74]. *CnKar2* is required for cellular response to ER stress and high temperature, and for maintenance of cell wall integrity [70,73].

Aside from the ER stress response, *CnIre1* has other functions. It also participates in the biosynthesis of the antiphagocytic capsule, in thermotolerance, in azole drug resistance, partially in the genotoxic stress response and in the maintenance of cell wall integrity [69,70]. Except for capsule production and thermotolerance these functions are at least partially mediated by *Hxl1*, while capsule biosynthesis seems to be dependent only on *CnIre1* [70]. Furthermore, *CnIre1* has a role in the sexual mating and unisexual differentiation of *C. neoformans*. While sexual mating is dependent on the activity of *CnKar2*, the same-sex mating is independent [68,74]. Both, opposite- and uni-sexual reproductions are independent of the *Hxl1* transcription factor [68]. This indicates that *C. neoformans* has evolved unique features of the UPR pathway that are not present in other eukaryotic organisms.

7. The UPR in *Candida albicans*

C. albicans is an opportunistic human fungal pathogen. The yeast-mycelia morphological transitions play an important role in its pathogenesis.

C. albicans contains a typical Ire1 protein. Its full length comprises 1224 amino acid residues. By primary sequence comparison *CaIre1* contains the common structural domains, i.e., the sensor-luminal

domain, the protein kinase domain and the ribonuclease domain (Figure 1). Overall CaIre1 displays 45% similarity and 31% identity with *ScIre1*. Like other yeasts, *CaIre1* conserves the amino acid residues involved in kinase and RNase activities. Although, no direct evidence of the involvement of *CaIre1* in the ER unfolded protein response has been obtained, its structural features indicate that it may activate a bZIP transcription factor (see below). It also appears that defective *CaIre1* mutants display high sensitivity to cell wall stress inducers such as caspofungin [75] and show defective filamentation that alters their pathogenic capacity [76]. *C. albicans* is able to synthesise inositol *de novo* and can take it up from the media; however, *CaIre1* has not been shown to participate in any of these processes [77].

In *C. albicans* the most studied component of the UPR pathway is the transcription factor Hac1. This protein displays high sequence similarity within the putative DNA-binding region to other yeast Hac1 proteins (Figure 2). Under ER stress conditions, the *CaHAC1* mRNA is processed analogously to the *S. cerevisiae HAC1* [78]. In contrast to other yeast species, however, the *CaHAC1* intron is only 19 bp long and it is located near the 3' end of the precursor mRNA (Figure 3), although it is apparently capable of forming the stem-loop structure characteristic of this kind of introns. Processing of the intron results in the synthesis of a transcription factor with a novel 27 C-terminus [78] that may form the transactivation domain. The sequence at the intron/exon boundaries in *CaHac1* are well conserved [78], but the unspliced form of *CaHac1* is unable to complement a *ScHac1Δ* mutant, indicating that *ScIre1* is unable to process the *CaHAC1* intron [78]. However, the fact that the spliced form of *CaHAC1* is able to complement the *S. cerevisiae* mutant indicates that *CaHac1* is the functional homologue of *ScHac1* [78]. Due to the small size of the *CaHAC1* intron, a translation attenuation mechanism similar to that present in *S. cerevisiae* and *K. lactis*, seems to be discarded.

CaHac1 is required in order to trigger a cellular response to ER stress inducers such as Tn and DTT. In fact, it appears that under ER stress, *CaHac1* triggers expression of a group of genes involved in secretion, cell wall biogenesis and vesicle transport among other processes [78].

Like in *C. glabrata*, the ER stress response in *C. albicans* is dependent on the calcineurin-CRZ1 pathway [79]. Nevertheless, it seems that in this species, the calcineurin pathway is required as an assisting mechanism to regulate the Hac1-dependent UPR genes [79]. Additionally, *C. albicans* cells that are defective in calcineurin and Crz1 activities are highly sensitive to Tn and DTT [80].

C. albicans expresses a Kar2 chaperone orthologue, which is essential for cell survival [81] but nothing is known regarding its participation in the ER stress response pathway. It has been determined that *CaKar2* can partially complement a lack of Kar2 in *S. cerevisiae*, alleviating the thermosensitivity displayed by the *Sckar2Δ* mutant. Additionally, *CaKar2* displays *in vitro* protein translocation activity, suggesting that it may participate in the secretory pathway of *C. albicans* [81].

8. Concluding Remarks

The unfolded protein response (UPR) is a signalling pathway that is activated in response to ER stress to restore and maintain ER homeostasis. In mammalian cells, it is composed by three branches: IRE1, PERK, and ATF6. IRE1 is the most conserved branch of the UPR. It is preserved in all eukaryotes and is the only branch present in yeast species. Even though the Ire1 sensor is highly conserved, the mechanisms to handle the ER stress response varies in different species. The kinase and RNase domains of Ire1 proteins are greatly similar among different species. In particular, the catalytic residues of those domains are highly conserved in all eukaryotes [82]. Upon ER stress, ER homeostasis can be restored in two ways: by increasing the protein folding capacity, and by decreasing the load of proteins arriving to the ER. The folding capacity may be increased through transcriptional upregulation, while the reduction of the protein load can be achieved by selective decay of ER-localised mRNAs. In any case, it seems that the RNase activity of Ire1 has a crucial role in the mechanism of the UPR, either degrading a large set of mRNAs or processing a very specific mRNA to produce a transcriptional response. In mammalian cells, both mechanisms are present, and are triggered depending on cellular conditions and cell type [52,53,56]. However, in yeast species the strategy is different; some yeasts rely on a transcriptional response to regulate genes needed to cope with unfolded protein accumulation,

while others initiate a selective decay of ER-localised mRNAs (Figure 9). In *S. cerevisiae*, *K. lactis*, *C. albicans* and *C. neoformans* Ire1 processes the pre-mRNA of a bZIP transcription factor, Hac1 (in *Sc.*, *Kl.*, and *Ca.*) or Hxl1 (in *Cn.*); while in *S. pombe* and *C. glabrata* the response is mediated by Ire1 through degradation of ER targeted-mRNAs by the RIDD pathway (Figure 9).

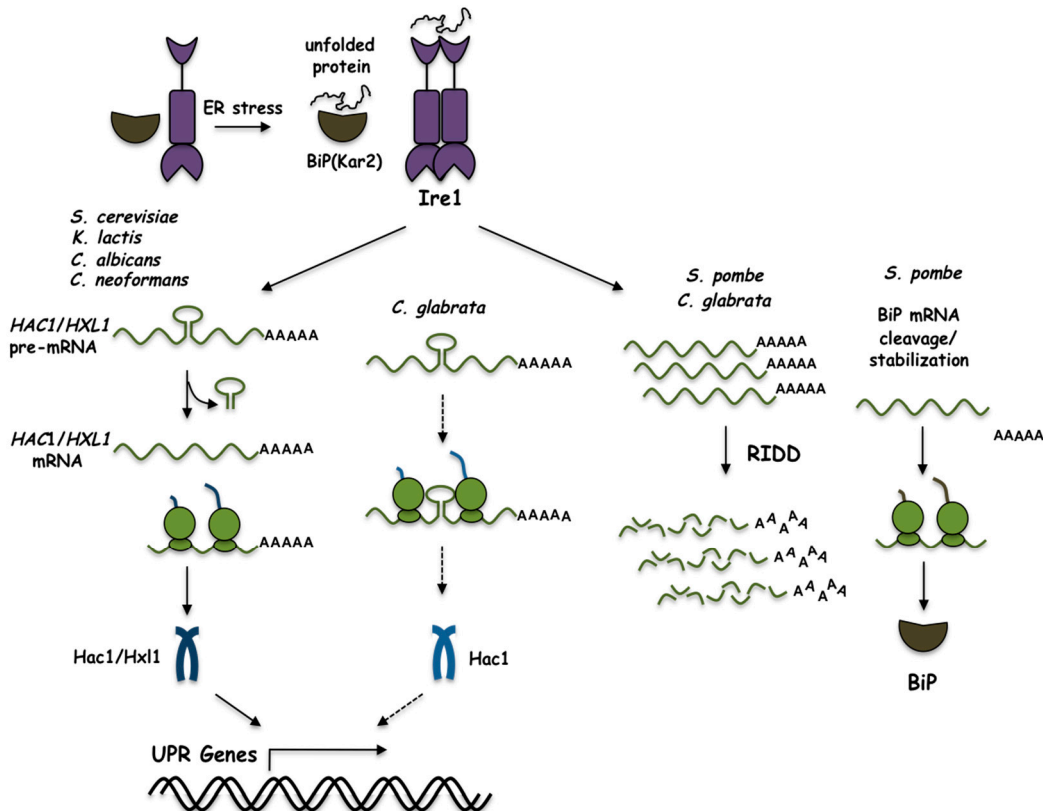


Figure 9. The unfolded protein response pathway in several yeast species. The accumulation of unfolded proteins in the ER leads to the activation of Ire1. In *Sc.*, *Kl.*, *Ca.*, and *Cn.*, Ire1 splices the *HAC1/HXL1* pre-mRNA leading to its translation. The synthesised bZIP factor (Hac1/Hxl1), regulates transcription of UPR-responsive genes. In *Sp.*, and *Cg.*, Ire1 cleaves ER-localised mRNAs through the Regulated Ire-Dependent Decay (RIDD) pathway. In *Sp.*, Ire1 also cleaves the BiP mRNA in the 3' UTR region leading to its stabilization and translation. As described in the text, the unspliced *HAC1* RNA of *Cg* may induce transcription of UPR-responsive genes in *S. cerevisiae* (depicted by the dotted arrows), although there is no evidence that this process can actually occur in *C. glabrata*.

It has been proposed that the RNase activity used in the RIDD process represents the ancestral mechanism, since it is less specific with a broader mRNA degradation capacity. Evolution of this process implied loss of this broad degradation capacity and the acquisition of a more specialised mechanism to splice a specific target [52]. Through this last mechanism Ire1 removes an unconventional intron; interestingly, it has been shown that the sequence of the Hac1/Hxl1 intron is conserved only at the splice recognition sites, while its size and structure vary among different species; it is very short in metazoan, filamentous fungi, and several yeasts, whereas some other yeasts have long introns [83]. The long intron of *S. cerevisiae* is shared by some closely related species, and it is suggested that the translation attenuation mechanism that depends on the 5' UTR described in *S. cerevisiae* is present only in this kind of long introns [42]. We have found that *K. lactis* presents a long intron containing a sequence complementary to the 5' UTR, which is similar to that of *S. cerevisiae*, therefore the attenuation mechanism could be conserved in *K. lactis*. Some yeasts lack the regulatory intron or even have lost the ortholog of the bZIP mRNA and therefore have evolved other mechanisms for the induction of the UPR. These different strategies indicate that yeast species have optimized the mechanisms of

their UPR to adapt to their specific lifestyles. The UPR pathways of the yeast species described in this review show intriguing differences that may expand our understanding of their phylogenetic relationships and the utility of the mechanisms present in each organism to deal with and adapt to their particular niche.

Author Contributions: M.H.-E. and E.D.-M. analysed data and wrote the paper; F.T.-Q. and A.E-A. made experiments and analysed data; L.K., L.O.-L., R.E. and R.C. wrote the paper.

Funding: This work was supported by grant numbers CONACyT: CB-254078 (to R.C.), and CB-238681 (to F.T.-Q.); PAPIIT, DAGAPA, UNAM: IN210616 (to E.D.-M., M.H.-E., and R.C.), and AI200315, IA202217 (to F.T.-Q.); BFU2015-64440-P (to R.E.) from the Spanish Ministerio de Economía, Industria y Competitividad and by FEDER.

Acknowledgments: M.H-E. is a PhD student from Programa de Doctorado en Ciencias Bioquímicas, Universidad Nacional Autónoma de México (UNAM), and received fellowship 366635 from CONACYT; E.D.-M. is a PhD candidate from Programa de Doctorado en Ciencias Biomédicas, Universidad Nacional Autónoma de México (UNAM), and received fellowship 380127 from CONACYT. We acknowledge the technical support from the Molecular Biology and Computer Facilities, IFC, UNAM. We also wish to recognise Patrick Weill for his assistance with the English language.

Conflicts of Interest: The authors declare no conflict of interest.

References

1. Domínguez-Martín, E.; Ongay-Larios, L.; Kawasaki, L.; Vincent, O.; Coello, G.; Coria, R.; Escalante, R. IreA controls endoplasmic reticulum stress-induced autophagy and survival through homeostasis recovery. *Mol. Cell. Biol.* **2018**, *38*, e00054-18. [[CrossRef](#)]
2. Domínguez-Martín, E.; Hernández-Elvira, M.; Vincent, O.; Coria, R.; Escalante, R. Unfolding the endoplasmic reticulum of a social amoeba: *Dictyostelium discoideum* as a new model for the study of endoplasmic reticulum stress. *Cells* **2018**, *7*, 56. [[CrossRef](#)] [[PubMed](#)]
3. Mori, K.; Ma, W.; Gething, M.J.; Sambrook, J. A transmembrane protein with a cdc2+/CDC28-related kinase activity is required for signaling from the ER to the nucleus. *Cell* **1993**, *74*, 743–756. [[CrossRef](#)] [[PubMed](#)]
4. Sidrauski, C.; Walter, P. The transmembrane kinase Ire1p is a site-specific endonuclease that initiates mRNA splicing in the unfolded protein response. *Cell* **1997**, *90*, 1031–1039. [[CrossRef](#)]
5. Bertolotti, A.; Zhang, Y.; Hendershot, L.M.; Harding, H.P.; Ron, D. Dynamic interaction of BiP and ER stress transducers in the unfolded protein response. *Nat. Cell Biol.* **2000**, *2*, 326–332. [[CrossRef](#)] [[PubMed](#)]
6. Okamura, K.; Kimata, Y.; Higashio, H.; Tsuru, A.; Kohno, K. Dissociation of Kar2p/BiP from an ER sensory molecule, Ire1p, triggers the unfolded protein response in yeast. *Biochem. Biophys. Res. Commun.* **2000**, *279*, 445–450. [[CrossRef](#)] [[PubMed](#)]
7. Credle, J.J.; Finer-Moore, J.S.; Papa, F.R.; Stroud, R.M.; Walter, P. On the mechanism of sensing unfolded protein in the endoplasmic reticulum. *Proc. Natl. Acad. Sci. USA* **2005**, *102*, 18773–18784. [[CrossRef](#)] [[PubMed](#)]
8. Oikawa, D.; Kimata, Y.; Kohno, K. Self-association and BiP dissociation are not sufficient for activation of the ER stress sensor Ire1. *J. Cell Sci.* **2007**, *120*, 1681–1688. [[CrossRef](#)] [[PubMed](#)]
9. Kimata, Y.; Ishiwata-Kimata, Y.; Ito, T.; Hirata, A.; Suzuki, T.; Oikawa, D.; Takeuchi, M.; Kohno, K. Two regulatory steps of ER-stress sensor Ire1 involving its cluster formation and interaction with unfolded proteins. *J. Cell Biol.* **2007**, *179*, 75–86. [[CrossRef](#)] [[PubMed](#)]
10. Gardner, B.M.; Walter, P. Unfolded proteins are Ire1-activating ligands that directly induce the unfolded protein response. *Science* **2011**, *333*, 1891–1894. [[CrossRef](#)] [[PubMed](#)]
11. Nikawa, J.; Yamashita, S. IRE1 encodes a putative protein kinase containing a membrane-spanning domain and is required for inositol phototrophy in *Saccharomyces cerevisiae*. *Mol. Microbiol.* **1992**, *6*, 1441–1446. [[CrossRef](#)] [[PubMed](#)]
12. Cox, J.S.; Shamu, C.E.; Walter, P. Transcriptional induction of genes encoding endoplasmic-reticulum resident proteins requires a transmembrane protein-kinase. *Cell* **1993**, *73*, 1197–1206. [[CrossRef](#)]
13. Sidrauski, C.; Cox, J.S.; Walter, P. tRNA ligase is required for regulated mRNA splicing in the unfolded protein response. *Cell* **1996**, *87*, 405–413. [[CrossRef](#)]

14. Cox, J.S.; Chapman, R.E.; Walter, P. The unfolded protein response coordinates the production of endoplasmic reticulum protein and endoplasmic reticulum membrane. *Mol. Biol. Cell* **1997**, *8*, 1805–1814. [[CrossRef](#)] [[PubMed](#)]
15. Chen, Y. Identification of mitogen-activated protein kinase signaling pathways that confer resistance to endoplasmic reticulum stress in *Saccharomyces cerevisiae*. *Mol. Cancer Res.* **2005**, *3*, 669–677. [[CrossRef](#)] [[PubMed](#)]
16. Shamu, C.E.; Walter, P. Oligomerization and phosphorylation of the Ire1p kinase during intracellular signaling from the endoplasmic reticulum to the nucleus. *EMBO J.* **1996**, *15*, 3028–3039. [[PubMed](#)]
17. Van Anken, E.; Pincus, D.; Coyle, S.; Aragón, T.; Osman, C.; Lari, F.; Gómez Puerta, S.; Korenykh, A.V.; Walter, P. Specificity in endoplasmic reticulum-stress signaling in yeast entails a step-wise engagement of HAC1 mRNA to clusters of the stress sensor Ire1. *eLife* **2014**, *3*, e05031. [[CrossRef](#)] [[PubMed](#)]
18. Goffin, L.; Vodala, S.; Fraser, C.; Ryan, J.; Timms, M.; Meusburger, S.; Catimel, B.; Nice, E.C.; Silver, P.A.; Xiao, C.-Y.; et al. The Unfolded Protein Response transducer Ire1p contains a nuclear localization sequence recognized by multiple β importins. *Mol. Biol. Cell* **2006**, *17*, 5309–5323. [[CrossRef](#)] [[PubMed](#)]
19. Mori, K.; Kawahara, T.; Yoshida, H.; Yanagi, H.; Yura, T. Signalling from endoplasmic reticulum to nucleus: Transcription factor with a basic-leucine zipper motif is required for the unfolded protein-response pathway. *Genes Cells* **1996**, *1*, 803–817. [[CrossRef](#)] [[PubMed](#)]
20. Fordyce, P.M.; Pincus, D.; Kimmig, P.; Nelson, C.S.; El-Samad, H.; Walter, P.; DeRisi, J.L. Basic leucine zipper transcription factor Hac1 binds DNA in two distinct modes as revealed by microfluidic analyses. *Proc. Natl. Acad. Sci. USA* **2012**, *109*, E3084–E3093. [[CrossRef](#)] [[PubMed](#)]
21. Fujii, Y.; Shimizu, T.; Toda, T.; Yanagida, M.; Hakoshima, T. Structural basis for the diversity of DNA recognition by bZIP transcription factors. *Nat. Struct. Biol.* **2000**, *7*, 889–893. [[CrossRef](#)] [[PubMed](#)]
22. Miller, M. The importance of being flexible: The case of basic region leucine zipper transcriptional regulators. *Curr. Protein Pept. Sci.* **2009**, *10*, 244–269. [[CrossRef](#)] [[PubMed](#)]
23. Nojima, H.; Leem, S.H.; Araki, H.; Sakai, A.; Nakashima, N.; Kanaoka, Y.; Ono, Y. Hac1: A novel yeast bZIP protein binding to the CRE motif is a multicopy suppressor for cdc10 mutant of *Schizosaccharomyces pombe*. *Nucleic Acids Res.* **1994**, *22*, 5279–5288. [[CrossRef](#)] [[PubMed](#)]
24. Nikawa, J.I.; Akiyoshi, M.; Hirata, S.; Fukuda, T. *Saccharomyces cerevisiae* IRE2/HAC1 is involved in IRE1-mediated KAR2 expression. *Nucleic Acids Res.* **1996**, *24*, 4222–4226. [[CrossRef](#)] [[PubMed](#)]
25. Cox, J.S.; Walter, P. A novel mechanism for regulating activity of a transcription factor that controls the unfolded protein response. *Cell* **1996**, *87*, 391–404. [[CrossRef](#)]
26. Chapman, R.E.; Walter, P. Translational attenuation mediated by an mRNA intron. *Curr. Biol.* **1997**, *7*, 850–859. [[CrossRef](#)]
27. Kawahara, T.; Yanagi, H.; Yura, T.; Mori, K. Endoplasmic reticulum stress-induced mRNA splicing permits synthesis of transcription factor Hac1p/Ern4p that activates the unfolded protein response. *Mol. Biol. Cell* **1997**, *8*, 1845–1862. [[CrossRef](#)] [[PubMed](#)]
28. Rüegsegger, U.; Leber, J.H.; Walter, P. Block of HAC1 mRNA translation by long-range base pairing is released by cytoplasmic splicing upon induction of the unfolded protein response. *Cell* **2001**, *107*, 103–114. [[CrossRef](#)]
29. Aragón, T.; Van Anken, E.; Pincus, D.; Serafimova, I.M.; Korenykh, A.V.; Rubio, C.A.; Walter, P. Messenger RNA targeting to endoplasmic reticulum stress signalling sites. *Nature* **2009**, *457*, 736–740. [[CrossRef](#)] [[PubMed](#)]
30. Mori, K.; Ogawa, N.; Kawahara, T.; Yanagi, H.; Yura, T. mRNA splicing-mediated C-terminal replacement of transcription factor Hac1p is required for efficient activation of the unfolded protein response. *Proc. Natl. Acad. Sci. USA* **2000**, *97*, 4660–4665. [[CrossRef](#)] [[PubMed](#)]
31. Mori, K.; Sant, A.; Kohno, K.; Normington, K.; Gething, M.J.; Sambrook, J.F. A 22 bp cis-acting element is necessary and sufficient for the induction of the yeast KAR2 (BiP) gene by unfolded proteins. *EMBO J.* **1992**, *11*, 2583–2593. [[PubMed](#)]
32. Kohno, K.; Normington, K.; Sambrook, J.; Gething, M.J.; Mori, K. The promoter region of the yeast KAR2 (BiP) gene contains a regulatory domain that responds to the presence of unfolded proteins in the endoplasmic reticulum. *Mol. Cell. Biol.* **1993**, *13*, 877–890. [[CrossRef](#)] [[PubMed](#)]

33. Mori, K.; Ogawa, N.; Kawahara, T.; Yanagi, H.; Yura, T. Palindrome with spacer of one nucleotide is characteristic of the cis-acting unfolded protein response element in *Saccharomyces cerevisiae*. *J. Biol. Chem.* **1998**, *273*, 9912–9920. [CrossRef] [PubMed]
34. Partaledis, J.A.; Berlin, V. The FKB2 gene of *Saccharomyces cerevisiae*, encoding the immunosuppressant-binding protein FKBP-13, is regulated in response to accumulation of unfolded proteins in the endoplasmic reticulum. *Proc. Natl. Acad. Sci. USA* **1993**, *90*, 5450–5454. [CrossRef] [PubMed]
35. Patil, C.K.; Li, H.; Walter, P. Gcn4p and novel upstream activating sequences regulate targets of the unfolded protein response. *PLoS Biol.* **2004**, *2*, e246. [CrossRef] [PubMed]
36. Bukau, B.; Horwich, A.L. The Hsp70 and Hsp60 Chaperone Machines. *Cell* **1998**, *92*, 351–366. [CrossRef]
37. Vogel, J.P.; Misra, L.M.; Rose, M.D. Loss of BiP/GRP78 function blocks translocation of secretory proteins in yeast. *J. Cell Biol.* **1990**, *110*, 1885–1895. [CrossRef] [PubMed]
38. Nishikawa, S.I.; Fewell, S.W.; Kato, Y.; Brodsky, J.L.; Endo, T. Molecular chaperones in the yeast endoplasmic reticulum maintain the solubility of proteins for retrotranslocation and degradation. *J. Cell Biol.* **2001**, *153*, 1061–1070. [CrossRef] [PubMed]
39. Kimata, Y.; Kimata, Y.I.; Shimizu, Y.; Abe, H.; Farcasanu, I.C.; Takeuchi, M.; Rose, M.D.; Kohno, K. Genetic evidence for a role of BiP/Kar2 that regulates Ire1 in response to accumulation of unfolded proteins. *Mol. Biol. Cell* **2003**, *14*, 2559–2569. [CrossRef] [PubMed]
40. Normington, K.; Kohno, K.; Kozutsumi, Y.; Gething, M.J.; Sambrook, J. *S. cerevisiae* encodes an essential protein homologous in sequence and function to mammalian BiP. *Cell* **1989**, *57*, 1223–1236. [CrossRef]
41. Wolfe, K.H.; Shields, D.C. Molecular evidence for an ancient duplication of the entire yeast genome. *Nature* **1997**, *387*, 708–713. [CrossRef] [PubMed]
42. Hooks, K.B.; Griffiths-Jones, S. Conserved RNA structures in the non-canonical Hac1/Xbp1 intron. *RNA Biol.* **2011**, *8*, 1–6. [CrossRef] [PubMed]
43. Mori, T.; Ogasawara, C.; Inada, T.; Englert, M.; Beier, H.; Takezawa, M.; Endo, T.; Yoshihisa, T. Dual functions of yeast tRNA ligase in the Unfolded Protein Response: Unconventional cytoplasmic splicing of HAC1 pre-mRNA is not sufficient to release translational attenuation. *Mol. Biol. Cell* **2010**, *21*, 3722–3734. [CrossRef] [PubMed]
44. Lewis, M.J.; Pelham, H.R. The sequence of the *Kluyveromyces lactis* BiP gene. *Nucleic Acids Res.* **1990**, *18*, 6438. [CrossRef] [PubMed]
45. Lewis, M.J.; Sweet, D.J.; Pelham, H.R. The ERD2 gene determines the specificity of the luminal ER protein retention system. *Cell* **1990**, *61*, 1359–1363. [CrossRef]
46. Pidoux, A.L.; Armstrong, J. The BiP protein and the endoplasmic reticulum of *Schizosaccharomyces pombe*: Fate of the nuclear envelope during cell division. *J. Cell. Sci.* **1993**, *105*, 1115–1120. [PubMed]
47. Frost, A.; Elgort, M.G.; Brandman, O.; Ives, C.; Collins, S.R.; Miller-Vedam, L.; Weibe Zahnh, J.; Hein, M.Y.; Poser, I.; Mann, M.; et al. Functional repurposing revealed by comparing *S. pombe* and *S. cerevisiae* genetic interactions. *Cell* **2012**, *149*, 1339–1352. [CrossRef] [PubMed]
48. Ridgway, G.J.; Douglas, H.C. Unbalanced growth of yeast due to inositol deficiency. *J. Bacteriol.* **1958**, *76*, 163–166. [PubMed]
49. Ingavale, S.S.; Bachhawat, A.K. Restoration of inositol prototrophy in the fission yeast *Schizosaccharomyces pombe*. *Microbiology* **1999**, *145*, 1903–1910. [CrossRef] [PubMed]
50. Voicu, P.-M.; Poitelea, M.; Schweingruber, E.; Rusu, M. Inositol is specifically involved in the sexual program of the fission yeast *Schizosaccharomyces pombe*. *Arch. Microbiol.* **2002**, *177*, 251–258. [CrossRef] [PubMed]
51. Niederberger, C.; Gräub, R.; Schweingruber, A.-M.; Fankhauser, H.; Rusu, M.; Poitelea, M.; Edenthaler, L.; Schweingruber, M.E. Exogenous inositol and genes responsible for inositol transport are required for mating and sporulation in *Schizosaccharomyces pombe*. *Curr. Genet.* **1998**, *33*, 255–261. [CrossRef] [PubMed]
52. Kimmig, P.; Diaz, M.; Zheng, J.; Williams, C.C.; Lang, A.; Aragón, T.; Li, H.; Walter, P. The unfolded protein response in fission yeast modulates stability of select mRNAs to maintain protein homeostasis. *eLife* **2012**, *2012*, e00048. [CrossRef] [PubMed]
53. Hollien, J.; Weissman, J.S. Decay of endoplasmic reticulum-localized mRNAs during the unfolded protein response. *Science* **2006**, *313*, 104–107. [CrossRef] [PubMed]
54. Mishiba, K.; Nagashima, Y.; Suzuki, E.; Hayashi, N.; Ogata, Y.; Shimada, Y.; Koizumi, N. Defects in IRE1 enhance cell death and fail to degrade mRNAs encoding secretory pathway proteins in the *Arabidopsis* unfolded protein response. *Proc. Natl. Acad. Sci. USA* **2013**, *110*, 5713–5718. [CrossRef] [PubMed]

55. Han, D.; Lerner, A.G.; Vande Walle, L.; Upton, J.-P.; Xu, W.; Hagen, A.; Backes, B.J.; Oakes, S.A.; Papa, F.R. IRE1alpha kinase activation modes control alternate endoribonuclease outputs to determine divergent cell fates. *Cell* **2009**, *138*, 562–575. [CrossRef] [PubMed]
56. Hollien, J.; Lin, J.H.; Li, H.; Stevens, N.; Walter, P.; Weissman, J.S. Regulated Ire1-dependent decay of messenger RNAs in mammalian cells. *J. Cell Biol.* **2009**, *186*, 323–331. [CrossRef] [PubMed]
57. Iqbal, J.; Dai, K.; Seimon, T.; Jungreis, R.; Oyadomari, M.; Kuriakose, G.; Ron, D.; Tabas, I.; Hussain, M.M. IRE1beta inhibits chylomicron production by selectively degrading MTP mRNA. *Cell Metab.* **2008**, *7*, 445–455. [CrossRef] [PubMed]
58. Pidoux, A.L.; Armstrong, J. Analysis of the BiP gene and identification of an ER retention signal in *Schizosaccharomyces pombe*. *EMBO J.* **1992**, *11*, 1583–1591. [PubMed]
59. Guydosh, N.R.; Kimmig, P.; Walter, P.; Green, R. Regulated Ire1-dependent mRNA decay requires no-go mRNA degradation to maintain endoplasmic reticulum homeostasis in *S. pombe*. *eLife* **2017**, *6*. [CrossRef] [PubMed]
60. Pineau, L.; Colas, J.; Dupont, S.; Beney, L.; Fleurat-Lessard, P.; Berjeaud, J.-M.; Bergès, T.; Ferreira, T. Lipid-induced ER stress: Synergistic effects of sterols and saturated fatty acids. *Traffic* **2009**, *10*, 673–690. [CrossRef] [PubMed]
61. Miyazaki, T.; Nakayama, H.; Nagayoshi, Y.; Kakeya, H.; Kohno, S. Dissection of Ire1 functions reveals stress response mechanisms uniquely evolved in *Candida glabrata*. *PLoS Pathog.* **2013**, *9*, e1003160. [CrossRef] [PubMed]
62. Miyazaki, T.; Kohno, S. ER stress response mechanisms in the pathogenic yeast *Candida glabrata* and their roles in virulence. *Virulence* **2014**, *5*, 365–370. [CrossRef] [PubMed]
63. Miyazaki, T.; Yamauchi, S.; Inamine, T.; Nagayoshi, Y.; Saijo, T.; Izumikawa, K.; Seki, M.; Kakeya, H.; Yamamoto, Y.; Yanagihara, K.; et al. Roles of calcineurin and Crz1 in antifungal susceptibility and virulence of *Candida glabrata*. *Antimicrob. Agents Chemother.* **2010**, *54*, 1639–1643. [CrossRef] [PubMed]
64. Babour, A.; Bicknell, A.A.; Tourtellotte, J.; Niwa, M. A surveillance pathway monitors the fitness of the endoplasmic reticulum to control its inheritance. *Cell* **2010**, *142*, 256–269. [CrossRef] [PubMed]
65. Chen, Y.-L.; Konieczka, J.H.; Springer, D.J.; Bowen, S.E.; Zhang, J.; Silao, F.G.S.; Bungay, A.A.C.; Bigol, U.G.; Nicolas, M.G.; Abraham, S.N.; et al. Convergent Evolution of calcineurin pathway roles in thermotolerance and virulence in *Candida glabrata*. *Genes Genome Genet.* **2012**, *2*, 675–691. [CrossRef] [PubMed]
66. Askew, D.S. Endoplasmic reticulum stress and fungal pathogenesis converge. *Virulence* **2014**, *5*, 331–333. [CrossRef] [PubMed]
67. Krishnan, K.; Askew, D.S. Endoplasmic reticulum stress and fungal pathogenesis. *Fungal Biol. Rev.* **2014**, *28*, 29–35. [CrossRef] [PubMed]
68. Jung, K.W.; So, Y.S.; Bahn, Y.S. Unique roles of the unfolded protein response pathway in fungal development and differentiation. *Sci. Rep.* **2016**, *6*, 1–14. [CrossRef] [PubMed]
69. Cheon, S.A.; Jung, K.-W.; Chen, Y.-L.; Heitman, J.; Bahn, Y.-S.; Kang, H.A. Unique evolution of the UPR pathway with a novel bZIP transcription factor, Hx11, for controlling pathogenicity of *Cryptococcus neoformans*. *PLoS Pathog.* **2011**, *7*, e1002177. [CrossRef] [PubMed]
70. Cheon, S.A.; Jung, K.W.; Bahn, Y.S.; Kang, H.A. The Unfolded Protein Response (UPR) pathway in *Cryptococcus*. *Virulence* **2014**, *5*, 341–350. [CrossRef] [PubMed]
71. Xue, C.; Liu, T.; Chen, L.; Li, W.; Liu, I.; Kronstad, J.W.; Seyfang, A.; Heitman, J. Role of an expanded inositol transporter repertoire in *Cryptococcus neoformans* sexual reproduction and virulence. *mBio* **2010**, *1*, e00084-10. [CrossRef] [PubMed]
72. Glazier, V.E.; Kaur, J.N.; Brown, N.T.; Rivera, A.A.; Panepinto, J.C. Puf4 regulates both splicing and decay of *HXL1* mRNA encoding the unfolded protein response transcription factor in *Cryptococcus neoformans*. *Eukaryot. Cell* **2015**, *14*, 385–395. [CrossRef] [PubMed]
73. Jung, K.W.; Kang, H.A.; Bahn, Y.S. Essential roles of the Kar2/BiP molecular chaperone downstream of the UPR pathway in *Cryptococcus neoformans*. *PLoS ONE* **2013**, *8*, e58956. [CrossRef] [PubMed]
74. Lee, S.C.; Heitman, J. Function of *Cryptococcus neoformans* KAR7 (SEC66) in karyogamy during unisexual and opposite-sex mating. *Eukaryot. Cell* **2012**, *11*, 783–794. [CrossRef] [PubMed]
75. Blankenship, J.R.; Fanning, S.; Hamaker, J.J.; Mitchell, A.P. An Extensive circuitry for cell wall regulation in *Candida albicans*. *PLoS Pathog.* **2010**, *6*, e1000752. [CrossRef] [PubMed]

76. Azadmanesh, J.; Gowen, A.M.; Creger, P.E.; Schafer, N.D.; Blankenship, J.R. Filamentation involves two overlapping, but distinct, programs of filamentation in the pathogenic fungus *Candida albicans*. *Genes Genome Genet.* **2017**, *7*, 3797–3808. [[CrossRef](#)] [[PubMed](#)]
77. Chen, Y.-L.; Kauffman, S.; Reynolds, T.B. *Candida albicans* uses multiple mechanisms to acquire the essential metabolite inositol during infection. *Infect. Immun.* **2008**, *76*, 2793–2801. [[CrossRef](#)] [[PubMed](#)]
78. Wimalasena, T.T.; Enjalbert, B.; Guillemette, T.; Plumridge, A.; Budge, S.; Yin, Z.; Brown, A.J.P.; Archer, D.B. Impact of the unfolded protein response upon genome-wide expression patterns, and the role of Hac1 in the polarized growth, of *Candida albicans*. *Fungal Genet. Biol.* **2008**, *45*, 1235–1247. [[CrossRef](#)] [[PubMed](#)]
79. Thomas, E.; Sircaik, S.; Roman, E.; Brunel, J.M.; Johri, A.K.; Pla, J.; Panwar, S.L. The activity of RTA2, a downstream effector of the calcineurin pathway, is required during tunicamycin-induced ER stress response in *Candida albicans*. *FEMS Yeast Res.* **2015**, *15*, fov095. [[CrossRef](#)] [[PubMed](#)]
80. Zhang, J.; Heitman, J.; Chen, Y.-L. Comparative analysis of calcineurin signaling between *Candida dubliniensis* and *Candida albicans*. *Commun. Integr. Biol.* **2012**, *5*, 122–126. [[CrossRef](#)] [[PubMed](#)]
81. Morrow, M.W.; Janke, M.R.; Lund, K.; Morrison, E.P.; Paulson, B.A. The *Candida albicans* Kar2 protein is essential and functions during the translocation of proteins into the endoplasmic reticulum. *Curr. Genet.* **2011**, *57*, 25–37. [[CrossRef](#)] [[PubMed](#)]
82. Zhang, L.; Zhang, C.; Wang, A. Divergence and conservation of the major UPR branch IRE1-bZIP signaling pathway across eukaryotes. *Sci. Rep.* **2016**, *6*, 27362. [[CrossRef](#)] [[PubMed](#)]
83. Montenegro-Montero, A.; Goity, A.; Larrondo, L.F. The bZIP transcription factor HAC-1 is involved in the unfolded protein response and is necessary for growth on cellulose in *Neurospora crassa*. *PLoS ONE* **2015**, *10*, e0131415. [[CrossRef](#)] [[PubMed](#)]



© 2018 by the authors. Licensee MDPI, Basel, Switzerland. This article is an open access article distributed under the terms and conditions of the Creative Commons Attribution (CC BY) license (<http://creativecommons.org/licenses/by/4.0/>).

Review

Unfolding the Endoplasmic Reticulum of a Social Amoeba: *Dictyostelium discoideum* as a New Model for the Study of Endoplasmic Reticulum Stress

Eunice Domínguez-Martín ^{1,2} , Mariana Hernández-Elvira ², Olivier Vincent ¹, Roberto Coria ^{2,*} and Ricardo Escalante ^{1,*}

¹ Instituto de Investigaciones Biomédicas “Alberto Sols” (CSIC-UAM), Arturo Duperier 4, 28029 Madrid, Spain; edominguez@iib.uam.es (E.D.-M.); ovincent@iib.uam.es (O.V.)

² Departamento de Genética Molecular, Instituto de Fisiología Celular, Universidad Nacional Autónoma de México, 04510 Ciudad de México, México; melvira@email.ifc.unam.mx (M.H.-E)

* Correspondence: rcoria@ifc.unam.mx (R.C.); rescalante@iib.uam.es (R.E.); Tel.: +52-55-56-22-56-52 (R.C.); +34-915-854-467 (R.E.); Fax: +34-915-854-401 (R.E.)

Received: 26 April 2018; Accepted: 5 June 2018; Published: 10 June 2018



Abstract: The endoplasmic reticulum (ER) is a membranous network with an intricate dynamic architecture necessary for various essential cellular processes. Nearly one third of the proteins trafficking through the secretory pathway are folded and matured in the ER. Additionally, it acts as calcium storage, and it is a main source for lipid biosynthesis. The ER is highly connected with other organelles through regions of membrane apposition that allow organelle remodeling, as well as lipid and calcium traffic. Cells are under constant changes due to metabolic requirements and environmental conditions that challenge the ER network’s maintenance. The unfolded protein response (UPR) is a signaling pathway that restores homeostasis of this intracellular compartment upon ER stress conditions by reducing the load of proteins, and by increasing the processes of protein folding and degradation. Significant progress on the study of the mechanisms that restore ER homeostasis was achieved using model organisms such as yeast, *Arabidopsis*, and mammalian cells. In this review, we address the current knowledge on ER architecture and ER stress response in *Dictyostelium discoideum*. This social amoeba alternates between unicellular and multicellular phases and is recognized as a valuable biomedical model organism and an alternative to yeast, particularly for the presence of traits conserved in animal cells that were lost in fungi.

Keywords: *Dictyostelium*; endoplasmic reticulum; endoplasmic reticulum stress; unfolded protein response; inositol-requiring enzyme 1 (IRE1)

1. *Dictyostelium* as a Model Organism for Experimental Biology Research

Owing to its simplicity and easy genetic manipulability, some microbial organisms prove to be powerful biology-research tools; for instance, *Saccharomyces cerevisiae* is one of the most widely studied eukaryotic organisms. Much of the current knowledge in biochemistry, and molecular and cellular biology arose from research performed with this yeast. However, since this fungal organism has some specific genetic, cellular, and metabolic traits that are not widely conserved, other eukaryotic microbial organisms emerged to address cellular processes that diverged greatly in yeast cells. One of these organisms is *Dictyostelium discoideum*, a social soil-dwelling protist, taxonomically classified in the Amoebozoa phylum, the sister group to animals and fungi [1]. Despite its phylogenetic classification, *Dictyostelium* displays cellular processes that are conserved in animal cells, but that are absent in fungal or plant cells, such as phagocytosis and chemotaxis. Interestingly, it also has traits that are conserved in

fungi and plants, but were lost in animal cells, such as phosphorelay signaling systems, and cellulose production [2,3].

Dictyostelium has a life cycle that alternates between unicellular and multicellular phases, depending on nutrient availability (Figure 1). As unicellular amoebas, they obtain nutrients from phagocytizing yeast or bacteria, and they multiply via fission about every 8 h. Remarkably, under starvation, *Dictyostelium* cells stop mitotic division, and start an intercellular signaling communication process mediated by the secretion of various molecules. One of them, the cyclic adenosine monophosphate (cAMP), acts as a chemoattractant that triggers the polarization, migration, and aggregation of groups of about 10^5 cells from the species *Dictyostelium discoideum*. These aggregates of apparently homogeneous cells enter a developmental program that generates a multicellular organism with distinct cell types. After various developmental stages, including one as a multicellular motile slug, the *Dictyostelium* differentiation program culminates in the formation of a fruiting body composed of a sorogen filled with spores, which is supported by a cellulose stalk made of dead cells (a detailed review of this process was addressed in Reference [4]).

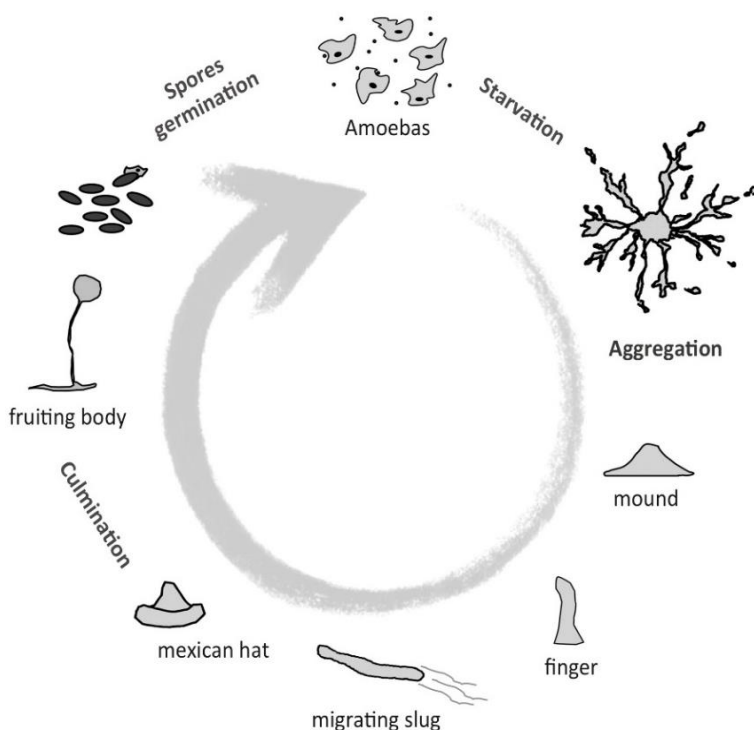


Figure 1. Diagram of the *Dictyostelium* life cycle. Individual amoebas feed on yeast and bacteria, and multiply via fission. When nutrients are scarce, cells aggregate and undergo a developmental program, comprised of distinct stages that culminate in the formation of a fruiting body, which is composed of a stalk, and a sorogen filled with spores. Under suitable environmental conditions, the spores germinate.

Since its first isolation and description more than 80 years ago, a growing number of studies used *Dictyostelium discoideum* to unravel diverse biological questions [2,3]. The genome of this haploid organism is fully sequenced [5], and many different techniques were developed allowing the study of a wide range of topics including infection and drug testing [6]. In addition, *Dictyostelium* was used in basic studies of cell and developmental signaling, among them, the pathways involved in endoplasmic reticulum (ER) homeostasis, maintenance, and regulation [7]. Conditions that interfere with ER homeostasis contribute to the pathogenesis of human chronic disorders including diabetes and some neurodegenerative syndromes, such as Alzheimer's, Parkinson's, and Huntington's diseases [8,9]. *Dictyostelium* emerged as an advantageous model for the study of signaling pathways involved in neurodegeneration (reviews on this topic were addressed in References [10–12]). In addition,

this amoeba is an interesting model for the study of pathways involved in neurological disorders associated with protein aggregation, since it efficiently regulates the accumulation of prion-like protein aggregates [13,14].

2. The Endoplasmic Reticulum of a Social Amoeba

The ER is the largest eukaryotic organelle. This complex membranous network is the place where essential functions such as protein folding and modification, lipid synthesis, and calcium (Ca^{2+}) storage are fulfilled. In the following sections, a general comparative description of the current knowledge on the *Dictyostelium* ER structure and function is presented. Table 1 contains a summary of all the *Dictyostelium* ER proteins that were discussed throughout this text.

2.1. A Membranous Network with an Intricate Structure

Two domains that maintain luminal continuity can be identified in the ER, the nuclear envelope (NE) and the peripheral ER, each with a particular structure and specific characteristics. In the NE, two stacked membranes of low curvature form the inner and outer nuclear membrane (INM and ONM), whereas the peripheral ER spreads across the cytosol, shaped by a network of interconnected tubules and flat sheet-like regions [15,16]. In mammalian cells, an array of constricted tubule clusters, enriched with three-way junctions, forms the peripheral ER matrices. This set of structures is relatively flat, and has a heterogeneous composition and topology [16]. In addition, there are some specialized ER regions formed through flattened membranes, which can be found shaping the nuclear envelope, in the perinuclear region or close to the plasma membrane [17–19]. A tubular network that expands from the NE and these matrices forms a system that connects all the ER domains. The tubules' surface is highly curved, which facilitates surface-dependent functions such as lipid synthesis, and signaling between the ER and other organelles [15].

The *Dictyostelium* ER can be visualized by expressing inositol-requiring enzyme A (IreA) tagged with a fluorescent protein. IreA is an ER-resident protein that participates in the unfolded protein response (UPR) pathway (see Section 3.1—The IreA Branch). The *Dictyostelium* ER can be divided into an NE region and a peripheral zone, consisting of a network of tubules and sheet-like regions, which spread throughout the cell (Figure 2). Domains with sheet-like appearance are distributed mainly in peripheral cell zones, and in close proximity to the NE, while tubules are spread throughout the cell, and can be observed as more defined structures in medial cell sections.

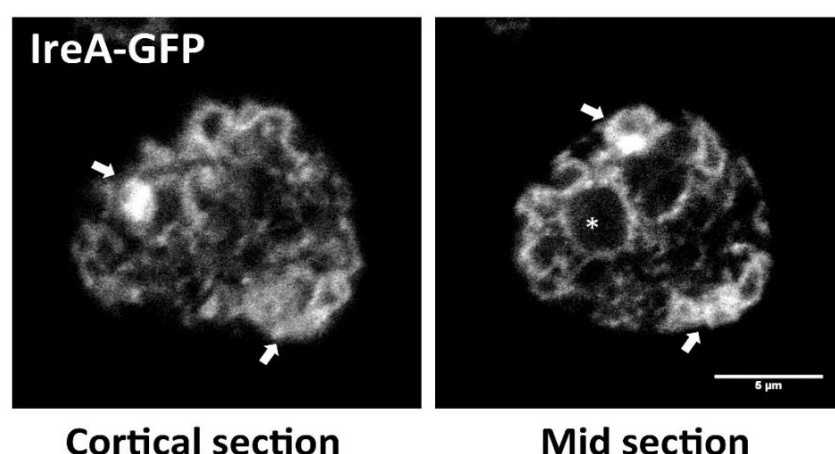


Figure 2. The *Dictyostelium* endoplasmic reticulum (ER). In vivo confocal microscopy pictures showing a cortical section and a mid-section of a wild-type (WT) cell expressing the ER marker, Inositol requiring enzyme A (IreA) fused to the GFP. The asterisk pinpoints the nucleus, surrounded by the perinuclear ER. Arrows highlight zones where sheet-like regions are evident. Tubules can be distinguished across the entire cell area. (Scale bar represents 5 μm).

Table 1. List of the endoplasmic reticulum (ER) protein orthologs mentioned throughout this text.

Function/Features	<i>Dictyostelium</i> ^a	<i>Human</i> ^a	<i>Saccharomyces cerevisiae</i> ^a	<i>Arabidopsis thaliana</i> ^a
ER structure				
Transmembrane protein that promotes membrane curvature, and participates in maintenance of tubular ER morphology	Reticulon-like group C (Rtnlc)/ Q54CA6	Reticulons-1 to 4 (RTN1 to RTN4)/ Q16799, O75298, O95197, Q9JK11	Reticulon-like proteins 1 (RTN1) and 2 (RTN2)/ A0A250W951, Q12443	Reticulon-like proteins B1 to 18, and 21 to 23 (RTNLB1 to 18 and RTNLB21 to 23)/ Q9SUR3, Q9SUT9, Q9SH59, Q9FFS0, O82352, Q6DBN4, Q9M145, Q9SS37, Q9LJQ5, Q6NPD8, Q9LT71, Q9M392, O64837, A2RVT6, Q9ZU43, Q8GYH6, Q6DR04, Q8LDS3, Q56X72, Q8GWH5, P0C941
Dynamin-like GTPase that mediates homotypic ER fusion	Sey1/ Q54W90	Atlastin-1 (ATL1)/ Q8WXF7	Sey1/ Q99287	Root hair defective 3 (RHD3) and root hair defective 3 homolog 2 (RHD3-2)/ P93042, Q9FKE9
ER contact sites				
Components of the mitochondria encounter sites (ERMES), which are involved in the tether between the ER and the mitochondria to promote inter-organelar calcium and phospholipid exchange	Maintenance of mitochondrial morphology-1 (Mmm1)/ Q54MI5	ND	Maintenance of mitochondrial morphology protein 1 (Mmm1)/ P41800	ND
	Mitochondrial distribution and morphology-10 (Mdm10)/ Q54XQ5	ND	Mitochondrial distribution and morphology 10 (Mdm10)/ P18409	ND
	Mitochondrial distribution and morphology 34 (Mdm34)/ Q869R5	ND	Mitochondrial distribution and morphology protein 34 (Mdm34)/ P53083	ND
Transmembrane protein required to regulate ER contact sites, essential for autophagy and proper ER homeostasis	Vacuole membrane protein 1 (Vmp1)/ Q54NL4	Vacuole membrane protein 1 (VMP1)/ Q96GC9	ND	Vacuole membrane proteins 1 (KMS1) and 2 (KMS2)/ Q5XF36, F4I8Q7

Table 1. Cont.

Function/Features	<i>Dictyostelium</i> ^a	<i>Human</i> ^a	<i>Saccharomyces cerevisiae</i> ^a	<i>Arabidopsis thaliana</i> ^a
Lipid metabolism				
Protein that associates to the lipid droplet surface	Perilipin (PlnA)/ Q54WC4	Perilipin proteins 1 to 5 (PLIN1 to 5)/ O60240, Q99541, O60664, Q96Q06, Q00G26	ND	ND
Catalyze the conversion of acyl coenzyme A (CoA) and 1,2-diacylglycerol to CoA and triacylglycerol.	Diacylglycerol O-acyltransferases 1 (Dgat1) and 2 (Dgat2)/ Q55BH9, Q54GC1	Diacylglycerol O-acyltransferases 1 (DGAT1), 2-acylglycerol O-acyltransferase 1 (MOGAT1)/ O75907, Q96PD6	Sterol O-acyltransferases 1 (Are1) and 2 (Are2)/ P25628, P53629	Diacylglycerol O-acyltransferase 1 (DGAT1)/ Q9SLD2
Protein folding and modification				
Subunits of the oligosaccharyl transferase complex, which catalyzes asparagine-linked glycosylation of newly synthesized proteins in the ER lumen	Oligosaccharyl transferase-1 (Ost1)/ Q54C27	Dolichyl-diphosphooligosaccharide-protein glycosyltransferase subunit 1 (RPN1)/ P04843	Dolichyl-diphosphooligosaccharide-protein glycosyltransferase subunit 1 (Ost1)/ P41543	Dolichyl-diphosphooligosaccharide-protein glycosyltransferase subunits 1A (OST1A) and 1B (OST1B)/ Q9SFX3, Q9ZUA0
	Oligosaccharyl transferase-2 (Ost2)/ Q54FB6	Dolichyl-diphosphooligosaccharide-protein glycosyltransferase subunit (DAD1)/ P61803	Dolichyl-diphosphooligosaccharide-protein glycosyltransferase subunit (OST2)/ P46964	Dolichyl-diphosphooligosaccharide-protein glycosyltransferase subunits 1 (DAD1) and 2 (DAD2)/ Q39080, O22622
	Oligosaccharyl transferase-3 (Ost3)/ Q54N33	ND	Dolichyl-diphosphooligosaccharide-protein glycosyltransferase subunit 3 (Ost3)/ P48439	Dolichyl-diphosphooligosaccharide-protein glycosyltransferase subunits 3A (OST3A) and 3B (OST3B)/ F4I8X8, Q9SYB5
	Oligosaccharyl transferase-4 (Ost4)/ Q54V54	Dolichyl-diphosphooligosaccharide-protein glycosyltransferase subunit 4 (OST4)/ P0C6T2	Dolichyl-diphosphooligosaccharide-protein glycosyltransferase subunit 4 (Ost4)/ Q99380	ND

Table 1. Cont.

Function/Features	<i>Dictyostelium</i> ^a	<i>Human</i> ^a	<i>Saccharomyces cerevisiae</i> ^a	<i>Arabidopsis thaliana</i> ^a
Oligosaccharyl transferase complex subunit C (Ostc)/ Q54X66	Oligosaccharyl transferase complex subunit OSTC (OSTC)/ Q9NRP0	Oligosaccharyltransferase complex subunit OSTC (OSTC)/ Q9NRP0	ND	Oligosaccharyl transferase complex/magnesium transporter family protein (At4g29870)/ Q9SZQ8
Wheat germ agglutinin-binding protein (Wbp1)/ Q54E62	Wheat germ agglutinin-binding protein (Wbp1)/ Q54E62	Dolichyl-diphosphooligosaccharide-protein glycosyltransferase 48 kDa subunit (DDOST)/ P39656	Dolichyl-diphosphooligosaccharide-protein glycosyltransferase subunit (Wbp1)/ P33767	Dolichyl-diphosphooligosaccharide-protein glycosyltransferase 48 kDa subunit (OST48)/ Q944K2
Suppressor of a WBP1 mutation (Swp1)/ Q54HG9	Suppressor of a WBP1 mutation (Swp1)/ Q54HG9	Dolichyl-diphosphooligosaccharide-protein glycosyltransferase subunit 2 (RPN2)/ P04844	Dolichyl-diphosphooligosaccharide-protein glycosyltransferase subunit (Swp1)/ Q02795	Dolichyl-diphosphooligosaccharide-protein glycosyltransferase subunit 2 (RPN2)/ Q93Z16
Staurosporine and temperature sensitivity (Stt3)/ Q54NM9	Staurosporine and temperature sensitivity (Stt3)/ Q54NM9	Dolichyl-diphosphooligosaccharide-protein glycosyltransferase subunits A (STT3A) and B (STT3B)/ P46977, Q8TCJ2	Dolichyl-diphosphooligosaccharide-protein glycosyltransferase subunit (Stt3)/ P39007	Dolichyl-diphosphooligosaccharide-protein glycosyltransferase subunits A (STT3A) and B (STT3B)/ Q93ZY3, Q9FX21
Heat shock protein 70 (Hsp70)-family chaperone	78 kDa Glucose-regulated protein (Grp78)/ Q8T869	Binding immunoglobulin protein/78 kDa glucose-regulated protein (BiP/Grp78)/ P11021	Binding immunoglobulin protein (BiP/Kar2)/ P16474	Binding immunoglobulin protein 2 (BIP2)/ F4K007
Hsp90-family chaperone	94 kDa Glucose-regulated protein (Dd-grp94)/ Q9NKX1	Endoplasmin (GRP94)/ P14625	ATP-dependent molecular chaperone (Hsp82)/ P02829	Endoplasmin homolog (HSP90-7)/ Q9STX5
Calcium-binding proteins with chaperone activity	Calreticulin (CrtA)/ Q23858	Calreticulin (CALR)/ P27797	ND	Calreticulin-1 (CRT1) and 2 (CRT2)/ O04151, Q388587
	Calnexin (CnxA)/ Q55BA8	Calnexin (CANX)/ P27824	Calnexin homolog (Cne1)/ P27825	Calnexin homolog 1 (CNX1) and 2 (CNX2)/ P29402, Q38798

Table 1. Cont.

Function/Features	<i>Dictyostelium</i> ^a	<i>Human</i> ^a	<i>Saccharomyces cerevisiae</i> ^a	<i>Arabidopsis thaliana</i> ^a
ER luminal protein that catalyzes the formation and remodeling of protein disulfide bonds	Protein disulfide isomerases 1 (Pdi1) and 2 (Pdi2)/ Q86IA3, Q54EN4	Protein disulfide isomerases (P4HB), A4 (PDIA4), A3 (PDIA3), and A6 (PDIA6)/ P07237, P13667, P30101, Q15084	Protein disulfide isomerase (Pdi1)/ P17967	Protein disulfide isomerase-like proteins 1-1 (PDIL1-1), 1-2 (PDIL1-2), 2-2 (PDIL2-2), and 2-3 (PDIL2-3)/ Q9XI01, Q9SRG3, O22263, O48773
<i>Unfolded Protein Response</i>				
ER transmembrane serine and threonine kinase with ribonuclease activity that senses ER stress	Inositol-requiring enzyme A (IreA)/ Q55GJ2	Inositol-requiring enzyme proteins 1α (IRE1 α or ERN1) and 1β (IRE1β or ERN2)/ O75460, Q76MJ5	Inositol-requiring enzyme 1 (Ire1)/ P32361	Inositol-requiring enzyme proteins 1a (IRE1a) and 1b (IRE1b)/ Q93VJ2,
<i>Calcium channel</i>				
Ion channel participates in calcium release from the ER, and is activated by inositol trisphosphate	Inositol 1,4,5-trisphosphate receptor (IplA)/ Q9NA13	Inositol 1,4,5-trisphosphate receptors type 1 (ITPR1), type 2 (ITPR2), and type 3 (ITPR3)/ Q14643, Q14571, Q14573	ND	ND

^a Protein orthologs/ UNIPROT identifiers. ND, no homology detected.

In mammalian cells, the curvature of the tubules is maintained by a highly conserved integral membrane family of proteins, referred to as reticulons (RTNs) [20]. RTN proteins contain a reticulon homology domain (RHD) at their C-terminus which is formed by two long hairpin transmembrane domains, separated by a hydrophilic linker [21]. These hairpins are inserted in the cytoplasmic leaflet of the ER membrane to provoke membrane bending. RTNs can also oligomerize in order to determine the diameter of the tubules [20–22].

Studies on how the *Dictyostelium* ER structure is maintained are still scarce; however, a homolog of the reticulon family was phylogenetically identified (annotated as *rtnlc*/DDB_G0293088) [23]. Owing to the presence in *Dictyostelium* of single orthologs of some of the proteins involved in the maintenance of ER architecture, it represents an advantageous model for combined genetic studies on ER dynamics and structure. For instance, reticulons were implicated in neurodegenerative disorders [24], but the study of this protein family in mammalian cells is challenging since they contain a large number of isoforms.

2.2. The ER Is a Dynamic Structure Continuously Rearranged

The ER is a highly dynamic network; its architecture is modified according to specific cellular demands or processes, such as changes in cellular morphology, cell migration, mitosis, and upon stressful conditions. For instance, specialized secretory cells require an increase in the number of sheet-like structures to synthesize large amounts of proteins, while adrenal, liver, and muscle cells require an ER network predominantly formed by tubules [25].

The synthesis of new tubules in the ER, together with the maintenance of its network and dynamics, depends greatly on the association of the ER with the cytoskeleton [26–28], while the maintenance of the reticulated network requires continuous events of contact and fusion between tubules. ER fusion events are mediated by atlastin (ATL) proteins, a dynamin-related family of GTPases that mediate homotypic membrane fusion [29,30]. During the fusion events, two GTP-bound ATLs, localized at opposing membranes, transdimerize, and GTP hydrolysis induces a conformational change that pulls the ER membrane close enough to fuse [31,32]. Plants and yeasts possess functional homolog GTPases of ATLs [33,34].

Recently, the role of the *Dictyostelium* ATL homolog Synthetic enhancement of YOP1 (Sey1) was evaluated during infection with the intracellular bacteria *Legionella pneumophila* (*L. pneumophila*) [35]. This pathogen exploits a conserved replication mechanism in mammalian macrophages and in *Dictyostelium* cells, based on the construction of a special ER-derived compartment known as a *Legionella*-containing vacuole (LCV). Interestingly, in *Dictyostelium* cells, Sey1 modulates *L. pneumophila* replication, possibly by mediating homotypic membrane fusion at later steps of LCV maturation.

2.3. A Well-Connected Membranous System

The ER interacts dynamically with other membranes, such as the plasma membrane, and has contacts with other organelles such as mitochondria, the Golgi body, and endosomes, among others. These interactions, known as membrane contact sites (MCSs), allow the transport of ER-synthesized lipids and Ca^{2+} to other organelles. In addition, MCSs are involved in organelle biogenesis, distribution, inheritance, and maintenance (a more extensive review on ER contact sites can be found in Reference [36]).

In yeasts, the mitochondria–ER membrane contacts (MERCs) are tethered by the ER–mitochondria encounter structure (ERMES), which organizes the contact between the ER and the mitochondrial outer membrane. Similarly, the mitochondrial contact site and cristae organizing system (MICOS) enables the contact between the mitochondrial inner and outer membranes. Together, both systems are referred to as the ER–mitochondria organizing network (ERMIONE). In addition, there is a heteromeric hexamer known as the ER membrane protein complex that participates in diverse ER processes, and in the tethering of MERCs, where it is presumably involved in phosphatidylserine traffic (a review with an evolutionarily analysis on the topic was given in Reference [37]).

In yeasts, the ERMES system comprises an ER transmembrane protein, maintenance of mitochondrial morphology-1 (Mmm1p), and a cytosolic protein, mitochondrial distribution and morphology 12 protein (Mdm12p), which form a complex with two outer mitochondrial membrane proteins, Mdm34p and Mdm10p [38]. Strikingly, orthologs of this complex are absent in mammalian cells, but proteins such as mitofusins, phosphofurin acid cluster sorting protein 2 (PACS2), the mitochondrial voltage-dependent anion channel (VDAC), and the vacuole membrane protein 1 (VMP1), among others, were implicated in the regulation of this contact site; however, a conclusive outlook on how MERCs are tethered in these organisms remains elusive [39,40].

In *Dictyostelium*, the architecture of the ER contact sites with other membranes has not been described. However, the ER–mitochondria contact sites may be regulated by a homolog of the fungal ERMES, since an ortholog of the Mdm12p ERMES protein was recently identified in this amoeba, and was purified for structural analysis [41]. In addition, ortholog genes of *mmm1* (DDB_G0285921), *mdm10* (DDB_G0278805), and *mdm34* (DDB_G0274475) were predicted and are annotated in the *Dictyostelium* genome database [42].

Interestingly, the *Dictyostelium* genome encodes a VMP1 ortholog. This ER transmembrane resident protein is conserved in plants and animals, but it is absent in yeast. *Dictyostelium vmp1* knock-out mutant cells show severe ER and Golgi structural alterations, together with a set of pleiotropic phenotypes, ranging from autophagy defects to deficient osmoregulation [43,44]. The phenotypes of *vmp1*[−] cells may be a consequence of the severe imbalance in ER homeostasis. Studies using this amoeba were crucial in unraveling the role of this still poorly understood ER protein and paved the way for further studies on other ER proteins that are conserved in *Dictyostelium*, but not in yeast cells.

2.4. The Main Source of Lipid Synthesis

The ER and the Golgi body are the major sites of membrane lipid synthesis in eukaryotic cells. Lipid synthesis occurs in specialized ER regions rich in tubules, and in vesicles that are adjacent to the Golgi body, called the ER–Golgi intermediate compartment (ERGIC) [45]. Once lipids reach the ERGIC, they are transported to their final destination through contact with other organelles, or via vesicle transport [46].

Dictyostelium total lipids are partitioned into approximately 60% phospholipids and 40% neutral lipids [47]. The membranes of this amoeba display a composition similar to that observed in mammalian cells, where phosphatidylserine, choline, and ethanolamine are the major constituents [47]; therefore, it can represent a comparative model for the study of ER lipid-associated processes. Of note, *Dictyostelium* contains several unsaturated fatty acid species, with stigmastenol as the major steroid [47,48], and ether inositol phospholipids [49]. As in other organisms, *Dictyostelium* maintains lipid homeostasis by packing excess lipids as inert neutral species sheltered in vesicles that emerge from the ER, which are referred to as lipid droplets (LDs). Upon addition of palmitic acid and cholesterol, *Dictyostelium* cells accumulate LDs which contain triacylglycerol (TAG) and sterol esters in an approximate ratio of 1:15, similar to the ratio observed in mammalian adipocytes [50]. These vesicles contain about 72 proteins, including perilipin, which is implicated in protecting LDs from lipolysis. Perilipin which is conserved in mammals, but absent in yeast and *Caenorhabditis* [51], has a homologous gene in *Dictyostelium*, *plnA*.

Analogously to mammalian organisms, *Dictyostelium* cells contain two acyl coenzyme A (CoA) diacyl-glycerol acyltransferases (DGATs) that participate in the synthesis of TAG. One of these enzymes, Dgat1, localizes to the ER membrane, and provides most of the TAG synthesis activity. As with human DGAT1, this enzyme participates in the synthesis of other lipids such as waxes and ether lipids. The other DGAT enzyme coded for in the *Dictyostelium* genome localizes at lipid droplets (LDs), and has a minor role in total cellular TAG synthesis [52].

2.5. A Perfect Compartment to Fold and Modify Proteins

The ER lumen contains a unique glycosylation machinery, and a particular environment enriched with Ca^{2+} , with a high oxidizing potential and a high viscosity. All these conditions make up a perfect situation for the synthesis, folding, and modification of integral and secreted proteins.

In order to achieve their functional state, proteins undergo various processes in the ER lumen; these include N-linked glycosylation, disulfide bond formation, folding cycles, and oligomerization.

N-linked glycosylation is a co-translational modification that consists of the addition of an oligosaccharide tree to the asparagine (Asn) residues contained in the Asn-X-serine/threonine motif of proteins. This reaction is triggered by the oligosaccharyl transferase (OST) enzyme, and it is essential for the recruitment of carbohydrate-binding factors in the ER lumen that stimulate protein folding. It serves to increase protein stability by masking hydrophobic stretches or proteolytic cleavage sites, and avoiding back-translocation [53]. Although the *Dictyostelium* OST enzyme is unstudied, it was inferred through comparative studies that it is formed by at least seven subunits, and that it shares similarity with its plant and fly homologs [54].

ER luminal chaperones help the newly synthesized proteins to reach their active conformation by promoting their folding, and by preventing aggregation. There are two groups of ER chaperones: the heat shock proteins (HSP), a protein family that can also be found in all cellular compartments, and the carbohydrate-binding chaperones (CBC), which are specifically located in the ER [55,56].

The ER is mainly enriched with members of the HSP70 and HSP90 families. These proteins recognize specific domains in glycosylated proteins, or exposed hydrophobic segments in the non-glycosylated ones, thus protecting intermediate folded precursors from aggregation by shielding these regions from intermolecular hydrophobic interactions. There is an ER resident HSP70 chaperone, called GRP78/binding immunoglobulin protein (BiP) in metazoans, or Kar2p in yeast, which participates in a broad number of processes besides protein folding [57]. Additionally, the calnexin and calreticulin proteins are two of the main CBCs. These chaperones interact with the glycan moiety to achieve protein maturation and quality control [55].

Orthologs of the broad spectrum of ER-resident folding proteins were identified and described in *Dictyostelium*, among them, the calcium-regulated chaperones—calreticulin and calnexin [58], the HSP70 chaperone—78 kDa glucose-regulated protein (Grp78) [7], and Dd-grp94, a member of the HSP90 family [59].

During the various stages of its life cycle, the *Dictyostelium* ER adapts to continuously changing metabolic demands. As vegetative amoebas, they obtain nutrients primarily via phagocytosis. Through this process, the ER transiently contacts the phagosome during the uptake process. This contact requires calreticulin and calnexin, which participate in Ca^{2+} storage [58]. These observations suggest that the ER participates during phagosome formation, possibly as a membrane source and as a regulator of Ca^{2+} homeostasis.

Two other non-chaperone protein families participate in the ER protein-folding process: the peptidyl-prolyl isomerases (PPIs), which catalyze cis/trans isomerization of peptide bonds, and the protein disulfide isomerases (PDIs) [56,60], a protein family that participates in the formation of disulfide bonds between inter- and intra-chain cysteine residues, a covalent linkage which provides stability to proteins. The formation and disruption of disulfide bonds can also act as a regulatory mechanism for protein activity control. PDI oxidoreductases exchange disulfide bonds with their substrates, which results either in the reduction of its active site and the oxidation of two adjacent cysteines in the substrate to form a disulfide bond, or in the opposite reaction. In yeasts, PDI is kept oxidized through an electron flow pathway catalyzed by the ER oxidase protein 1 (Ero1) [61].

The *Dictyostelium* genome codes for two members of the PDI family (*pdi1* and *pdi2*). Remarkably, PDI (*pdi1*) lacks the canonical C-terminus retrieval signal motif for ER localization composed by the amino acids HDEL, and instead, requires a sequence in its last 57 C-terminal amino acids [62]. This motif allows the retention of PDIs at the ER when overexpressed in yeast cells, indicating that this ER-retention mechanism might be conserved in evolution [63].

3. Endoplasmic Reticulum Stress and the Unfolded Protein Response in a Social Amoeba

To support ER protein homeostasis, the cell must achieve equilibrium between the protein load and the concentration of the ER folding machinery. Conditions that alter this equilibrium may cause defects in protein folding and modification, thus leading to the accumulation of misfolded proteins in the ER lumen, a condition termed as ER stress (ERS) [64].

Dictyostelium development is regulated via a variety of secreted extracellular signals; it was observed that about 2.6% of the 12,257 proteins predicted to be encoded in its genome are secreted during this process [65]. In addition to the fluctuating metabolic demands of its life cycle, *Dictyostelium* cells encounter various stressful conditions derived from the complex ecosystem it inhabits, some of which cause ER homeostasis imbalances. For instance, this amoeba might share a habitat with the *Streptomyces* species, which evolved competitive survival mechanisms based on the production of antibiotics.

Recently, it was demonstrated that tunicamycin (TN), a fatty acyl nucleoside antibiotic produced by *Streptomyces lysosuperificus* and *Streptomyces chartreusis*, which interferes with N-glycosylation, induces ERS in *Dictyostelium* [7]. In *Dictyostelium*, this antibiotic effectively inhibits protein glycosylation [66]. The TN effects on *Dictyostelium* development were first determined in the early 1980s. Since then, TN was widely used to evaluate the role of N-glycosylated cell-adhesion proteins during the aggregation process. This antibiotic was found to inhibit cellular growth, and to impair development [66–73]. In addition, TN blocks cell fusion during *Dictyostelium* sexual development, mainly due to its effects on glycoprotein production [74]. Interestingly, TN can partially suppress the developmental phenotypes, but not allore cognition impairment, as presented by null-mutants of Transmembrane IPT/IG/E-set repeat protein (TgrB1) and TgrC1, two immunoglobulin-like proteins required for kin discrimination and cell type differentiation during *Dictyostelium* development [72].

After TN treatment, *Dictyostelium* cells undergo evident morphological changes by adopting a spherical shape [7]. Likewise, upon hyperosmotic stress, *Dictyostelium* cells suffer morphological changes due to a cytoskeletal reorganization [75]. Interestingly, a similar rounded morphology was also described for a subpopulation of stress- and detergent-resistant *Dictyostelium* cells, in which the expression of some lipid-metabolism genes were modified [76].

To cope with ERS, eukaryotic cells evolved a conserved system referred to as the unfolded protein response (UPR), which restores ER homeostasis through the activation of a complex transcriptional program that changes the expression of genes encoding proteins associated with the synthesis of membranes, and for chaperones and degradative enzymes [77]. In addition, the UPR decreases the protein load at the ER through the selective degradation of messenger RNAs (mRNAs) that are targeted to this compartment, and by decreasing the translation rates [78,79]. In metazoans, the UPR is activated in parallel by three ER transmembrane sensors: the inositol-requiring enzyme 1 (IRE1), the protein kinase RNA-like ER kinase (PERK), and the activating transcription factor 6 (ATF6) (Figure 3). Each of these branches senses the folding environment in the ER lumen and activates several transcription factors upon ERS.

After ERS, *Dictyostelium* cells trigger an adaptive transcriptional response, which diminishes the ER protein load, increases ER protein folding, and favours the cellular degradation processes [7]. Interestingly, ERS induces transcriptional changes in some genes that code for proteins of the actin cytoskeleton, and some genes involved in lipid metabolism [7], which suggests that the round cellular morphology caused by ERS might be the consequence of membrane and cytoskeletal rearrangements. Adopting a round morphology devoid of pseudopodia might be advantageous to *Dictyostelium* cells, by aiding in the lipid-balance maintenance in the plasma membrane, and by decreasing energy requirements.

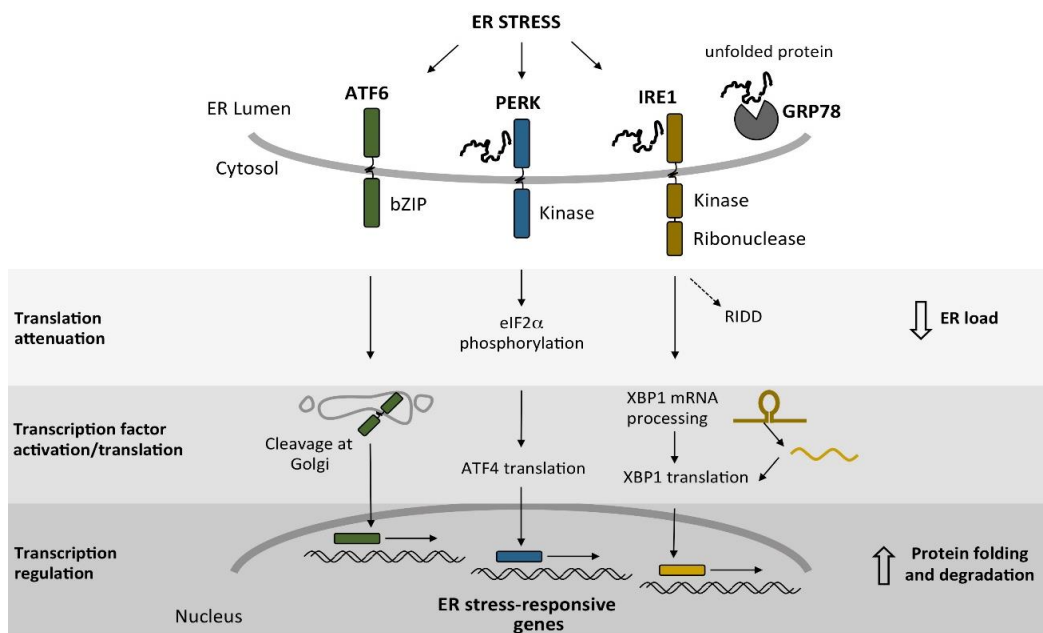


Figure 3. Signaling pathways involved in the unfolded protein response (UPR). In mammalian cells, three signaling branches that depend on the ER transmembrane sensor proteins—activating transcription factor 6 (ATF6), protein kinase RNA-like ER kinase (PERK), and inositol-requiring enzyme 1 (IRE1)—are activated upon ER stress (ERS). PERK and IRE1 can sense ERS by interacting directly with unfolded proteins through their luminal sensor domain. In addition, ATF6, PERK, and IRE1 detect an increase in unfolded proteins when they lose their association with the ER chaperone GRP78/binding immunoglobulin protein (BiP). When these transducers detect ERS, a recovery response is activated. This response mainly regulates two events: the reduction of ER protein load, and an increase in the protein-folding and degradation capacity of the cell. The former is accomplished via translation inhibition, triggered by the PERK-mediated phosphorylation of the eukaryotic initiation factor 2 α (eIF2 α), and by the degradation of certain messenger RNAs (mRNAs) in the regulated IRE1-dependent decay (RIDD). The second event regulates the activation or translation of transcription factors that, when transported to the nucleus, reprogram transcription to increase the expression of ER homeostatic genes, thus promoting protein folding and modification of the ER.

3.1. The IreA Branch

As in other organisms, the transcriptional response to ERS in *Dictyostelium* is mediated by the IRE1 pathway, which is, until now, the only UPR signaling branch identified in this amoeba. In plants, yeasts, and mammals, this pathway is constituted by the type I ER-resident transmembrane protein, IRE1, and a basic zipper leucine transcription factor known as the X-box binding protein 1 (XBP1) in mammalian cells, HAC1 in yeast, and bZIP60 in plants.

IRE1, the most conserved UPR transducer, contains an amino N-terminal ER luminal stress-sensor domain, and a carboxy C-terminal cytoplasmic region that harbors a kinase and a kinase extension nuclelease (KEN) domain [80]. IRE1 plays a prominent role in the UPR of plants and animals, and it is the only sensor in *Saccharomyces cerevisiae* [81]. Mammalian cells contain two IRE1 isoforms, IRE1 α , which is ubiquitously expressed, and IRE1 β , which is exclusively expressed in the intestinal and lung epithelia [82,83]. *Arabidopsis thaliana* also has two IRE1 orthologs (IRE1A and IRE1B) that display differential expression patterns [84].

When the cell is under ERS conditions, IRE1 is activated via a conformational change triggered by direct interaction with unfolded proteins through its sensor domain and/or by the release of the chaperone GRP78/Kar2p from the same domain. This leads to the formation of high-order IRE1 oligomers, and their transautophosphorylation [85–87]. Once activated, IRE1 processes the mRNA of a

transcription factor through an unconventional splicing event that eliminates an intron. The processed mRNA is translated into a bZIP that upregulates the transcription of genes encoding ER-resident chaperones and modification enzymes, among others [88]. Although the protein sequence of this transcription factor is poorly conserved between species, the IRE1 cleavage site and the stem-loop structure of the unconventional intron are widely preserved [89–91].

In mammalian cells, IRE1 is able to regulate its protein levels via the degradation of its own mRNA. The IRE1 N-terminus can bind to the 5' end of its own mRNA while the nascent protein is translated and attached to the ribosome. After the release of the nascent protein, IRE1 can dimerize, and activates its RNase domain to degrade the mRNA [92]. The yeast Ire1p kinase domain participates in the downregulation of the pathway through an autophosphorylation process that requires a 28-amino-acid region in its kinase domain; this hyperphosphorylation destabilizes Ire1p oligomers [93].

The *Dictyostelium* genome encodes a single IRE1 sensor ortholog, IreA, an ER-localized protein with a single predicted transmembrane domain [7]. IreA comprises two regions, one localized in the ER lumen, which is poorly conserved and likely functions as the ER environment sensor, and the other region that is predicted to be at the cytosolic face of the ER and contains a serine/threonine kinase and a KEN domain (Figure 4A). Both kinase and ribonuclease domains are required in *Dictyostelium* cells to survive ER stress, and both must be fully active to regulate IreA oligomer-formation dynamics during sustained ERS [7]. Upon ER stress, IreA forms transient high-order oligomers (Figure 4B). Oligomerization in the yeast Ire1p is required for the recruitment of unprocessed *HAC1* mRNA [94], and to trigger Ire1p RNase activation [95]. However, in *Dictyostelium*, the possible transcription factor is yet unidentified.

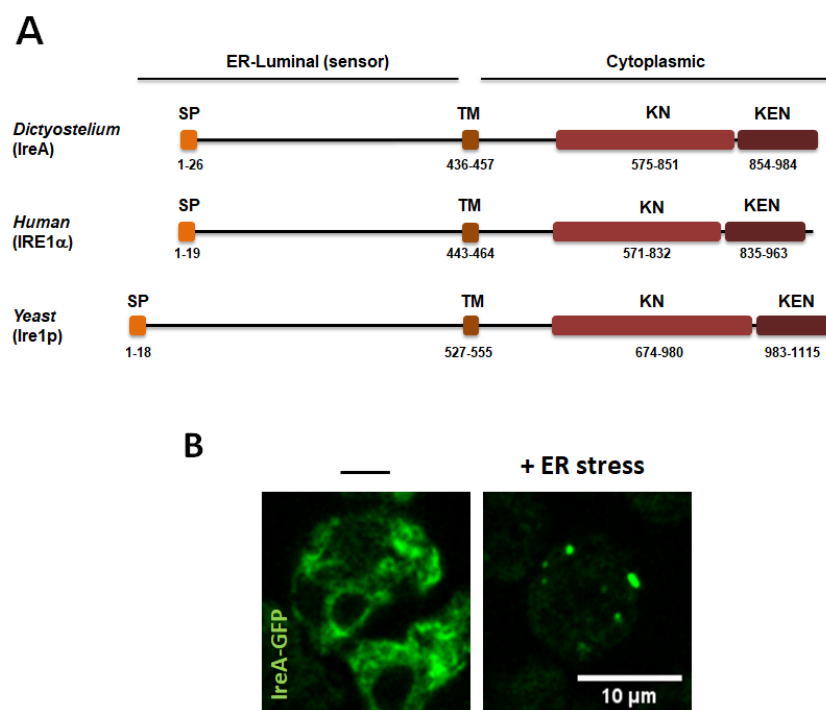


Figure 4. (A) Diagram of the structural domains of *Dictyostelium* IreA, compared with its *Saccharomyces cerevisiae* and human orthologs. SP (signal peptide), TM (transmembrane domain), KN (kinase domain), and KEN (kinase extension nuclease domain). Proteins were drawn to scale. Numbers indicate amino acid coordinates. Protein domains were obtained from www.uniprot.org. (B) Live-cell confocal microscopy of *ireA*[−] cells expressing the IreA-GFP construct after 4 h, in the absence or in the presence of an ER-stress inducer. The IreA-GFP signal forms large puncta (possibly high-order oligomers). (Scale bar corresponds to 10 μ m).

In animal cells, IRE1 regulates transcript abundance in a branched fashion, since it splices the XBP1 transcript, but also degrades mRNAs through its RNase domain via a mechanism named regulated IRE1-dependent decay (RIDD) [78,79,96]. The RIDD pathway decreases the ER protein load of secreted and transmembrane proteins, and can activate apoptosis by degrading anti-apoptotic pre-mRNAs [97]. Interestingly, the yeasts *Schizosaccharomyces pombe* and *Candida glabrata* possess the RIDD pathway, but lack any XBP1/HAC1-like transcription factors [90,91], and thus, their UPR-dependent transcriptional changes are solely regulated by RIDD in a single-component pathway [91,98]. In *Dictyostelium*, a considerable number of transcripts are downregulated in an IreA-dependent manner, thus suggesting the existence of a RIDD pathway. However, the ERS response also increases the abundance of specific transcripts, suggesting the existence of an IreA-dependent transcription factor; however, an XBP1 ortholog is yet unidentified [7]. Therefore, the *Dictyostelium* ERS response pathway may resemble that of the IRE1-branched animal mechanism.

3.2. *IreA*-Independent UPR Pathways in *Dictyostelium*

In contrast to the yeast UPR, in which the entire transcriptional response depends on the IRE1 pathway, in *Dictyostelium*, the response is only partially dependent on IreA [7], which suggests that, as in plants and animals, additional input signaling pathways must exist in this amoeba. The IreA-dependent transcriptional reprogramming primarily triggers an increase in the degradative capacity of the cell, and a decrease in protein load at the ER. As in yeast, the *Dictyostelium* IRE1 pathway regulates the expression of genes that participate in degradative processes, such as ubiquitin and ubiquitin ligases, together with ester-bond hydrolases and peptidases [7]. However, the expression of only a few ER chaperones depends on IreA, suggesting that, as in animal cells, IRE1-independent pathways may be implicated in the regulation of these components.

In animal cells, there are two UPR pathways that account for additional inputs, besides IRE1, to regulate the UPR (Figure 3). One of them is regulated by ATF6, a type II transmembrane ER-resident protein that bears a bZIP transcription factor domain in its cytosolic N-terminal portion. This UPR component is present in metazoan cells, and functional homologs were identified in plants (bZIP28 and bZIP17) [99,100]. Upon ERS, ATF6 is translocated from the ER to the Golgi body, where its transcription factor domain is released via a proteolytic cleavage triggered by the site-1 and site-2 proteases (S1P and S2P) [101,102]. The ATF6-dependent transcriptional reprogramming is required to induce the expression of genes that code for chaperones and degradative enzymes, and of genes involved in ER-membrane remodeling [103]. ATF6 signaling participates in senescence-associated ER expansion [104], and variants of this gene underlie the pathogenesis of inherited retinal and cone photoreceptor disorders [105,106].

In addition, in animals, the UPR is regulated by PERK, a transmembrane kinase that regulates protein translation through phosphorylating the eukaryotic initiation factor 2 α (eIF2 α) [107]. In plants, the presence of PERK orthologs is unreported.

Identification of ATF6 and PERK orthologs in *Dictyostelium* was unsuccessful; nevertheless, the existence of homolog components of these pathways cannot be ruled out. ATF6 belongs to the bZIP transcription factor family, and *Dictyostelium* contains a large number of these transcription factors. It was suggested that bZIPs evolved from a single common ancestor, which expanded and diversified greatly during evolution [108]. The current opisthokont bZIP transcription factors emerged from three ancestral groups that appeared during the evolution of this phylogenetic branch. One of these ancestral groups gave rise to the ATF6/HAC1 set of transcription factors, which is absent in other phylogenetic branches, such as the Amoebozoa or Plantae [108]. However, ER transmembrane bZIP transcription factors, which are activated upon ERS by a mechanism analogous to the one that regulates ATF6 and XBP1, were identified in plants [99,109]. *Dictyostelium* transcription factors may have diverged largely, so further characterization of the potential 19 bZIP transcription factors coded for in its genome may unravel the presence of ATF6 and XBP1 functional homologs.

4. ER Stress and the Autophagy Pathway in *Dictyostelium*

Degradative pathways also participate in homeostasis recovery upon ERS. Protein degradation is mainly achieved through two mechanisms. One is the ER-associated degradation (ERAD), which is accomplished by the proteasome, and thus, requires protein retro-translocation from the ER to the cytoplasm [110,111]. The other is autophagy, which delivers cytoplasmic material to the lysosome through double-membrane vesicles, known as autophagosomes [112]. If cells are not able to recover from ERS, the UPR represses the adaptive response, and triggers cell death [113].

In mammalian and plant cells, IRE1 activity is not only devoted to mRNA processing. In addition to the activation of its RNase domain, IRE1 kinase can regulate other signaling pathways that orchestrate a more complex response. In animal cells, upon persistent ER stress, IRE1 can activate the Jun N-terminal kinase (JNK) by interacting with the adaptor protein TNF-receptor associated factor 2 (TRAF2) [114]. Depending on the severity of the stress, this signaling leads either to autophagy induction or to apoptosis activation [97,115]. Similarly, in plants, it was observed that the IRE1 kinase domain is required for the induction of autophagy upon ERS [116]. However, the JNK pathway is absent in *Dictyostelium*, and in other organisms outside the animal kingdom, such as plants or fungi [117,118]. The JNKs belong to the high osmolarity glycerol (HOG1)-like mitogen-activated protein kinase (MAPK) family, a group that emerged through duplication from a common ancestor that gave rise in fungi to a single HOG1 kinase. In contrast to p38, the other animal MAPK of this group, JNK genes underwent rapid evolution [118]. Thus, the IRE1-mediated JNK signaling, triggered by ERS in animal cells, might be a specialized trait of this phylogenetic group that emerged later during animal evolution.

Recently, we determined that autophagy is required for cell survival in response to ER stress in *Dictyostelium* cells [7]. However, in contrast with the animal and plant scenario, we found that IreA is not required for this autophagy induction. This suggests the presence of IRE1-independent pathways that may sense ERS and induce autophagy as a survival response. However, the IreA-mediated recovery of ER homeostasis was required to achieve a fully functional autophagy-dependent degradation, thus highlighting the functional connection of the ER with autophagosome biogenesis [7].

Dictyostelium cells not only lack JNK signaling pathways, but also caspase-dependent apoptotic cell death. However, there is a pathway of programmed cell death that is displayed by these amoebas with the characteristics of autophagic cell death (ACD) [119]. ACD is a death process characterized by cytoplasm vacuolization without chromatin condensation as in apoptosis, or organelle swelling as in necrosis [120]. It was described that ACD participates in cell death during *Drosophila* development [121], in hypersensitive cell death in plants [122], and in mammalian cell death under certain conditions [123]. Still, the nature and specific mechanisms that regulate ACD remain poorly defined.

In *Dictyostelium*, stalk cells die through ACD during fruiting-body formation [124,125]. Interestingly, research using this amoeba uncovered a novel link between the ER and ACD regulation, since it was observed that this type of cell death depends on the ER Ca²⁺-channel inositol 1,4,5-trisphosphate receptor (IP3R). Presumably, it is required to increase the cytosolic concentration of Ca²⁺ [126]. Since changes in calcium homeostasis at the ER might imbalance several cellular functions (for example, ER protein-folding and chaperone functions), studies on the participation of the UPR pathways in ACD regulation in this amoeba might unravel novel links between both pathways. It can also be inferred that, due to the absence of caspase-dependent apoptosis in *Dictyostelium*, the UPR may only be devoted to survival responses; thus, the study of the cellular effects of sustained ER stress in *Dictyostelium* may shed light on conserved survival responses that are hindered in animal cells by apoptotic signaling.

5. Assessing ER Stress in *Dictyostelium*

The onset of a stress response is usually evaluated by analyzing changes in the expression of marker genes. In *Dictyostelium*, ERS induces an increase in the abundance of several transcripts [7], whose levels can be analyzed to determine whether or not a defined treatment or growth condition

leads to ERS. In Table 2, we present a selected list of IreA-dependent and independent genes, whose expression showed significant changes upon a TN treatment, and that can be useful as ERS markers. In addition, the changes in the expression of proteins such as cell division cycle protein D (CdcD), a conserved ATPase that participates in protein retro-translocation from the ER [127], can be evaluated via western blotting. It can also be determined whether a certain stimulus activates an IreA-dependent response, by following IreA clustering behavior in a time-lapse confocal microscopy assay of IreA-GFP-expressing cells that were exposed to the stimulus under study (Figure 4B).

Table 2. List of selected genes that showed a significant transcript increase upon a 16 h tunicamycin treatment, and that are suggested for evaluation as ER stress markers (list extracted from Domínguez-Martín, E. et al., 2018 [7]).

Gene ID	Name	Description	IreA-Dependent
DDB_G0276445	Grp78	Heat shock protein Hsp70 family protein.	no
DDB_G0274199	DDB_G0274199	Putative metallophosphoesterase.	no
DDB_G0278477	sarB	ADP ribosylation factors/ Secretion-associated and Ras-related (ARF/SAR) superfamily protein. GTP-binding protein Sar1B involved in vesicular transport between the endoplasmic reticulum and the Golgi body.	no
DDB_G0283867	cprC	Cysteine proteinase 3.	no
DDB_G0278371	spc1	Ortholog of the conserved microsomal signal peptidase 12 kDa subunit; the signal peptidase complex is a membrane-bound endo-proteinase that removes signal peptides from nascent proteins as they are translocated into the lumen of the endoplasmic reticulum.	no
DDB_G0281833	DDB_G0281833	Ubiquitin-conjugating enzyme E2.	no
DDB_G0283113	eriA	RNA exonuclease.	no
DDB_G0290227	npl4	Ortholog of nuclear protein localization 4 (NPL4), which, together with ubiquitin fusion degradation protein 1 (Ufd1) and cell division cycle protein D (CdcD), is involved in recognition of polyubiquitinated proteins, and their presentation to the 26S proteasome for degradation.	no
DDB_G0287685	cinC	Elongation factor 2. Translocates the peptidyl-tRNA from the aminoacyl site to the peptidyl site on the ribosome during protein synthesis; induced by cycloheximide; knockdown has significantly reduced ability for protein synthesis.	yes
DDB_G0269462	DDB_G0269462	Large protein containing two ubiquitin domains.	yes
DDB_G0291121	cinB	Esterase/lipase/thioesterase domain-containing protein.	yes
DDB_G0285131	derl2	Derlin-2. component of endoplasmic reticulum-associated degradation (ERAD) for misfolded luminal proteins.	yes
DDB_G0270272	uae1	Ubiquitin activating enzyme E1.	yes

Changes in ER morphology upon ERS can be followed using immunofluorescence staining. Specific antibodies against *Dictyostelium* ER-resident proteins, such as calnexin and PDI [62,128], are available. As depicted in Figure 5, ER morphology defects in ERS-sensitive strains, such as the *ireA*[−] mutant, can be easily detected with this technique.

The sensitivity of mutant strains to ER stressors, such as TN, can be evaluated via serial dilution spotting assays, as described previously [7] (Figure 6). This assay is performed by spotting serial dilutions of cells that were previously treated with various concentrations of the ERS inducer and/or for various treatment times, over agar plates with bacteria (Figure 6A). It is recommended to evaluate cell morphology before spotting cells (Figure 6B). After removal of the stressor, cells that survived the treatment can reinstate growth in association with bacteria. The inability of a certain strain to restore growth after treatment with ERS inducers reflects its sensitivity to this condition (Figure 6C). Currently, the only reported ER stress-sensitive strain is the *ireA*[−] mutant, which can be included as a control in this sort of assay [7].

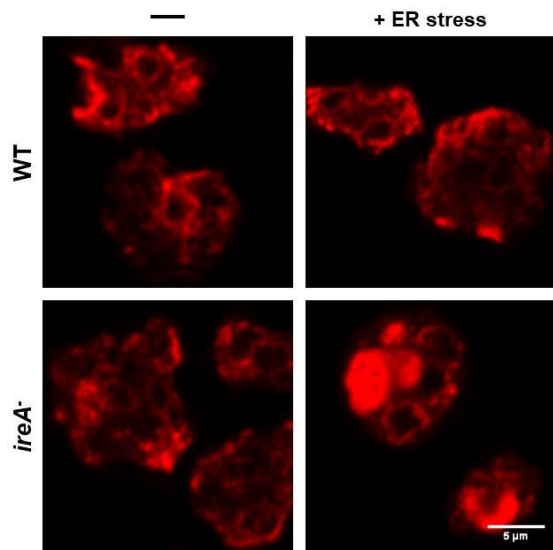


Figure 5. WT and *ireA*[−] cells, after an ER stress treatment or mock, were fixed and prepared for the detection of the ER-resident protein disulfide isomerase (PDI) via an immunofluorescence assay and were visualized using confocal microscopy. An ER stress treatment severely impaired the ER morphology of the sensitive *ireA*[−] cells. (Scale bar corresponds to 5 μ m).

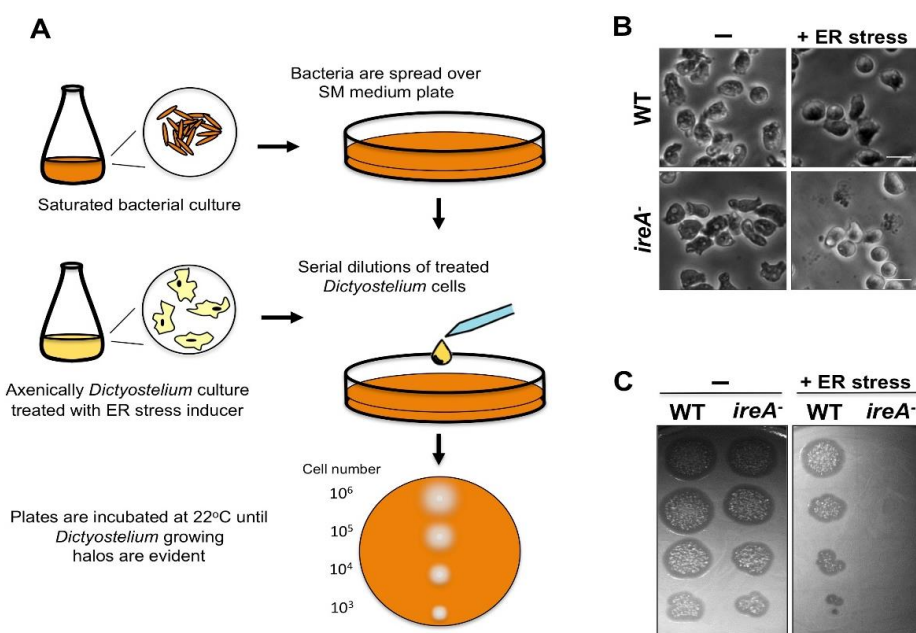


Figure 6. (A) Descriptive diagram of a serial dilution spotting assay used to test if a certain strain is sensitive to an ER stress inducer. A culture of bacterial cells (*Dictyostelium* is usually fed with *Klebsiella aerogenes* or *Escherichia coli*) is grown to saturation, and an aliquot is spread over an SM agar plate. Axenically growing *Dictyostelium* strains in the mid-logarithmic growth phase (with a density of around 1×10^6 cells/mL) are prepared and treated for the desired times with the ER stress inducer. After the treatment, *Dictyostelium* cells are collected, and serial dilutions are prepared and spotted on the SM agar plates. Plates are incubated at 22 °C until lysis plaques emerge due to the presence of growing amoebas feeding on bacteria. (B) Light microscopy pictures of WT and ER stress-sensitive *ireA*[−] cells treated with a stress inducer. Morphological changes and cell lysis can be analyzed before the spotting assay. Notice the presence of round cells and the cell debris in the *ireA*[−] strain after the treatment. (C) Picture of a spotting assay where a WT and an ER stress-sensitive strain (*ireA*[−] cells) were tested with mock or ER stress inducer treatment.

6. Concluding Remarks

Dictyostelium proved to be an advantageous model in cell biology, and more recently, it emerged as a valuable organism for the study of ER-associated processes, such as the pathways involved in the ER stress response. These pathways show intriguing similarities, but also some differences between *Dictyostelium* and other organisms, expanding our knowledge of this conserved pathway across evolution. In addition, *Dictyostelium* poses an interesting model to unravel the role of proteins with unknown functions that are conserved in animals, but absent in yeast, and whose study may lead to a deeper understanding of how the complex regulation of the ER network is attained.

Author Contributions: E.D.-M analyzed data and wrote the paper; M.H.-E. analyzed data and wrote the paper; O.V., R.C. and R.E. wrote the paper.

Funding: This work was supported by grant numbers (to E.D.-M., O.V., and R.E.) BFU2012-32536 and BFU2015-64440-P from Ministerio de Economía Industria y Competitividad, and by FEDER and CONACYT: CB-254078; PAPIIT, DAGAPA, UNAM: IN210616 (to E.D.-M., M.H.-E., and R.C.).

Acknowledgments: E.D.-M is a PhD candidate from Programa de Doctorado en Ciencias Biomédicas, Universidad Nacional Autónoma de México (UNAM), and received fellowship 380127 from CONACYT. M.H.-E. is a PhD student from Programa de Doctorado en Ciencias Bioquímicas, Universidad Nacional Autónoma de México (UNAM), and received fellowship 366635 from CONACYT.

Conflicts of Interest: The authors declare no conflicts of interest.

References

1. Sheikh, S.; Thulin, M.; Cavender, J.C.; Escalante, R.; Kawakami, S.; Lado, C.; Landolt, J.C.; Nanjundiah, V.; Queller, D.C.; Strassmann, J.E.; et al. A New Classification of the Dictyostelids. *Protist* **2018**, *169*, 1–28. [[CrossRef](#)] [[PubMed](#)]
2. Annesley, S.; Fisher, P. *Dictyostelium discoideum*—A model for many reasons. *Mol. Cell. Biochem.* **2009**, *329*, 73–91. [[CrossRef](#)] [[PubMed](#)]
3. Muñoz-Braceras, S.; Mesquita, A.; Escalante, R. *Dictyostelium discoideum* as a model in biomedical research. In *Dictyostelids. Evolution, Genomics and Cell Biology*; Romeralo, M., Baldauf, S., Escalante, R., Eds.; Springer: Berlin/Heiderberg, Germany, 2013; pp. 1–34. ISBN 978-3-642-38486-8.
4. Loomis, W.F. Cell signaling during development of *Dictyostelium*. *Dev. Biol.* **2014**, *391*, 1–16. [[CrossRef](#)] [[PubMed](#)]
5. Eichinger, L.; Pachebat, J.A.; Glockner, G.; Rajandream, M.-A.; Sucgang, R.; Berriman, M.; Song, J.; Olsen, R.; Szafranski, K.; Xu, Q.; et al. The genome of the social amoeba *Dictyostelium discoideum*. *Nature* **2005**, *435*, 43–57. [[CrossRef](#)] [[PubMed](#)]
6. Williams, J.G. *Dictyostelium* finds new roles to model. *Genetics* **2010**, *185*, 717–726. [[CrossRef](#)] [[PubMed](#)]
7. Domínguez-Martín, E.; Ongay-Larios, L.; Kawasaki, L.; Vincent, O.; Coello, G.; Coria, R.; Escalante, R. IreA controls endoplasmic reticulum stress-induced autophagy and survival through homeostasis recovery. *Mol. Cell. Biol.* **2018**, MCB.00054-18. [[CrossRef](#)]
8. Roussel, B.D.; Kruppa, A.J.; Miranda, E.; Crowther, D.C.; Lomas, D.A.; Marciniak, J.S. Endoplasmic reticulum dysfunction in neurological disease. *Lancet Neurol.* **2013**, *12*, 105–118. [[CrossRef](#)]
9. Ozcan, L.; Tabas, I. Role of Endoplasmic Reticulum Stress in Metabolic Disease and Other Disorders. *Annu. Rev. Med.* **2012**, *63*, 317–328. [[CrossRef](#)] [[PubMed](#)]
10. Annesley, S.J.; Chen, S.; Francione, L.M.; Sanislav, O.; Chavan, A.J.; Farah, C.; De Piazza, S.W.; Storey, C. L.; Ilievská, J.; Fernando, S.G.; et al. *Dictyostelium*, a microbial model for brain disease. *Biochim. Biophys. Acta Gen. Subj.* **2014**, *1840*, 1413–1432. [[CrossRef](#)] [[PubMed](#)]
11. Huber, R.J. Using the social amoeba *Dictyostelium* to study the functions of proteins linked to neuronal ceroid lipofuscinosis. *J. Biomed. Sci.* **2016**, *23*, 83. [[CrossRef](#)] [[PubMed](#)]
12. Myre, M.A.; Huber, R.J.; Day, D.H.O. *Functional Analysis of Proteins Involved in Neurodegeneration Using the Model Organism Dictyostelium: Alzheimer's, Huntington's, and Batten Disease*; Elsevier Inc.: New York, NY, USA, 2018; ISBN 9780128040782.

13. Malinovska, L.; Palm, S.; Gibson, K.; Verbavatz, J.-M.; Alberti, S. *Dictyostelium discoideum* has a highly Q/N-rich proteome and shows an unusual resilience to protein aggregation. *Proc. Natl. Acad. Sci. USA* **2015**, *112*, E2620–E2629. [[CrossRef](#)] [[PubMed](#)]
14. Santarriaga, S.; Petersen, A.; Ndukwe, K.; Brandt, A.; Gerges, N.; Scaglione, J.B.; Scaglione, K.M. The social amoeba *Dictyostelium discoideum* is highly resistant to polyglutamine aggregation. *J. Biol. Chem.* **2015**, *290*, 25571–25578. [[CrossRef](#)] [[PubMed](#)]
15. Westrate, L.M.; Lee, J.E.; Prinz, W.A.; Voeltz, G.K. Form Follows Function: The Importance of Endoplasmic Reticulum Shape. *Annu. Rev. Biochem.* **2015**, *84*, 791–811. [[CrossRef](#)] [[PubMed](#)]
16. Nixon-Abell, J.; Obara, C.J.; Weigel, A.V.; Li, D.; Legant, W.R.; Xu, C.S.; Pasolli, H.A.; Harvey, K.; Hess, H.F.; Betzig, E.; et al. Increased spatiotemporal resolution reveals highly dynamic dense tubular matrices in the peripheral ER. *Science* **2016**, *354*, aaf3928. [[CrossRef](#)] [[PubMed](#)]
17. Fernández-Busnadio, R.; Saheki, Y.; de Camilli, P. Three-dimensional architecture of extended synaptotagmin-mediated endoplasmic reticulum—Plasma membrane contact sites. *Proc. Natl. Acad. Sci. USA* **2015**, *112*, E2004–E2013. [[CrossRef](#)] [[PubMed](#)]
18. Hetzer, M.W. The nuclear envelope. *Cold Spring Harb. Perspect. Biol.* **2010**. [[CrossRef](#)] [[PubMed](#)]
19. Terasaki, M.; Shemesh, T.; Kashuri, N.; Klemm, R.W.; Schalek, R.; Hayworth, K.J.; Hand, A.R.; Yankova, M.; Huber, G.; Lichtman, J.W.; et al. Stacked endoplasmic reticulum sheets are connected by helicoidal membrane motifs. *Cell* **2013**, *154*, 285–296. [[CrossRef](#)] [[PubMed](#)]
20. Zurek, N.; Sparks, L.; Voeltz, G. Reticulon short hairpin transmembrane domains are used to shape ER tubules. *Traffic* **2011**, *12*, 28–41. [[CrossRef](#)] [[PubMed](#)]
21. di Sano, F.; Bernardoni, P.; Piacentini, M. The reticulons: Guardians of the structure and function of the endoplasmic reticulum. *Exp. Cell Res.* **2012**, *318*, 1201–1207. [[CrossRef](#)] [[PubMed](#)]
22. Shibata, Y.; Voss, C.; Rist, J.M.; Hu, J.; Rapoport, T.A.; Prinz, W.A.; Voeltz, G.K. The reticulon and Dp1/Yop1p proteins form immobile oligomers in the tubular endoplasmic reticulum. *J. Biol. Chem.* **2008**, *283*, 18892–18904. [[CrossRef](#)] [[PubMed](#)]
23. Oertle, T.; Klinger, M.; Stuermer, C.A.O.; Schwab, M.E. A reticular rhapsody: Phylogenetic evolution and nomenclature of the RTN/Nogo gene family. *FASEB J.* **2003**, *17*, 1238–1247. [[CrossRef](#)] [[PubMed](#)]
24. Chiurchiù, V.; Maccarrone, M.; Orlacchio, A. The role of reticulons in neurodegenerative diseases. *NeuroMol. Med.* **2014**, *16*, 3–15. [[CrossRef](#)] [[PubMed](#)]
25. Schwarz, D.S.; Blower, M.D. The endoplasmic reticulum: Structure, function and response to cellular signaling. *Cell. Mol. Life Sci.* **2016**, *73*, 79–94. [[CrossRef](#)] [[PubMed](#)]
26. Bola, B.; Allan, V. How and why does the endoplasmic reticulum move? *Biochem. Soc. Trans.* **2009**, *37 Pt 5*, 961–965. [[CrossRef](#)] [[PubMed](#)]
27. Fehrenbacher, K.L.; Davis, D.; Wu, M.; Boldogh, I.; Pon, L.A. Endoplasmic reticulum dynamics, inheritance, and cytoskeletal interactions in budding yeast. *Mol. Biol. Cell* **2002**, *13*, 854–865. [[CrossRef](#)] [[PubMed](#)]
28. Boevink, P.; Oparka, K.; Cruz, S.S.; Martin, B.; Betteridge, A.; Hawes, C. Stacks on tracks: The plant Golgi apparatus traffics on an actin/ER network. *Plant J.* **1998**, *15*, 441–447. [[CrossRef](#)] [[PubMed](#)]
29. Liu, T.Y.; Bian, X.; Sun, S.; Hu, X.; Klemm, R.W.; Prinz, W.A.; Rapoport, T.A.; Hu, J. Lipid interaction of the C terminus and association of the transmembrane segments facilitate atlastin-mediated homotypic endoplasmic reticulum fusion. *Proc. Natl. Acad. Sci. USA* **2012**, *109*, E2146–E2154. [[CrossRef](#)] [[PubMed](#)]
30. McNew, J.A.; Sondermann, H.; Lee, T.; Stern, M.; Brandizzi, F. GTP-Dependent Membrane Fusion. *Annu. Rev. Cell Dev. Biol.* **2013**, *29*, 529–550. [[CrossRef](#)] [[PubMed](#)]
31. Bian, X.; Klemm, R.W.; Liu, T.Y.; Zhang, M.; Sun, S.; Sui, X.; Liu, X.; Rapoport, T.A.; Hu, J. Structures of the atlastin GTPase provide insight into homotypic fusion of endoplasmic reticulum membranes. *Proc. Natl. Acad. Sci. USA* **2011**, *108*, 3976–3981. [[CrossRef](#)] [[PubMed](#)]
32. Byrnes, L.J.; Sondermann, H. Structural basis for the nucleotide-dependent dimerization of the large G protein atlastin-1/SPG3A. *Proc. Natl. Acad. Sci. USA* **2011**, *108*, 2216–2221. [[CrossRef](#)] [[PubMed](#)]
33. Wang, H.; Lockwood, S.K.; Hoeltzel, M.F.; Schiefelbein, J.W. The Root Hair Defective3 gene encodes an evolutionarily conserved protein with GTP-binding motifs and is required for regulated cell enlargement in Arabidopsis. *Genes Dev.* **1997**, *11*, 799–811. [[CrossRef](#)] [[PubMed](#)]
34. Hu, J.; Shibata, Y.; Zhu, P.P.; Voss, C.; Rismanchi, N.; Prinz, W.A.; Rapoport, T.A.; Blackstone, C. A Class of Dynamin-like GTPases Involved in the Generation of the Tubular ER Network. *Cell* **2009**, *138*, 549–561. [[CrossRef](#)] [[PubMed](#)]

35. Steiner, B.; Swart, A.L.; Welin, A.; Weber, S.; Personnic, N.; Kaech, A.; Freyre, C.; Ziegler, U.; Klemm, R. W.; Hilbi, H. ER remodeling by the large GTPase atlastin promotes vacuolar growth of *Legionella pneumophila*. *EMBO Rep.* **2017**, *18*, 1–20. [[CrossRef](#)] [[PubMed](#)]
36. Phillips, M.J.; Voeltz, G.K. Structure and function of ER membrane contact sites with other organelles. *Nat. Rev. Mol. Cell Biol.* **2016**, *17*, 69–82. [[CrossRef](#)] [[PubMed](#)]
37. Wideman, J.G.; Muñoz-Gómez, S.A. The evolution of ERMIONE in mitochondrial biogenesis and lipid homeostasis: An evolutionary view from comparative cell biology. *Biochim. Biophys. Acta Mol. Cell Biol. Lipids* **2016**, *1861*, 900–912. [[CrossRef](#)] [[PubMed](#)]
38. Kornmann, B.; Currie, E.; Collins, S.R.; Schuldiner, M.; Nunnari, J.; Weissman, J.S.; Walter, P. An ER-mitochondria tethering complex revealed by a synthetic biology screen. *Science* **2009**, *325*, 477–481. [[CrossRef](#)] [[PubMed](#)]
39. Tabara, L.C.; Escalante, R. VMP1 establishes ER-microdomains that regulate membrane contact sites and autophagy. *PLoS ONE* **2016**, *11*, 18892–18904. [[CrossRef](#)] [[PubMed](#)]
40. Herrera-Cruz, M.S.; Simmen, T. Of yeast, mice and men: MAMs come in two flavors. *Biol. Direct* **2017**, *12*, 1–21. [[CrossRef](#)] [[PubMed](#)]
41. AhYoung, A.P.; Lu, B.; Cascio, D.; Egea, P.F. Crystal structure of Mdm12 and combinatorial reconstitution of Mdm12/Mmm1 ERMES complexes for structural studies. *Biochem. Biophys. Res. Commun.* **2017**, *488*, 129–135. [[CrossRef](#)] [[PubMed](#)]
42. Fey, P.; Gaudet, P.; Pilcher, K.E.; Franke, J.; Chisholm, R.L. dictyBase and the Dicty Stock Center. *Methods Mol. Biol.* **2006**, *346*, 51–74. [[PubMed](#)]
43. Calvo-garrido, J.; Carilla-latorre, S.; La, F.; Egea, G.; Escalante, R. Vacuole Membrane Protein 1 Is an Endoplasmic Reticulum Protein Required for Organelle Biogenesis, Protein Secretion, and Development. *Mol. Biol. Cell.* **2008**, *19*, 3442–3453. [[CrossRef](#)] [[PubMed](#)]
44. Calvo-Garrido, J.; King, J.S.; Muñoz-Braceras, S.; Escalante, R. Vmp1 regulates PtdIns3P signaling during autophagosome formation in *Dictyostelium discoideum*. *Traffic* **2014**, *11*, 1235–1246. [[CrossRef](#)] [[PubMed](#)]
45. Fagone, P.; Jackowski, S. Membrane phospholipid synthesis and endoplasmic reticulum function. *J. Lipid Res.* **2009**, *50*, S311–S316. [[CrossRef](#)] [[PubMed](#)]
46. Appenzeller-Herzog, C. The ER-Golgi intermediate compartment (ERGIC): In search of its identity and function. *J. Cell Sci.* **2006**, *119*, 2173–2183. [[CrossRef](#)] [[PubMed](#)]
47. Davidoff, F.; Korn, E.D. Fatty acid and phospholipid composition of the cellular slime mold, *Dictyostelium discoideum*. *J. Biol. Chem.* **1963**, *238*, 3199–3209. [[PubMed](#)]
48. Weeks, G.; Herring, F.G. The lipid composition and membrane fluidity of *Dictyostelium discoideum* plasma membranes at various stages during differentiation. *J. Lipid Res.* **1980**, *21*, 681–686. [[PubMed](#)]
49. Clark, J.; Kay, R.R.; Kielkowska, A.; Niewczas, I.; Fets, L.; Oxley, D.; Stephens, L.R.; Hawkins, P.T. *Dictyostelium* uses ether-linked inositol phospholipids for intracellular signalling. *EMBO J.* **2014**, *33*, 2188–2200. [[CrossRef](#)] [[PubMed](#)]
50. Du, X.; Barisch, C.; Paschke, P.; Herrfurth, C.; Bertinetti, O.; Pawolleck, N.; Otto, H.; Rühling, H.; Feussner, I.; Herberg, F.W.; et al. *Dictyostelium* lipid droplets host novel proteins. *Eukaryot. Cell* **2013**, *12*, 1517–1529. [[CrossRef](#)] [[PubMed](#)]
51. Lu, X.; Gruia-Gray, J.; Copeland, N.G.; Gilbert, D.J.; Jenkins, N.A.; Londos, C.; Kimmel, A.R. The murine perilipin gene: The lipid droplet-associated perilipins derive from tissue-specific, mRNA splice variants and define a gene family of ancient origin. *Mamm. Gen.* **2001**, *12*, 741–749. [[CrossRef](#)]
52. Du, X.; Herrfurth, C.; Gottlieb, T.; Kawelke, S.; Feussner, I.; Rühling, H.; Feussner, I.; Maniak, M. *Dictyostelium discoideum* Dgat2 can substitute for the essential function of Dgat1 in triglyceride production but not in ether lipid synthesis. *Eukaryot. Cell* **2014**, *13*, 517–526. [[CrossRef](#)] [[PubMed](#)]
53. Xu, C.; Ng, T.W.D. Glycosylation-directed quality control of protein folding. *Nat. Rev. Mol. Cell Biol.* **2015**, *16*, 742–752. [[CrossRef](#)] [[PubMed](#)]
54. Kelleher, D.J.; Gilmore, R. An evolving view of the eukaryotic oligosaccharyltransferase. *Glycobiology* **2006**, *16*, 47R–62R. [[CrossRef](#)] [[PubMed](#)]
55. Braakman, I.; Hebert, D.N. Protein folding in the endoplasmic reticulum. *Cold Spring Harb. Perspect. Biol.* **2013**, *5*, a013201. [[CrossRef](#)] [[PubMed](#)]
56. Halperin, L.; Jung, J.; Michalak, M. The many functions of the endoplasmic reticulum chaperones and folding enzymes. *IUBMB Life* **2014**, *66*, 318–326. [[CrossRef](#)] [[PubMed](#)]

57. Gidalevitz, T.; Stevens, F.; Argon, Y. Orchestration of secretory protein folding by ER chaperones. *Biochim. Biophys. Acta Mol. Cell Res.* **2013**, *1833*, 2410–2424. [CrossRef] [PubMed]
58. Müller-Taubenberger, A.; Lupas, N.; Li, H.; Ecke, M.; Simmeth, E.; Gerisch, G. Calreticulin and calnexin in the endoplasmic reticulum are important for phagocytosis. *EMBO J.* **2001**, *20*, 6772–6782. [CrossRef] [PubMed]
59. Morita, T.; Saitoh, K.; Takagi, T.; Maeda, Y. Involvement of the glucose-regulated protein 94 (Dd-GRP94) in starvation response of Dictyostelium discoideum cells. *Biochem. Biophys. Res. Commun.* **2016**, *274*, 323–331. [CrossRef] [PubMed]
60. Braakman, I.; Bulleid, N.J. Protein Folding and Modification in the Mammalian Endoplasmic Reticulum. *Annu. Rev. Biochem.* **2011**, *80*, 71–99. [CrossRef] [PubMed]
61. Bulleid, N.J. Disulfide Bond Formation in the Mammalian Endoplasmic Reticulum. *Cold Spring Harb. Perspect. Biol.* **2012**, *4*, a013219. [CrossRef] [PubMed]
62. Monnat, J.; Hacker, U.; Geissler, H.; Rauchenberger, R.; Neuhaus, E.M.; Maniak, M.; Soldati, T. Dictyostelium discoideum protein disulfide isomerase, an endoplasmic reticulum resident enzyme lacking a KDEL-type retrieval signal. *FEBS Lett.* **1997**, *418*, 357–362. [CrossRef]
63. Monnat, J.; Neuhaus, E.M.; Pop, M.S.; Ferrari, D.M.; Kramer, B.; Soldati, T. Identification of a Novel Saturable Endoplasmic Reticulum Localization Mechanism Mediated by the C-Terminus of a *Dictyostelium* Protein Disulfide Isomerase. *Mol. Biol. Cell* **2000**, *11*, 3469–3484. [CrossRef] [PubMed]
64. Oslowski, C.M.; Urano, F. *Measuring ER Stress and the Unfolded Protein Response Using Mammalian Tissue Culture System*, 1st ed.; Elsevier Inc.: New York, NY, USA, 2011; Volume 490.
65. Bakthavatsalam, D.; Gomer, R.H. The secreted proteome profile of developing Dictyostelium discoideum cells. *Proteomics* **2010**, *10*, 2556–2559. [CrossRef] [PubMed]
66. Lam, T.Y.; Siu, C.-H. Inhibition of cell differentiation and cell cohesion by tunicamycin in Dictyostelium discoideum. *Dev. Biol.* **1982**, *92*, 398–407. [CrossRef]
67. Yamada, H.; Takatsuki, A.; Hirano, T.; Miyazaki, T.; Tamura, G. Effects of Tunicamycin on Cell Adhesion and Biosynthesis of Glycoproteins in Aggregation-Competent Cells of Dictyostelium discoideum. *J. Biochem.* **1982**, *92*, 399–406. [CrossRef] [PubMed]
68. Ochiai, H.; Stadler, J.; Westphal, M.; Wagle, G.; Merkl, R.; Gerisch, G. Monoclonal antibodies against contact sites A of Dictyostelium discoideum: Detection of modifications of the glycoprotein in tunicamycin-treated cells. *EMBO J.* **1982**, *1*, 1011–1016. [PubMed]
69. Hirano, T.; Yamada, H.; Miyazaki, T. Inhibition of cell adhesion in Dictyostelium discoideum by tunicamycin is prevented by leupeptin. *J. Biochem.* **1983**, *93*, 1249–1257. [CrossRef] [PubMed]
70. McDonald, C.J.; Sampson, J. The effects of inhibition of protein glycosylation on the aggregation of Dictyostelium discoideum. *J. Embryol. Exp. Morphol.* **1983**, *78*, 229–248. [PubMed]
71. Sadeghi, H.; Klein, C. Inhibition of N-linked glycosylation in Dictyostelium discoideum: Effects of aggregate formation. *Differentiation* **1988**, *38*, 99–103. [CrossRef] [PubMed]
72. Frank, L.C.-L.; Chen, G.; Nicole, W.A.; Shaulsky, G. Altered N-glycosylation modulates TgrB1/TgrC1-mediated development but not allore cognition in Dictyostelium. *J. Cell Sci.* **2015**, *128*, 3990–3996. [CrossRef]
73. Huber, R.J.; Myre, M.A.; Cotman, S.L. Aberrant adhesion impacts early development in a Dictyostelium model for juvenile neuronal ceroid lipofuscinosis. *Cell Adhes. Migr.* **2017**, *11*, 399–418. [CrossRef] [PubMed]
74. Browning, D.D.; O’Day, D.H. Concanavalin A and wheat germ agglutinin binding glycoproteins associated with cell fusion and zygote differentiation in Dictyostelium discoideum: Effects of calcium ions and tunicamycin on glycoprotein profiles. *Biochem. Cell Biol.* **1991**, *69*, 282–290. [CrossRef] [PubMed]
75. Kuwayama, H.; Ecke, M.; Gerisch, G.; VanHaastert, P.J.M. Protection against osmotic stress by cDGMP-mediated myosin phosphorylation. *Science* **1996**, *271*, 207–209. [CrossRef] [PubMed]
76. Serafimidis, I.; Bloomfield, G.; Skelton, J.; Ivens, A.; Kay, R.R. A new environmentally resistant cell type from Dictyostelium. *Microbiology* **2007**, *153*, 619–630. [CrossRef] [PubMed]
77. Travers, K.J.; Patil, C.K.; Wodicka, L.; Lockhart, D.J.; Weissman, J.S.; Walter, P. Functional and genomic analyses reveal an essential coordination between the unfolded protein response and ER-associated degradation. *Cell* **2000**, *101*, 249–258. [CrossRef]
78. Hollien, J.; Weissman, J.S. Decay of Endoplasmic Reticulum-Localized mRNAs During the Unfolded Protein Response. *Science* **2006**, *313*, 104–107. [CrossRef] [PubMed]

79. Hollien, J.; Lin, J.H.; Li, H.; Stevens, N.; Walter, P.; Weissman, J.S. Regulated Ire1-dependent decay of messenger RNAs in mammalian cells. *J. Cell Biol.* **2009**, *186*, 323–331. [CrossRef] [PubMed]
80. Lee, K.P.K.; Dey, M.; Neculai, D.; Cao, C.; Dever, T.E.; Sicheri, F. Structure of the Dual Enzyme Ire1 Reveals the Basis for Catalysis and Regulation in Nonconventional RNA Splicing. *Cell* **2008**, *132*, 89–100. [CrossRef] [PubMed]
81. Shamu, C.; Cox, J.; Walter, P. The unfolded-protein-response pathway in yeast. *Trends Cell Biol.* **1994**, *4*, 56–60. [CrossRef]
82. Bertolotti, A.; Wang, X.Z.; Novoa, I.; Jungreis, R.; Schlessinger, K.; Cho, J.H.; West, A.B.; Ron, D. Increased sensitivity to dextran sodium sulfate colitis in IRE1 β -deficient mice. *J. Clin. Investig.* **2001**, *107*, 585–593. [CrossRef] [PubMed]
83. Martino, M.B.; Jones, L.; Brighton, B.; Ehre, C.; Abdulah, L.; Davis, C.W.; Ron, D.; O’Neal, W.K.; Ribeiro, C.M.P. The ER stress transducer IRE1 β is required for airway epithelial mucin production. *Mucosal Immunol.* **2013**, *6*, 639–654. [CrossRef] [PubMed]
84. Fanata, W.I.D.; Lee, S.Y.; Lee, K.O. The unfolded protein response in plants: A fundamental adaptive cellular response to internal and external stresses. *Proteomics. J.* **2013**, *93*, 356–368. [CrossRef] [PubMed]
85. Okamura, K.; Kimata, Y.; Higashio, H.; Tsuru, A.; Kohno, K. Dissociation of Kar2p/BiP from an ER Sensory Molecule, Ire1p, Triggers the Unfolded Protein Response in Yeast. *Biochem. Biophys. Res. Commun.* **2000**, *279*, 445–450. [CrossRef] [PubMed]
86. Kimata, Y.; Ishiwata-Kimata, Y.; Ito, T.; Hirata, A.; Suzuki, T.; Oikawa, D.; Takeuchi, M.; Kohno, K. Two regulatory steps of ER-stress sensor Ire1 involving its cluster formation and interaction with unfolded proteins. *J. Cell Biol.* **2007**, *179*, 75–86. [CrossRef] [PubMed]
87. Gardner, B.M.; Walter, P. Unfolded proteins are Ire1-activating ligands that directly induce the unfolded protein response. *Science* **2011**, *333*, 1891–1894. [CrossRef] [PubMed]
88. Bowring, C.E.; Llewellyn, D.H. Differences in HAC1 mRNA processing and translation between yeast and mammalian cells indicate divergence of the eukaryotic ER stress response. *Biochem. Biophys. Res. Commun.* **2001**, *287*, 789–800. [CrossRef] [PubMed]
89. Hooks, K.B.; Griffiths-Jones, S. Conserved RNA structures in the non-canonical Hac1/Xbp1 intron. *RNA Biol.* **2011**, *8*, 552–556. [CrossRef] [PubMed]
90. Wu, H.; Ng, B.S.H.; Thibault, G. Endoplasmic reticulum stress response in yeast and humans. *Biosci. Rep.* **2014**, *34*, 321–330. [CrossRef] [PubMed]
91. Kimmig, P.; Diaz, M.; Zheng, J.; Williams, C.C.; Lang, A.; Aragón, T.; Li, H.; Walter, P. The unfolded protein response in fission yeast modulates stability of select mRNAs to maintain protein homeostasis. *Elife* **2012**, *1*, e00048. [CrossRef] [PubMed]
92. Tirasophon, W.; Lee, K.; Callaghan, B.; Welihinda, A.; Kaufman, R.J. The endoribonuclease activity of mammalian IRE1 autoregulates its mRNA and is required for the unfolded protein response. *Genes Dev.* **2000**, *14*, 2725–2736. [CrossRef] [PubMed]
93. Rubio, C.; Pincus, D.; Korennyykh, A.; Schuck, S.; El-Samad, H.; Walter, P. Homeostatic adaptation to endoplasmic reticulum stress depends on Ire1 kinase activity. *J. Cell Biol.* **2011**, *193*, 171–184. [CrossRef] [PubMed]
94. van Anken, E.; Pincus, D.; Coyle, S.; Aragón, T.; Osman, C.; Lari, F.; Gómez Puerta, S.; Korennyykh, A.V.; Walter, P. Specificity in endoplasmic reticulum-stress signaling in yeast entails a step-wise engagement of HAC1 mRNA to clusters of the stress sensor Ire1. *Elife* **2014**, *3*, 1–17. [CrossRef] [PubMed]
95. Aragón, T.; van Anken, E.; Pincus, D.; Serafimova, I.M.; Korennyykh, A.V.; Rubio, C.A.; Walter, P. Messenger RNA targeting to endoplasmic reticulum stress signalling sites. *Nature* **2009**, *457*, 736–740. [CrossRef] [PubMed]
96. Coelho, D.S.; Cairão, F.; Zeng, X.; Pires, E.; Coelho, A.V.; Ron, D.; Ryoo, H.D.; Domingos, P.M. Xbp1-Independent Ire1 Signaling Is Required for Photoreceptor Differentiation and Rhabdomere Morphogenesis in Drosophila. *Cell Rep.* **2013**, *5*, 791–801. [CrossRef] [PubMed]
97. Chen, Y.; Brandizzi, F. IRE1: ER stress sensor and cell fate executor. *Trends Cell Biol.* **2013**, *23*, 547–555. [CrossRef] [PubMed]
98. Miyazaki, T.; Nakayama, H.; Nagayoshi, Y.; Kakeya, H.; Kohno, S. Dissection of Ire1 functions reveals stress response mechanisms uniquely evolved in *Candida glabrata*. *PLoS Pathog.* **2013**, *9*, e1003160. [CrossRef] [PubMed]

99. Liu, J.-X.; Srivastava, R.; Che, P.; Howell, S.H. An endoplasmic reticulum stress response in Arabidopsis is mediated by proteolytic processing and nuclear relocation of a membrane-associated transcription factor, bZIP28. *Plant Cell* **2007**, *19*, 4111–4119. [CrossRef] [PubMed]
100. Che, P.; Bussell, J.D.; Zhou, W.; Estavillo, G.M.; Pogson, B.J.; Smith, S.M. Signaling from the endoplasmic reticulum activates brassinosteroid signaling and promotes acclimation to stress in Arabidopsis. *Sci. Signal.* **2010**, *3*, ra69. [CrossRef] [PubMed]
101. Chen, X.; Shen, J.; Prywes, R. The luminal domain of ATF6 senses endoplasmic reticulum (ER) stress and causes translocation of ATF6 from the ER to the Golgi. *J. Biol. Chem.* **2002**, *277*, 13045–13052. [CrossRef] [PubMed]
102. Yamamoto, K.; Yoshida, H.; Kokame, K.; Kaufman, R.J.; Mori, K. Differential contributions of ATF6 and XBP1 to the activation of endoplasmic reticulum stress-responsive cis-acting elements ERSE, UPRE and ERSE-II. *J. Biochem.* **2004**, *136*, 343–350. [CrossRef] [PubMed]
103. Okada, T.; Yoshida, H.; Akazawa, R.; Negishi, M.; Mori, K. Distinct roles of activating transcription factor 6 (ATF6) and double-stranded RNA-activated protein kinase-like endoplasmic reticulum kinase (PERK) in transcription during the mammalian unfolded protein response. *Biochem. J.* **2002**, *366 Pt 2*, 585–594. [CrossRef] [PubMed]
104. Druelle, C.; Drullion, C.; Desl  , J.; Martin, N.; Saas, L.; Cormenier, J.; Malaquin, N.; Huot, L.; Slomianny, C.; Bouali, F.; et al. ATF6 α regulates morphological changes associated with senescence in human fibroblasts. *Oncotarget* **2016**, *7*, 67699–67715. [CrossRef] [PubMed]
105. Skorczyk-Werner, A.; Chiang, W.C.; Wawrocka, A.; Wicher, K.; Jarmuz-Szymczak, M.; Kostrzewska-Poczekaj, M.; Jamsheer, A.; P  oski, R.; Rydzanicz, M.; Pojda-Wilczek, D.; et al. Autosomal recessive cone-rod dystrophy can be caused by mutations in the ATF6 gene. *Eur. J. Hum. Genet.* **2017**, *25*, 1210–1216. [CrossRef] [PubMed]
106. Chiang, W.-C.; Chan, P.; Wissinger, B.; Vincent, A.; Skorczyk-Werner, A.; Krawczyński, M.R.; Kaufman, R.J.; Tsang, S.H.; H  on, E.; Kohl, S.; et al. Achromatopsia mutations target sequential steps of ATF6 activation. *Proc. Natl. Acad. Sci. USA* **2017**, *114*, 400–405. [CrossRef] [PubMed]
107. Marciak, S.J.; Garcia-Bonilla, L.; Hu, J.; Harding, H.P.; Ron, D. Activation-dependent substrate recruitment by the eukaryotic translation initiation factor 2 kinase PERK. *J. Cell Biol.* **2006**, *172*, 201–209. [CrossRef] [PubMed]
108. Jindrich, K.; Degnan, B.M. The diversification of the basic leucine zipper family in eukaryotes correlates with the evolution of multicellularity. Genome evolution and evolutionary systems biology. *BMC EBiol.* **2016**, *16*, 1–12.
109. Nagashima, Y.; Mishiba, K.; Suzuki, E.; Shimada, Y.; Iwata, Y.; Koizumi, N. Arabidopsis IRE1 catalyses unconventional splicing of bZIP60 mRNA to produce the active transcription factor. *Sci. Rep.* **2011**, *1*, 29. [CrossRef] [PubMed]
110. Ruggiano, A.; Foresti, O.; Carvalho, P. ER-associated degradation: Protein quality control and beyond. *J. Cell Biol.* **2014**, *204*, 869–879. [CrossRef] [PubMed]
111. Tsai, B.; Ye, Y.; Rapoport, T.A. Retro-translocation of proteins from the endoplasmic reticulum into the cytosol. *Nat. Rev. Mol. Cell Biol.* **2002**, *3*, 246–255. [CrossRef] [PubMed]
112. Klionsky, D.J.; Emr, S.D. Autophagy as a regulated pathway of cellular degradation. *Science* **2000**, *290*, 1717–1721. [CrossRef] [PubMed]
113. Walter, P.; Ron, D. The unfolded protein response: From stress pathway to homeostatic regulation. *Science* **2011**, *334*, 1081–1086. [CrossRef] [PubMed]
114. Urano, F.; Wang, X.-Z.; Bertolotti, A.; Zhang, Y.; Chung, P.; Harding, H.P.; Ron, D. Coupling of Stress in the Endoplasmic Reticulum to Activation of JNK Protein Kinases by Transmembrane Protein Kinase IRE1. *Science* **2000**, *287*, 664–666. [CrossRef] [PubMed]
115. Ogata, M.; Hino, S.; Saito, A.; Morikawa, K.; Kondo, S.; Kanemoto, S.; Murakami, T.; Taniguchi, M.; Tanii, I.; Yoshinaga, K.; et al. Autophagy is activated for cell survival after endoplasmic reticulum stress. *Mol. Cell. Biol.* **2006**, *26*, 9220–9231. [CrossRef] [PubMed]
116. Liu, Y.; Burgos, J.S.; Deng, Y.; Srivastava, R.; Howell, S.H.; Bassham, D.C. Degradation of the endoplasmic reticulum by autophagy during endoplasmic reticulum stress in Arabidopsis. *Plant Cell* **2012**, *24*, 4635–4651. [CrossRef] [PubMed]

117. Goldberg, J.M.; Manning, G.; Liu, A.; Fey, P.; Pilcher, K.E.; Xu, Y.; Smith, J.L. The dictyostelium kinome—Analysis of the protein kinases from a simple model organism. *PLoS Genet.* **2006**, *2*, e38. [[CrossRef](#)] [[PubMed](#)]
118. Caffrey, D.R.; O'Neill, L.A.; Shields, D.C. The evolution of the MAP kinase pathways: Coduplication of interacting proteins leads to new signaling cascades. *J. Mol. Evol.* **1999**, *49*, 567–582. [[CrossRef](#)] [[PubMed](#)]
119. Giusti, C.; Tresse, E.; Luciani, M.F.; Golstein, P. Autophagic cell death: Analysis in Dictyostelium. *Biochim. Biophys. Acta Mol. Cell Res.* **2009**, *1793*, 1422–1431. [[CrossRef](#)] [[PubMed](#)]
120. Kroemer, G.; Galluzzi, L.; Vandenebeele, P.; Abrams, J.; Alnemri, E.S.; Baehrecke, E.H.; Blagosklonny, M.V.; El-Deiry, W.S.; Golstein, P.; Green, D.R.; et al. Classification of cell death: Recommendations of the Nomenclature Committee on Cell Death 2009. *Cell Death Differ.* **2009**, *16*, 3–11. [[CrossRef](#)] [[PubMed](#)]
121. Baehrecke, E.H. Autophagic programmed cell death in Drosophila. *Cell Death Differ.* **2003**, *10*, 940–945. [[CrossRef](#)] [[PubMed](#)]
122. Hofius, D.; Schultz-Larsen, T.; Joensen, J.; Tsitsigiannis, D.I.; Petersen, N.H.T.; Mattsson, O.; Jørgensen, L.B.; Jones, J.D.G.; Mundy, J.; Petersen, M. Autophagic Components Contribute to Hypersensitive Cell Death in Arabidopsis. *Cell* **2009**, *137*, 773–783. [[CrossRef](#)] [[PubMed](#)]
123. Liu, Y.; Levine, B. Autosis and autophagic cell death: The dark side of autophagy. *Cell Death and Differentiation* **2015**, *22*, 367–376. [[CrossRef](#)] [[PubMed](#)]
124. Whittingham, W.F.; Raper, K.B. Non-Viability of Stalk Cells in Dictyostelium. *Proc. Natl. Acad. Sci. USA* **1960**, *46*, 642–649. [[CrossRef](#)] [[PubMed](#)]
125. Levraud, J.-P.; Adam, M.; Luciani, M.-F.; de Chastellier, C.; Blanton, R.L.; Golstein, P. Dictyostelium cell death: Early emergence and demise of highly polarized paddle cells. *J. Cell Biol.* **2003**, *160*, 1105–1114. [[CrossRef](#)] [[PubMed](#)]
126. Lam, D.; Golstein, P. A specific pathway inducing autophagic cell death is marked by an IP3R mutation. *Autophagy* **2008**, *8*, 347–350. [[CrossRef](#)]
127. Wolf, D.H.; Stoltz, A. The Cdc48 machine in endoplasmic reticulum associated protein degradation. *Biochim. Biophys. Acta Mol. Cell Res.* **2012**, *1823*, 117–124. [[CrossRef](#)] [[PubMed](#)]
128. Müller-Taubenberger, A. Application of fluorescent protein tags as reporters in live-cell imaging studies. *Meth. Mol. Biol.* **2006**, *346*, 229–246.



© 2018 by the authors. Licensee MDPI, Basel, Switzerland. This article is an open access article distributed under the terms and conditions of the Creative Commons Attribution (CC BY) license (<http://creativecommons.org/licenses/by/4.0/>).